



Field Validation of Air-Source Heat Pumps for Cold Climates

Jon Winkler and Sugi Ramaraj

National Renewable Energy Laboratory

**NREL is a national laboratory of the U.S. Department of Energy
Office of Energy Efficiency & Renewable Energy
Operated by the Alliance for Sustainable Energy, LLC**

This report is available at no cost from the National Renewable Energy Laboratory (NREL) at www.nrel.gov/publications.

Contract No. DE-AC36-08GO28308

Technical Report
NREL/TP-5500-84745
May 2023



Field Validation of Air-Source Heat Pumps for Cold Climates

Jon Winkler and Sugi Ramaraj

National Renewable Energy Laboratory

Suggested Citation

Winkler, Jon and Sugi Ramaraj. 2023. *Field Validation of Air-Source Heat Pumps for Cold Climates*. Golden, CO: National Renewable Energy Laboratory. NREL/TP-5500-84745.
<https://www.nrel.gov/docs/fy23osti/84745.pdf>.

**NREL is a national laboratory of the U.S. Department of Energy
Office of Energy Efficiency & Renewable Energy
Operated by the Alliance for Sustainable Energy, LLC**

This report is available at no cost from the National Renewable Energy Laboratory (NREL) at www.nrel.gov/publications.

Contract No. DE-AC36-08GO28308

Technical Report
NREL/TP-5500-84745
May 2023

National Renewable Energy Laboratory
15013 Denver West Parkway
Golden, CO 80401
303-275-3000 • www.nrel.gov

NOTICE

This work was authored by the National Renewable Energy Laboratory, operated by Alliance for Sustainable Energy, LLC, for the U.S. Department of Energy (DOE) under Contract No. DE-AC36-08GO28308. Funding provided by the U.S. Department of Energy Office of Energy Efficiency and Renewable Energy Building Technologies Office. The views expressed herein do not necessarily represent the views of the DOE or the U.S. Government.

This report is available at no cost from the National Renewable Energy Laboratory (NREL) at www.nrel.gov/publications.

U.S. Department of Energy (DOE) reports produced after 1991 and a growing number of pre-1991 documents are available free via www.OSTI.gov.

Cover Photos by Dennis Schroeder: (clockwise, left to right) NREL 51934, NREL 45897, NREL 42160, NREL 45891, NREL 48097, NREL 46526.

NREL prints on paper that contains recycled content.

Preface

This project measured the in-field performance of centrally ducted, variable-capacity air-source heat pumps in cold climates to validate performance and develop field-based performance maps. The work presented in this report does not represent performance of any product relative to regulated minimum efficiency requirements.

The laboratory and field site used for this work are not certified rating test facilities. The conditions and methods under which products were characterized for this work differ from standard rating conditions, as described.

Because the methods and conditions differ, the reported results are not comparable to rated product performance and should only be used to estimate performance under the measured conditions.

Acknowledgments

We would like to thank Dale Hoffmeyer and Catherine Rivest at the U.S. Department of Energy for their support of our work. We would like to acknowledge Bob Davis at Ecotope, Inc. for his efforts to recruit participants during the COVID-19 pandemic, lead the installation of the monitoring equipment and house data collection, and routinely assure data collection was running smoothly. We appreciate the assistance from Greg Barker and Ed Hancock at Mountain Energy Partnerships for their expertise with configuring and programming Campbell data logging systems. This project benefited from a strong collaboration with Rebecca Trojanowski and Tom Butcher at Brookhaven National Laboratory.

List of Acronyms

ACCA	Air Conditioning Contractors of America
ACH	air changes per hour
AHRI	Air-Conditioning, Heating, and Refrigeration Institute
BNL	Brookhaven National Laboratory
COP	coefficient of performance
CT	current transformer
DOE	U.S. Department of Energy
DSE	distribution system efficiency
EIA	U.S. Energy Information Agency
HDD ₆₅	heating degree days
HSPF	heating seasonal performance factor
IDU	indoor unit
IECC	International Energy Conservation Code
MSHP	mini-split heat pump
NEEP	Northeast Energy Efficiency Partnerships
NREL	National Renewable Energy Laboratory
ODU	outdoor unit
RH	relative humidity
SEER	seasonal energy efficiency ratio
SRTM	Site-Responsible Team Member
WBT	wet-bulb temperature

Executive Summary

Heating energy is the largest end-use for U.S. residential buildings, accounting for approximately one-third of residential building energy consumption (EIA 2021). Historically, air-source heat pumps have been limited to temperate climates because of subpar performance at extremely cold outdoor air temperatures. However, recent advances to cold-climate air-source heat pump technology, which typically rely on inverter-driven, variable-speed compressors and variable-speed fans, have significantly improved low-temperature heat pump performance, enabling the technology to save energy for many homes in cold climates.

Many researchers have field validated single-zone, ductless mini-split heat pumps (MSHPs), typically used to displace a home's existing heating system in cold climates. However, most U.S. homes utilize a central, forced air heating system to distribute warm air throughout the home. In the mid-2000s, central split heat pump systems with variable-speed compressors were introduced to the market. However, despite the availability of inverter-driven central heat pump systems, questions remain regarding in-field performance when installed in cold climates.

In fall 2018, the National Renewable Energy Laboratory (NREL) and Brookhaven National Laboratory (BNL) embarked on a U.S. Department of Energy funded study to measure in-field performance of both MSHPs and centrally ducted, variable-speed heat pumps in cold climates. NREL and BNL collaborated to develop a common field test protocol to guide these two independent, yet coordinated, studies. Monitoring equipment installation started in February 2021 and was completed by the following September. Because the focus of the study was on heating performance, data was collected for at least one full winter and concluded in summer 2022. The NREL study discussed in this report focused exclusively on centrally ducted heat pumps.

The primary objective of this project was to measure in-field performance of centrally ducted, variable-capacity air-source heat pumps in cold climates to validate performance and develop field-based performance maps. The project focused on quantifying heat pump performance at cold temperatures.

We fulfilled the project objective by monitoring 13 central heat pump systems installed in single-family residential buildings located in a cold climate for at least one full winter season. This report describes the house characteristics and heat pump specifications, field monitoring and data analysis methodologies, and measured heating and cooling field performance. Due to an instrumentation issue, this report includes data on 12 of the 13 monitored heat pumps.

The sites identified for the study were primarily located in the northwest United States, as homes in the region tend to have all-electric space heating systems and high-efficiency heat pumps have been incentivized in the region for several years. NREL partnered with Ecotope, Inc., a small energy consulting firm located in Seattle, for site recruitment, monitoring equipment installation, and data quality management. All the sites included in the study had previously installed a high-efficiency central heat pump system. One site in a Denver suburb had the only dual fuel heat pump in the study.

We used airside and power measurements, collected at five-second intervals, to quantify heat pump capacity, coefficient of performance (COP), and auxiliary heater energy consumption. We

developed algorithms to automatically determine the heat pump operating mode including defrost and auxiliary heating operation. A whole-house thermal and duct audit was completed during the initial site visit to estimate winter heating loads and assess heat pump sizing. Whole-home heating design loads were calculated at ASHRAE 99% design temperatures (ASHRAE 2017) and compared to manufacturer-reported maximum capacities to assess the heat pump sizing at each site.

Figure ES-1 compares the estimated fraction of the building load met by compressor-based heating to the heat pump sizing, where a value of 100% represents a heat pump that has been perfectly sized to match the building’s heating load at the 99% design temperature. Several heat pumps in the study were undersized based on this metric. The fraction of the heating load served by the compressor depends on the heat pump sizing, winter weather, occupant thermostat settings and schedule, heat pump controls, and heat pump capacity retention at cold temperatures.

The heat pump at Site 8 was undersized due to an inefficient distribution system and thus the system relied on the electric resistance auxiliary heater to meet ~20% of the building’s heating load during winter 2021–2022. The heat pump at Site 8 also ran the auxiliary heater for approximately six minutes following every defrost cycle and occasionally relied on the auxiliary heater to recover from thermostat setback periods. These three factors significantly decreased the overall performance of the heat pump.

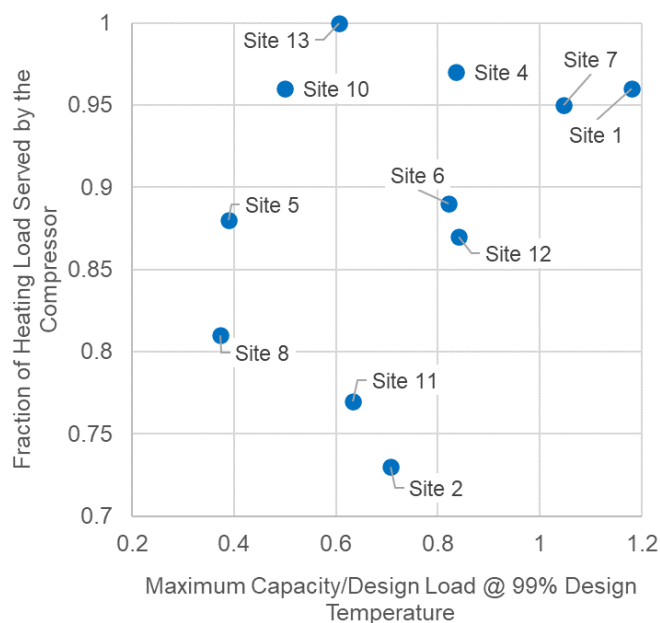


Figure ES-1. Fraction of the building heating load served by the compressor compared to the heat pump sizing percentage at the 99% heating design temperature winter 2021-2022.

In contrast, the heat pump at Site 10 satisfied nearly 95% of the heating load despite being undersized as well; however, the weather during the winter was warmer than normal when compared to the heating design temperature. The weather at Site 13 was also warmer than normal and the auxiliary heat rarely turned on, resulting in the compressor meeting most of the

building’s heating load. The winter weather at Site 11 was colder than normal and the heat pump was sized to meet 63% of the design heating load, which resulted in the compressor meeting less than 80% of the heating load. The heat pump at Site 2 had a clear operational and/or control fault midway through the winter resulting in poor system performance, where the auxiliary heat was over-utilized. As a result, a low fraction of the building’s heating load was served by the compressor.

The heat pumps at Sites 1 and 7 were the only two heat pumps in the study sized with excess heating capacity and as expected, both sites utilized the compressor to meet more than 95% of the season’s heating load.

Figure ES-2 plots the compressor-based heating seasonal COP and the overall system heating COP for the twelve sites. The compressor-based heating COP was calculated by summing the total heat delivered divided by the total indoor and outdoor unit energy consumption during time periods with compressor-based heating. The average seasonal compressor-based heating COP across all twelve sites averaged 2.5, ranging from 1.7 (Site 6) to 3.5 (Site 8). Though Site 8 had the highest heat pumping (i.e., compressor-based heating) COP, the auxiliary heater consumed a significant amount of energy, lowering the overall heating COP.

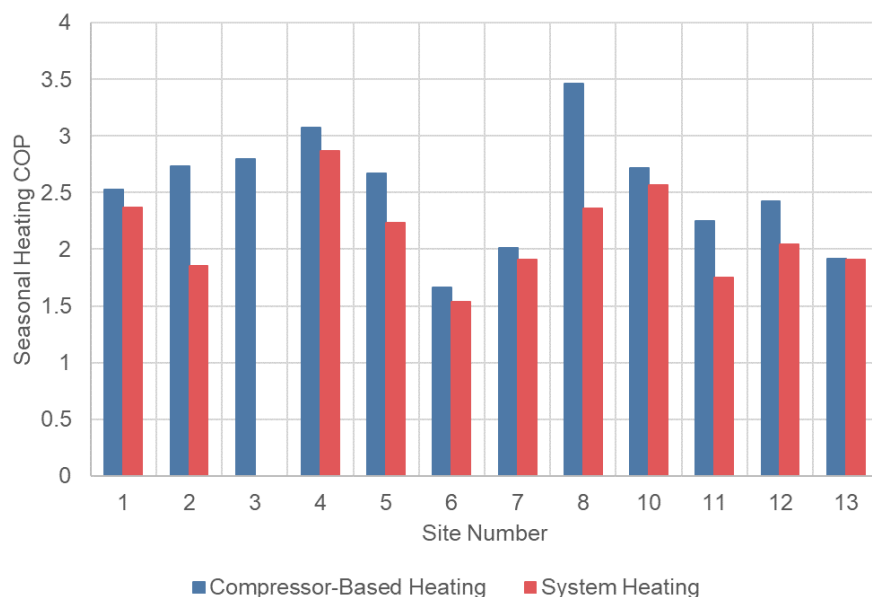


Figure ES-2. Seasonal compressor-based heating and system heating COPs during winter 2021–2022 for each site.

The seasonal system heating COP accounts for auxiliary heat energy consumption, which lowers the overall COP because the auxiliary heater operates at a COP of 1. This significantly lowered the overall heating COP for several sites. Specifically at Sites 2 and 8, the auxiliary heat lowered the overall system COP by more than 30%. Six sites (Sites 1, 4, 6, 7, 10, and 13) had relatively

little auxiliary heater usage and thus the heating COP was lowered by less than 7% for these homes.

Additional conclusions include:

- Heating COP: Heating COPs were compared to manufacturer-reported values attained from either the Northeast Energy Efficiency Partnership's Cold-Climate Air Source Heat Pump Product Listing (NEEP 2022) or manufacturer-published expanded performance tables. Steady state COPs at 7 of the 12 sites aligned closely with expected performance. For the remaining sites, the measured COPs were lower than expected. One potential cause for low COP is a low indoor airflow rate. However, sites with lower-than-expected COPs did not consistently have low indoor unit airflow rates.
- Heating capacity: The measured capacity tended to be closer to the minimum manufacturer-reported capacity rather than the maximum. For 5 of the 12 sites, the measured capacity aligned well with maximum manufacturer-reported capacity at cold outdoor air temperatures.
- Capacity modulation: Heat pumps at 11 of the sites included variable-capacity compressors. However, despite having modulation capabilities, the heat pumps were off for a significant fraction of the time at outdoor temperatures where we expected the system to run continuously. This could be due to occupant thermostat setpoint schedules or the equipment controls.
- Auxiliary heat use: The electric resistance auxiliary heater energy use exceeded 40% of the compressor-based heating energy at 5 of the 11 reported-on all-electric sites. At 2 of those 5 sites, the auxiliary heating consumed more energy than compressor-based heating operation. This was due to one system being undersized and use of auxiliary heat after defrost and during setback recovery (Site 8) and a control and/or sensor fault in one system (Site 2).
- Defrost operation: All systems spent a relatively small fraction of the operating hours in defrost mode. However, the energy consumed by defrost operation exceeded 20% of the compressor-based heating energy at 4 of 12 sites as the auxiliary heater was turned on during defrost. Two sites ran the auxiliary heater for more than five minutes following the defrost cycle. Defrost operation was the primary consumer of auxiliary heating at 3 of 11 sites. (Defrost energy use was not fully accounted for at the dual fuel site because natural gas consumption was not directly measured. However, the natural gas furnace did operate during defrost.)
- Heating supply air temperature: The supply air temperature for all sites rarely exceeded 100°F. Five sites maintained a relatively constant supply air temperature independent of outdoor air temperature, while the supply air temperature decreased at colder outdoor air temperatures for six of the sites. Supply air temperatures around 80°F were not uncommon.

Table of Contents

1	Introduction	1
1.1	Project Overview and Objective.....	2
1.2	Key Research Questions.....	3
1.3	Approach Overview	3
2	Site Characteristics and Heat Pump Information	5
2.1	Site Locations.....	5
2.2	Site Issues and Resolutions	6
2.2.1	Heat Pump Installation Issues	6
2.2.2	Data Logging Issues.....	6
2.3	Weather Data During Monitoring	7
2.4	Site Characteristics.....	10
2.5	Heat Pump Specifications and Settings.....	10
2.6	House Heating Loads and Heat Pump Sizing	16
3	Field Monitoring Methodology	19
3.1	Field Protocol	19
3.2	Data Acquisition.....	19
3.3	Blower Airflow Data and Correlations	20
4	Data Analysis Approach	24
4.1	Determining Heat Pump Operating Modes.....	27
4.1.1	System Off Mode	27
4.1.2	Fan-Only Mode	28
4.1.3	Compressor Heating Mode.....	29
4.1.4	Auxiliary Heating Mode.....	31
4.1.5	Compressor + Auxiliary Heating Mode	32
4.1.6	Defrost Mode	33
4.1.7	Cooling Mode.....	34
4.2	Determining Steady State Periods.....	36
4.3	Performance Calculations	37
5	Heating Mode Performance Results and Discussion	39
5.1	Heating Season Summary Data.....	39
5.2	Heating Season Operating Modes	42
5.3	Compressor-Based Heating COP and Capacity	44
5.4	Auxiliary Heater Use.....	51
5.5	Cycling and Capacity Modulation.....	54
5.6	Defrost.....	62
5.7	Heating Supply Air Temperature	65
5.8	Standby Power Consumption	65
6	Cooling Mode Performance Results and Discussion	72
6.1	Cooling Season Operating Modes.....	72
6.2	Cooling Capacity and Coefficient of Performance	72
6.3	Capacity Modulation and Cycling.....	77
7	Summary and Conclusions	81
7.1	Recommendations to Improve Installed Performance	82
7.2	Recommendations to Improve the Field Protocol.....	83
	References	84
	Appendix A. Field Protocol Data Entry Forms	86
	Checklist (Condensed Protocol) and Data Entry Form for Air-Source Heat Pumps Cold-Climate Field Performance Project	86
	Form 1a: Ducted Systems: House Information Table	87
	Form 2a: Home’s Heating Energy Use	88

Form 2b: Home’s Cooling Energy Use.....	90
Form 3: Site Photos of Heat Pump.....	92
Form 4: Heat Pump Information and Product Data.....	93
Form 5: Commissioning Data*	94
Form 6a: Ducted Systems – Blower Airflow Data.....	95
Form 7: Data Logger Channel List.....	96
Indoor Data Logger (CR1000)	96
Outdoor Data Logger (CR1000).....	97
Form 8: Home Thermal Audit.....	98
Ducts.....	99
Blower Door Test.....	100
Exterior Duct Leakage Testing.....	101

List of Figures

Figure ES-1. Fraction of the building heating load served by the compressor compared to the heat pump sizing percentage at the 99% heating design temperature winter 2021-2022.	vii
Figure ES-2. Seasonal compressor-based heating and system heating COPs during winter 2021–2022 for each site.....	viii
Figure 1. Residential heat pump market penetration in the United States (EIA 2020).....	1
Figure 2. (a) Northwest site locations and (b) IECC climate zone map.....	6
Figure 3. Outdoor temperature histograms for the monitoring period for each site.	9
Figure 4. House heating load lines (blue) and manufacturer-reported maximum and minimum heating capacities (red solid and dashed lines, respectively).....	17
Figure 5. Schematic depicting key measurements on the IDU and ODU used to meet project objectives.	20
Figure 6. Measured blower airflow rate and power (points) and correlation used for performance calculations (lines).	21
Figure 7. Flow plate used for IDU airflow measurement.	22
Figure 8. Comparison of field-measured indoor unit airflow rate to manufacturer-reported airflow rates listed in the AHRI Directory of Certified Products.....	23
Figure 9. Flow chart outlining the data processing approach along with the decision tree for determining the heat pump operating mode.	26
Figure 10. Automatically detected heat pump operation mode during a cold winter period.....	27
Figure 11. Outdoor power and compressor inverter frequency during a period with cycling.	28
Figure 12. Automatically detected system off operation mode during a period with cycling.	28
Figure 13. Blower power, outdoor power, and compressor inverter frequency during a period with fan-only operation.	29
Figure 14. Automatically detected operation mode during an example period with fan-only operation....	29
Figure 15. Blower power, outdoor power, and compressor inverter frequency during a period with heating cycle.	30
Figure 16. Supply and return air temperature during a period with heating cycle.....	30
Figure 17. Automatically detected compressor heating operation mode during an example period.	30
Figure 18. Blower power and supply and return air temperature during a period with auxiliary heating operation.....	31
Figure 19. Automatically detected operation mode during an example period with auxiliary heating operation.....	31
Figure 20. Blower power, outdoor and indoor power, and compressor inverter frequency during a period with compressor + auxiliary heating operation.....	32
Figure 21. Supply and return air temperature during a period with compressor + auxiliary heating operation.....	32
Figure 22. Automatically detected compressor + auxiliary heating operation mode during an example period.	33
Figure 23. Air and refrigerant temperatures during a defrost cycle.....	33
Figure 24. ODU and IDU power during a defrost cycle.	34
Figure 25. Automatically detected defrost cycle.....	34
Figure 26. Blower power, outdoor power, and compressor inverter frequency during a period with cooling cycle.	35
Figure 27. Air and refrigerant temperatures during a period with cooling cycle.....	35
Figure 28. Automatically detected cooling operation mode during an example period.	35
Figure 29. Supply air temperature and inverter frequency over a moving data window.	36
Figure 30. Steady state detection using hybrid online steady state detection method.	37
Figure 31. Heat pump operational modes at cold temperatures during winter 2021–2022.	43
Figure 32. Box and whisker plot of steady-state compressor-based heating COPs (blue boxes) and manufacturer-reported COPs at minimum and maximum speeds (red lines).	46

Figure 33. Mean steady-state compressor-based heating COPs (blue bars) and manufacturer-reported COPS at minimum and maximum speeds (red lines).	47
Figure 34. Box and whisker plot of steady-state compressor-based heating capacity (blue boxes) and manufacturer-reported capacities at minimum and maximum speeds (red lines).....	48
Figure 35. Mean steady-state compressor-based heating capacity binned by outdoor temperature (blue bars) and manufacturer-reported capacities at minimum and maximum speeds (red lines). .	49
Figure 36. Box and whisker plot of steady-state compressor-based heating IDU airflow rate (blue boxes) and manufacturer-reported full load and minimum speed airflow rates (red lines).....	50
Figure 37. Site 2 daily ODU and auxiliary heater energy use during winter 2021–2022.....	52
Figure 38. Operating modes for Sites 2 and 8 to highlight auxiliary heat use.....	52
Figure 39. High cycling rate at Site 13 during mild temperatures.	55
Figure 40. High cycling rate resolved at Site 13.....	56
Figure 41. Auxiliary heater energy in heating (blue) and defrost (orange) modes during winter 2021–2022.....	57
Figure 42. Mean compressor heating runtime fraction.	58
Figure 43. Box and whisker plot of compressor cycles per hour during winter 2021–2022.	59
Figure 44. Box and whisker plot of inverter frequency during steady-state compressor-based heating operation.....	60
Figure 45. Fraction of time spent at a given inverter frequency during steady-state compressor-based heating operation during winter 2021–2022.	61
Figure 46. An example day with frequent defrost cycles for the heat pump at Site 7.	62
Figure 47. ODU, IDU, and blower power and compressor inverter frequency during a day with frequent defrost cycles at Site 7.	63
Figure 48. Air and refrigerant temperatures during a day with frequent defrost cycles at Site 7.	63
Figure 49. An example day with a long defrost cycle at Site 7.....	64
Figure 50. ODU, IDU, and compressor inverter frequency during a long defrost cycle at Site 7.	64
Figure 51. Air and refrigerant temperatures during a long defrost cycle at Site 7.....	64
Figure 52. Time spent in defrost mode during winter 2021–2022.....	67
Figure 53. Total number of defrost cycles during winter 2021–2022.....	68
Figure 54. Box and whisker plot showing the defrost cycle length during winter 2021–2022.....	69
Figure 55. Box and whisker plot showing heat pump supply air temperature during periods of steady-state compressor-based heating.	70
Figure 56. Average ODU (orange) and IDU (blue) standby power during winter 2021–2022.	71
Figure 57. Heat pump operational modes at warm outdoor air temperatures.	73
Figure 58. Box and whisker plot of steady-state cooling COPs.	74
Figure 59. Mean steady-state cooling COPs.....	75
Figure 60. Box and whisker plot of steady-state cooling total capacity.	76
Figure 61. Box and whisker plot of compressor cycles per hour during cooling mode operation for Sites 1, 2, 3, and 10.....	77
Figure 62. Mean cooling runtime fraction.	79
Figure 63. Box and whisker plot of inverter frequency during steady-state cooling operation.	80

List of Tables

Table 1. Heat Pump Site Information	5
Table 2. Number of Hours with Cold Temperatures.....	8
Table 3. House Characteristics, Site Design Temperatures, and House Design Heating Loads for the Northwestern Sites	13
Table 4. Heat Pump Product Data and Specifications	14
Table 5. Heat Pump Installation and Operation Information and Auxiliary Heat Specifications.....	15

Table 6. Heat Pump Sizing and Site Balance Temperatures.....	18
Table 7. List of Key Sensor Types.....	20
Table 8. Coefficients for the Blower Fan Curve.....	22
Table 9. Measurements Used for Data Processing and Calculations.....	24
Table 10. Calculated Moist Air Properties.....	25
Table 11. Summary of Heating Data for Winter 2021–2022.....	41
Table 12. Auxiliary Heat Runtime at Cold Temperatures During Winter 2022–2023	54
Table 13. Auxiliary Heat Use Following a Defrost Cycle During Winter 2021–2022.....	65

1 Introduction

Heating energy is the largest end-use for U.S. residential buildings, accounting for approximately one-third of residential building energy consumption (EIA 2021). Historically, air-source heat pumps have been limited to temperate climates because of subpar performance at extremely cold outdoor air temperatures. Heat pumps have also not seen significant market penetration in regions with access to natural gas. However, recent advances to cold-climate air-source heat pump technology, which typically rely on inverter-driven, variable-speed compressors and variable-speed fans, have significantly improved low-temperature heat pump performance enabling the technology to potentially save energy for many homes in cold climates. Despite the relatively recent technology advancements, heat pump technology is more common in warmer climates, as shown in Figure 1, which provides a breakdown of heat pump use throughout the United States based on the U.S. Energy Information Agency *2020 Residential Energy Consumption Survey* (EIA 2020).

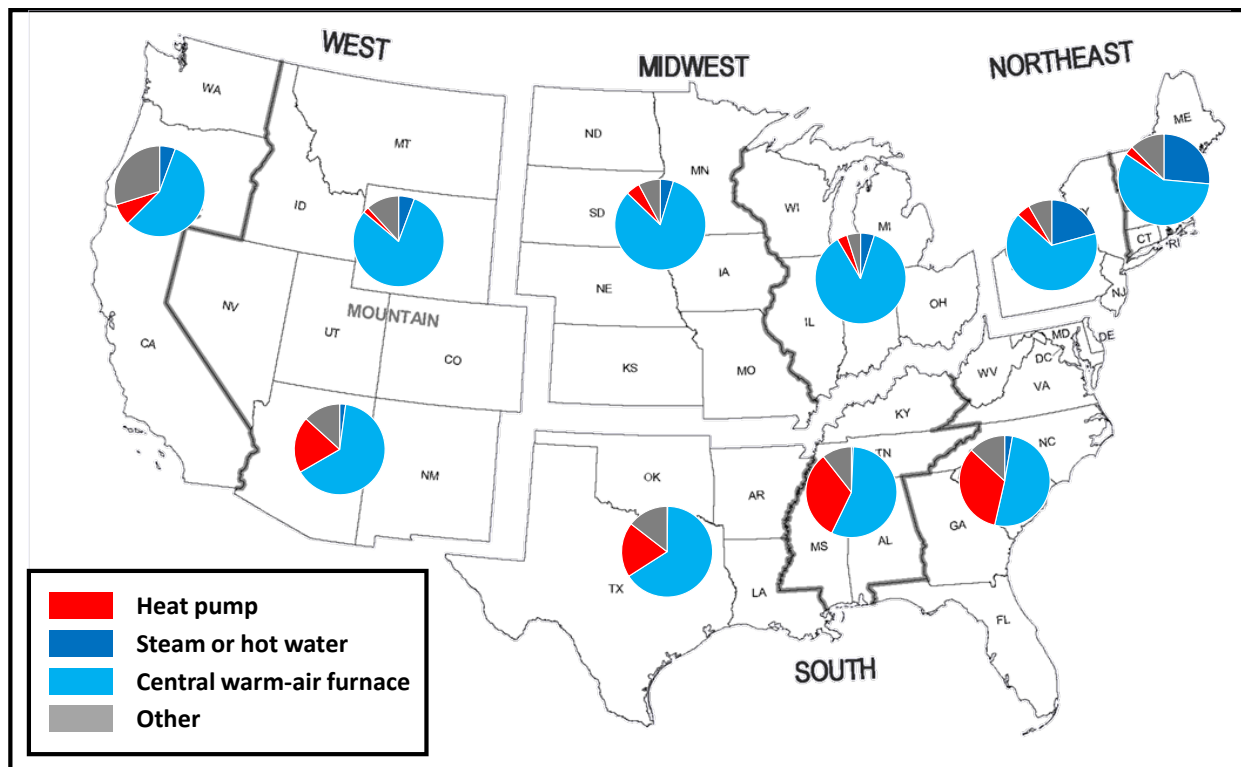


Figure 1. Residential heat pump market penetration in the United States (EIA 2020).

Inverter-driven compressor technology was developed in the 1970s and 1980s for mini-split heat pumps (MSHPs) and nowadays nearly all MSHPs on the market incorporate an inverter-driven compressor. An inverter modulates the compressor speed, allowing the heat pump to dynamically adjust the heating and cooling capacity to better match the building load. Inverter-driven heat pumps are more efficient at part-loads and offer improved cold-climate performance because the system increases the compressor speed at low outdoor temperatures. Inverter-driven compressors are commonly also referred to as variable-speed and variable-capacity.

Many researchers have field validated single-zone ductless MSHPs, which are typically used to displace a home's existing heating system in cold climates (CADMUS 2016; CADMUS 2017; Larson et al. 2013). The majority of MSHPs provide point-source heating and cooling, eliminating the need for an air distribution system and making MSHPs an attractive solution in homes lacking ductwork such as those with hydronic or electric baseboard heating. However, two-thirds of U.S. homes utilize a central, forced air heating system to distribute warm air throughout the home, which is reflected in the proportion of homes that utilize a central warm-air furnace shown in Figure 1. Though MSHPs are not limited to ductless configurations, the compact-ducted MSHP air handlers do not typically have the heating capacity necessary to condition an entire U.S. home. Multi-split heat pumps (MSHPs with more than one indoor unit) condition multiple rooms within a home and are available in larger capacities than those of single-zone MSHPs.

In the mid-2000s, central heat pump systems with variable-speed compressors were introduced to the market. Fixed capacity and two-stage central heat pump systems continue to dominate sales; however, manufacturers continue to routinely introduce variable-speed models to the market (Salmonsén 2018). Variable-speed, central heat pumps were initially offered by top brands at the highest efficiency levels; however, central heat pumps with variable-speed compressors are now offered by nearly every brand at a range of efficiencies. Despite the availability of inverter-driven, central heat pump systems, questions remain regarding in-field performance when installed in cold climates.

In fall 2018, the National Renewable Energy Laboratory (NREL) and Brookhaven National Laboratory (BNL) embarked on a U.S. Department of Energy (DOE) funded study to measure in-field performance of both MSHPs and centrally ducted variable-speed heat pumps in cold climates. NREL and BNL collaborated to develop a common field test protocol to guide the two independent, yet coordinated, studies. Monitoring equipment installation started in February 2021 and was completed by the following September. Because the focus of the study was heating performance, data was collected for at least one full winter and concluded in summer 2022. The NREL study focused exclusively on centrally ducted heat pumps. Specific monitoring equipment installation dates and system types are listed for each site in Section 2.

1.1 Project Overview and Objective

The primary objective of this project was to measure in-field performance of centrally ducted, variable-capacity air-source heat pumps in cold climates to validate performance and develop field-based performance maps. The project focused on quantifying heat pump performance at cold temperatures.

We fulfilled the project objective by monitoring 13 central heat pump systems installed in single-family detached residential buildings located in a cold climate for at least one full winter season. This report describes the house characteristics and heat pump specifications (Section 2), field monitoring and data analysis methodologies (Sections 3 and 4, respectively), and heating and cooling measured field performance (Sections 5 and 6, respectively).

1.2 Key Research Questions

The project's key research questions are broken down into five key areas, listed below. The research questions focus on heating mode performance with interest specifically at cold temperatures.

1. Heat Pump Installed Capacity and Efficiency (Section 5.3)
 - a. What is the measured heating capacity and efficiency of installed, central, variable-capacity heat pump systems, specifically at cold temperatures?
 - b. How does the measured performance in the field compare to the expected performance?
2. Auxiliary Heat Use (Section 5.4)
 - a. How much energy is consumed by the electric resistance auxiliary heater?
 - b. How often does the auxiliary heat turn on and what factors determine usage, such as outdoor air temperature or defrost mode?
3. Variable-Capacity Modulation and Heat Pump Sizing (Section 5.5)
 - a. How does the cycling rate and runtime of the variable-capacity heat pumps depend on outdoor air temperature?
 - b. What fraction of the home's heating load is satisfied by compressor-based heating at cold temperatures?
4. Defrost Mode Energy (Section 5.6)
 - a. How much energy is consumed by the heat pump while in defrost mode?
 - b. How often do defrost cycles occur, what is the duration, and how does the frequency and duration depend on outdoor air temperature?
5. Supply Air Temperature (Section 5.7)
 - a. What is the heat pump supply air temperature when using compressor-based heating at various outdoor air temperatures?

1.3 Approach Overview

The sites identified for the study were primarily located in the northwest United States because homes in the region tend to have all-electric space heating systems, and high-efficiency heat pumps have been incentivized for several years. NREL partnered with Ecotope, Inc., a small energy consulting firm located in Seattle, for site recruitment, monitoring equipment installation, and data quality management. All the sites included in the study had previously installed a high-efficiency, central heat pump system.

We used airside and power measurements to quantify heat pump capacity, coefficient of performance (COP), and auxiliary heater energy consumption. Two independent, standalone data loggers were used at each site—one located within proximity of the heat pump outdoor unit (ODU) and the other close to indoor unit (IDU). This approach minimized time on site by reducing the need to run wires, and data was combined during post-processing. The ODU data

logger included a weather station to monitor outdoor air dry-bulb temperature and relative humidity.

During the initial site visit, Ecotope correlated the IDU airflow rate to the blower power consumption by temporary installing an air handler flow plate or duct blaster to measure the indoor airflow at a range of blower speeds. Blower power was measured throughout the study to estimate the indoor airflow rate during the long-term monitoring. A whole-house thermal and duct audit was also completed during the initial site visit to assess the winter heating loads and heat pump sizing. A full description of the approach can be found in Section 3.

2 Site Characteristics and Heat Pump Information

2.1 Site Locations

We monitored 13 central heat pump systems for this study. Twelve of the sites were in the northwestern United States (Washington and Montana) and one site was located close to NREL in Colorado. Table 1 summarizes the site location details including the site heating degree days (HDD₆₅) (ASHRAE 2017), elevation, which is important for data processing, and monitoring equipment installation date.

Table 1. Heat Pump Site Information

Site ID	Location	HDD ₆₅	Elevation (ft)	Monitoring Install Date
1	Paterson, WA	5,097	380	2/1/2021
2	Prosser, WA	4,936	666	2/2/2021
3	Broomfield, CO	5,667	5,597	12/14/2020
4	Benton City, WA	4,936	499	2/3/2021
5	Nine Mile Falls, WA	6,130	1,648	2/11/2021
6	Spokane Valley, WA	6,130	2,002	2/24/2021
7	S. Spokane, WA	6,130	1,876	2/23/2021
8	Valleyford, WA	6,627	2,487	3/22/2021
9	Cheney, WA	6,776	2,352	3/25/2021
10	Hamilton, MT	7,372	3,570	6/23/2021
11	Spokane, WA	6,627	1,843	7/6/2021
12	Spokane, WA	6,627	1,843	7/8/2021
13	Glenwood, WA	5,898	1,900	9/15/2021

Figure 2 shows the Northwest site locations and the International Energy Conservation Code (IECC) climate zone map for reference (PNNL 2022). All the sites in Washington and Colorado were in IECC Climate Zone 5, which has a similar climate to Connecticut, Massachusetts, and southern Vermont. Site 10, which was in Montana, is in IECC Climate Zone 6. Sites 1, 2, and 4 were in southern Washington, east of the Cascades, while Sites 5–9, 11, and 12 were near Spokane in northern Washington. Site 13 was close to Mount Adams (located at ~2,000 ft above sea level). Sites 1–4 were selected to be close to NREL and Ecotope office locations to minimize travel during the COVID-19 pandemic.



Figure 2. (a) Northwest site locations and (b) IECC climate zone map.

2.2 Site Issues and Resolutions

2.2.1 Heat Pump Installation Issues

Site 2: Site 2 was instrumented in February 2021. We quickly observed that there were lengthy time periods in which the compressor would not run, and the system would exclusively use auxiliary heat to condition the building. Ecotope revisited the site in March 2021 with a manufacturer service technician to resolve the issue. System performance did subsequently improve; however, as Section 5 will show, Site 2 often used the auxiliary heater to heat the home.

Site 4: While Ecotope field researchers were measuring the indoor airflow rate during the initial site visit, the blower failed to operate at more than one airflow rate. At that time, the building occupant mentioned the system did not modulate as expected. Ecotope contacted a manufacturer service technician and the IDU control board was replaced during a service call in March 2021. Ecotope revisited the site to collect a set of airflow measurements, which were used for the data analysis.

Site 7: Site 7 instrumentation was installed in late February 2021. Despite having a limited amount of heating data, we concluded the heating COP at Site 7 was lower than expected and the system was using too much auxiliary heat. Ecotope and the homeowner engaged with the service technician, who reluctantly admitted there was a performance issue due to undersized return ductwork. The return plenum was reconstructed in June 2021 and Ecotope remeasured the blower airflow rates for the airflow rate correlation. Following the repair, the capacity increased and modulation improved; however, as Section 5 will show, the COP was still lower than expected.

2.2.2 Data Logging Issues

Site 3: The ODU power measurement enclosure leaked during summer 2021 and was replaced a few months later. Thus, we lost a few months of summer data.

Site 9: Site 9 was in a rural location without a reliable cell phone signal. We routinely made connections to the indoor logger to download the data but could not resolve connection issues to the outdoor logger despite relocating the antenna and adding a diversity antenna to the cell

modem. All the data loggers included a back-up memory module. However, after a site visit in October 2021 to manually download the data, the backup memory module failed to record future readings, resulting in significant data loss. Because only a complete set of IDU data was obtained, Site 9 is not included in this report.

Site 12: Site 12 was also in a rural location without a reliable cell phone signal and there were random errors with writing data to the backup memory module. Thus, the data set for Site 12 is not as extensive as other sites in the study.

Site 13: The ODU inverter frequency measurement at Site 13 failed early during the monitoring period and was not fixed. However, all other measurements reliably collected data, allowing us to determine the heat pump's capacity and COP.

2.3 Weather Data During Monitoring

Because the study was primarily focused on quantifying cold temperature performance, it is useful to compare the measured temperature data to typical weather for each site. One approach is to count the hours of data at or below the heating design temperatures. Table 2 lists the 99% and 99.6% ASHRAE heating design temperatures for each site and the number of hours below the corresponding temperature. The 99% heating design temperature is defined as the outdoor temperature that a given location stays above for 99% of the hours in a year using a 30-year average (ASHRAE 2017). Accordingly, the outdoor temperature at a location would be colder than the 99% heating design temperature for approximately 88 hours per year (on average). Based on this metric, Sites 2, 4, 8, 10, 12, and 13 had warmer than average temperatures during the monitoring period. The data logging issue for Site 12 explains the relatively few hours of cold temperature data.

As some sites were monitored for more than a single winter, we include the number of hours during the entire monitoring period as well as during winter 2021–2022. It is useful to have a consistent monitoring period across all sites when comparing performance for some metrics, such as auxiliary heat energy, which is why we included two different hour counts in Table 2. However, with exception of Site 3, there were very few hours with cold temperatures prior to winter 2021–2022.

Figure 3 plots outdoor temperature histograms for the entire monitoring periods for each site.

Table 2. Number of Hours with Cold Temperatures

Site ID	Design Temperature [°F]		Number Hours Colder than the Design Temperature			
			Entire Monitoring Period		Winter 2021–2022	
	99%	99.6%	99%	99.6%	99%	99.6%
1	18.3	11.7	98	22.4	86.5	22.4
2	15.6	7.4	79.8	3.7	76.7	3.7
3	5.1	-1.4	134.1	46.6	71.6	15.3
4	15.6	7.4	69.8	8.4	69.2	8.4
5	13.8	7.6	144.3	10.8	133	10.8
6	13.8	7.6	130.3	13.3	130.3	13.3
7	13.8	7.6	137.5	21.9	137.5	21.9
8	11	4.7	51.8	3.3	51.8	3.3
10	3.1	-3.8	48.3	13	48.3	13
11	11	4.7	106.8	6.2	106.8	6.2
12	11	4.7	8	0	8	0
13	13.7	7.8	26.9	6.5	26.9	6.5

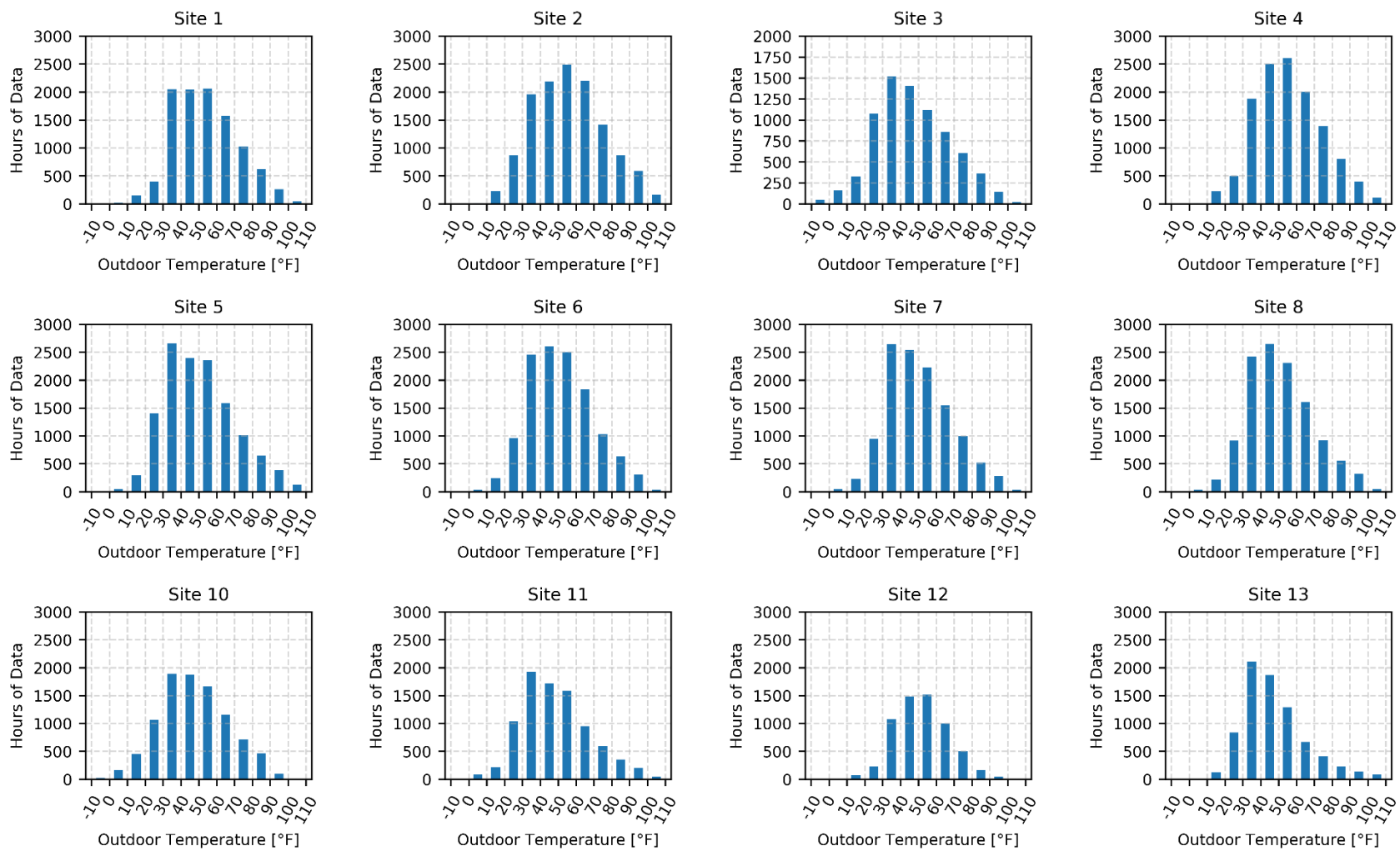


Figure 3. Outdoor temperature histograms for the monitoring period for each site.

2.4 Site Characteristics

A whole-house thermal and duct audit was completed for all the northwest U.S. sites during the initial site visit to calculate the design heating load. The following parameters were assessed:

- Exterior and interzonal wall surface area and insulation R-value
- Ceiling surface area and insulation R-value
- Foundation type, surface area, and insulation R-value
- Glazing surface area and U-value
- Whole-house air changes per hour (ACH) at 50 Pascals depressurization
- Distribution system efficiency (DSE) calculation inputs, such duct surface area, insulation R-value, and air leakage.

The design heating load was calculated for each site using procedures based on Air Conditioning Contractors of America Manual J (ACCA 2016). However, we assumed an indoor temperature of 65°F rather than the Manual J assumption of 70°F to account for internal gains and building thermal mass. Table 3 lists the whole-house total heat transfer coefficient, distribution system efficiency, and design heating loads assuming a 99% heating design temperature. A distribution system efficiency of 100% indicates the home's ductwork was located within the thermal envelope. Sites 5, 8, and 13 had notably poor ductwork resulting in high heating design loads.

The whole-home design heating load was calculated using the whole-house total heat transfer coefficient (UA_{wh}), the distribution system efficiency (DSE), and the 99% heating design temperature (T_{design}) based on the following equation.

$$\dot{Q}_{design,htg} = \frac{UA_{wh}}{DSE} * (65 - T_{design}) \quad (1)$$

where

$$UA_{wh} = UA_{env} + \left(\frac{ACH_{50}}{20}\right) V_{house} \left(\frac{1.1}{60}\right) \quad (2)$$

where UA_{env} is the overall heat transfer coefficient of the thermal enclosure, ACH_{50} is single-point, whole-house ACH measured at 50 Pascal depressurization converted to an estimated natural ACH¹, and V_{house} is the house interior volume.

2.5 Heat Pump Specifications and Settings

Table 4 lists the heat pump product data and specifications for each site. All systems were variable-capacity systems except for Site 12, which was a two-stage system. Additionally, all sites were fully electric except for Site 3, which had a dual fuel system with a natural gas furnace for backup heating.

¹ <http://www.homeenergy.org/show/article/nav/blowerdoor/id/1015>

The nominal heating and cooling capacities, heating seasonal performance factors (HSPFs), and seasonal energy efficiency ratios (SEERs) were sourced from the Air-Conditioning, Heating, and Refrigeration Institute (AHRI) Directory of Certified Products (AHRI 2022).

The Northeast Energy Efficiency Partnerships (NEEP) developed and published a cold-climate air-source heat pump specification and maintains a product listing of manufacturer-submitted data for heat pumps that meet the specification (NEEP 2021). The product list is popular in the industry and is often used by utility programs to define rebate requirements. Nine of the 13 monitored heat pumps are currently listed as meeting the specification. For ducted heat pump systems, the NEEP Cold-Climate Air-Source Heat Pump Specification Version 3.1 requirements include the following:

- $HSPF \geq 9.0$
- $COP \geq 1.75$ at 5°F
- $SEER \geq 15.0$
- Reporting of capacity and COP at minimum, rated, and maximum speeds at 47°F, 17°F, and 5°F.

Version 4, which requires performance based on HSPF2 and SEER2, became effective starting January 1, 2023 (NEEP 2022).

NEEP requires manufacturers to report heat pump capacity and COP at 5°F whereas the AHRI Directory of Certified Products only reports the capacity at 17°F, which is the coldest temperature required during the ratings test. The updated heat pump DOE test procedure (Appendix M1) now allows for an optional cold temperature test to be conducted at 5°F (10 CFR Part 430 2022, AHRI 2020). The DOE Cold Climate Heat Pump Challenge allows for an optional test condition of -15°F (DOE 2021).

Table 4 lists the manufacturer-reported maximum capacity at 5°F; however, the data source of the maximum capacity varied across the sites. The manufacturer-reported data in the NEEP heat pump list was used for systems included in the product listing. Otherwise, manufacturer expanded performance table data was used. The coldest outdoor temperature listed in expanded performance table data for Sites 3 and 6 was 7°F, which is noted in Table 4 with italicized text. The heating capacity retention at cold temperatures can be assessed by comparing the nominal heating capacity, which is measured at an outdoor temperature of 47°F, to the maximum heating capacity at 5°F. The capacity retention ranged from 48% to 68% for the sites with data at 5°F.

Table 4 also lists the minimum heating capacity at 47°F for the variable-capacity systems, which was sourced from the NEEP product list or manufacturer expanded performance tables. The equipment's turndown ratio can be assessed by comparing the nominal heating capacity at 47°F to the minimum heating capacity, which varied from 0.2 (Site 3) to 0.7 (Site 11).

All the systems installed at the northwestern U.S. locations utilized a draw-through blower configuration, meaning the blower was downstream of the indoor heat pump coil. The dual fuel system at Site 3 used a blow-through configuration because the indoor coil was installed downstream of the furnace.

Table 5 lists information regarding the heat pump installation, operation, and auxiliary heat. The compressor lockout temperature is defined as the minimum outdoor temperature at which the compressor operates that can be specified using the system's communicating thermostat. Most systems have a hard-coded compressor lockout temperature at a colder temperature to protect the equipment. The auxiliary heat lockout temperature is defined as the maximum outdoor temperature at which the auxiliary heat source operates. When the outdoor temperature is above the compressor lockout temperature and below the auxiliary lockout temperature, the compressor and electric resistance auxiliary heater should be allowed to operate simultaneously. The heating setpoints were self-reported by the building occupants at the onset of the study and collected via the occupant survey included in Appendix A.

As previously noted, all systems included an auxiliary electric resistance heater except for Site 3, which had a natural gas backup furnace. The electric resistance auxiliary heating elements were wired using multiple stages and included a lockout temperature above which the auxiliary heater should not operate.

All variable-speed heat pumps, except for the heat pump at Site 10, used manufacturer-specific, communicating thermostats. A communicating heat pump system utilizes a proprietary serial communication protocol to send operational and performance data to all the components (thermostat, IDU, and ODU) in the system. In a noncommunicating system, the thermostat energizes a set of individual wires to control the heat pump. Most variable-speed heat pumps utilize communicating thermostats to control the compressor and blower speeds.

Table 3. House Characteristics, Site Design Temperatures, and House Design Heating Loads for the Northwestern Sites

Site ^a	Conditioned Floor Area [ft ²]	ACH ₅₀ ^b	Total Heat Transfer Coeff. (UA) [kBtu/h-°F]		Distribution System Efficiency ^e	Design Temperature [°F]		Design Heating Load [kBtu/h] ^f
			Envelope ^c	Whole-house ^d		99%	99.6%	
1	3,800	4.5	497	637	91%	18.3	11.7	32.7
2	1,750	4.4	523	600	81%	15.6	7.4	36.6
4	3,600	4.2	480	579	77%	15.6	7.4	37.1
5	3,600	6.9	464	601	58%	13.8	7.6	53.1
6	3,325	5.1	628	754	100%	13.8	7.6	38.6
7	2,340	9.9	595	736	100%	13.8	7.6	37.7
8	3,300	6.2	576	824	53%	11	4.7	84.0
9	3,000	4.2	419	496	100%	11.7	6.8	26.4
10	1,240	10.6	377	481	76%	3.1	-3.8	39.2
11	3,020	6.2	468	604	73%	11	4.7	44.7
12	3,600	3.2	483	568	100%	11	4.7	30.7
13	1,940	8.8	390	513	57%	13.7	7.8	46.2

^a Thermal audit was completed at all sites except for Site 3.

^b ACH measured using a blower door whole-house depressurization test at 50 Pascals.

^c Total heat transfer coefficient for walls, floors, ceilings, and windows.

^d Whole-house total heat transfer coefficient accounting for natural infiltration.

^e Distribution system efficiency determined using methodology specified in ASHRAE Standard 152.

^f Design heating load calculated using the 99% design temperature and indoor temperature of 65°F.

Table 4. Heat Pump Product Data and Specifications

Site	NEEP Listed ^a	HSPF ^b [Btu/W]	SEER ^b [Btu/W]	Nominal Capacity ^b		Heating Capacity		Heating COP	
				Heating [kBtu/h]	Cooling [kBtu/h]	Maximum @ 5°F [kBtu/h]	Minimum@ 47°F [kBtu/h]	Maximum Speed @ 5°F	Minimum Speed @ 47°F
1	Yes	11	19	56	58.5	30.5	16.9	2.2	5.0
2	Yes	9.6	19	45	48	22	18.3	2.0	4.5
3	No	8.5	15.5	33	32.6	16.5 ^c	6.7	1.7 ^c	2.3
4	Yes	9.6	19.5	46.5	46.5	26.8	18.8	2.0	4.6
5	Yes	10	20	33	34.8	18.6	9.4	2.2	3.9
6	No	11	18	46	46	22.1 ^c	15.9	2.3 ^c	4.9
7	Yes	11	22	46	46	31.1	12	2.3	4.5
8	Yes	10	19.3	42.5	47	28.4	12.1	1.8	4.7
9	Yes	9.8	19.5	35.2	35.2	22.1	13.4	1.9	4.9
10	Yes	10	19	34.4	34.8	20.2	16.5	2.3	4.8
11	No	10	19	44.5	45	25.6 ^d	32.1	2.7	4.7
12	No	9	16	46.5	47.5	22.4 ^d	N/A	2.6	N/A
13	Yes	10.4	16.5	39	36	25.9	11.8	2.3	3.2

^a Based on whether an exact outdoor and indoor unit match was found in NEEP's Cold Climate Air Source Heat Pump List.

^b Listed values based on information attained from the AHRI Directory of Certified Product Performance.

^c Values based on expanded performance table data at 7°F outdoor air temperature, which was the minimum temperature included.

^d Values based on expanded performance table data since the equipment was not included in NEEP's Cold Climate Air Source Heat Pump List.

Table 5. Heat Pump Installation and Operation Information and Auxiliary Heat Specifications

Site	Heat Pump Install Date	IDU Location	Compressor Lockout ^a	Auxiliary Heat Specifications			Number of Zones	Heating Setpoints [°F]	
				Capacity	Stages	Lockout ^b		Occupied	Setback
1	3/31/2019	Living Zone	Disabled	15 kW	3	35°F	3	73	70
2	7/20/2019	Garage	Disabled	20 kW	4	25°F	1	71	66
3	9/11/2020	Attic	~5°F	90 kBtu/h ^c	2	~25°F	1	68	68
4	4/23/2019	Attic	N/A	15 kW	3	N/A	2	N/A	N/A
5	3/18/2019	Crawlspace	5°F	20 kW	4	35°F	1	70	66
6	4/1/2016	Basement	6°F	15 kW	1	35°F	1	68	62
7	2/15/2021	Crawlspace	0°F	20 kW	4	40°F	1	70	67
8	6/24/2019	Garage	5°F	20 kW	3	35°F	1	70	65
9	3/27/2019	Basement	15°F	15 kW	N/A	35°F	1	69	69
10	10/30/2018	Crawlspace	Disabled	10 kW	2	30°F	1	70	68
11	11/1/2018	Living Zone	N/A	20 kW	2	N/A	1	72	68
12	3/1/2018	Basement	5°F	9 kW	N/A	35°F	1	73	67
13	8/17/2021	Garage	Disabled	10 kW	2	20°F	1	70	67

^a Compressor lockout temperature defined as the minimum outdoor temperature at which the compressor operates that can specified using the thermostat.

^b Auxiliary heat lockout temperature defined as the maximum outdoor temperature at which the auxiliary heat source operates.

^c Site 3 included a dual-fuel heat pump with a two-stage natural gas furnace with the capacity specified in kBtu/h.

2.6 House Heating Loads and Heat Pump Sizing

Figure 4 plots the house heating loads (blue lines) using the total heat transfer coefficients and distribution system efficiencies from Table 3 along with the manufacturer-provided maximum and minimum heating capacities (red solid and dashed lines, respectively). Site 3 is not shown in Figure 4 because a thermal audit at this site was not completed. The house heating loads, calculated using Equation 1, are shown for the 99.6% and 99% heating design temperatures for each site. The heating load was assumed to equal zero at an outdoor temperature of 65°F. The maximum and minimum heat pump capacities are plotted using manufacturer data at 5°F, 17°F, and 47°F, which tends to neglect capacity loss due to defrost cycles. Table 6 lists the estimated heat pump maximum capacity using manufacturer data at the 99% design temperature and calculates the percent of under- or oversizing by dividing the estimated heat pump capacity by the building's heating load. Thus, an undersized system has a value less than 100%.

Comparing the heating load and heating capacity lines indicates the amount the heat pump is either under- or oversized for the house. The heat pumps installed at Sites 5 and 8 are clearly very undersized for the house, given that the heat pump is expected to satisfy less than 40% of the heating load at the design temperature. Sites with undersized heat pumps have high balance point temperatures, which is the temperature at which the heating load and maximum capacity lines intersect. Presumably, at temperatures colder than the balance point, auxiliary heat is required to satisfy the building heating load. The heat pumps at Sites 10, 11, and 13 also appear to be undersized. The auxiliary heat usage, analyzed in Section 5, is a good indicator of undersizing.

The temperature at which the minimum capacity and heating load lines intersect is used to estimate when the equipment will have to cycle on and off to meet load because the heat pump has reached the minimum turndown. For example, the heat pump at Site 6 should be capable of modulating the compressor to run continuously at temperatures below ~47°F. However, because the heating loads lines do not account for solar and internal gains and thermostat temperature setback schedules, the equipment will likely cycle at cooler temperatures than indicated in Figure 4.

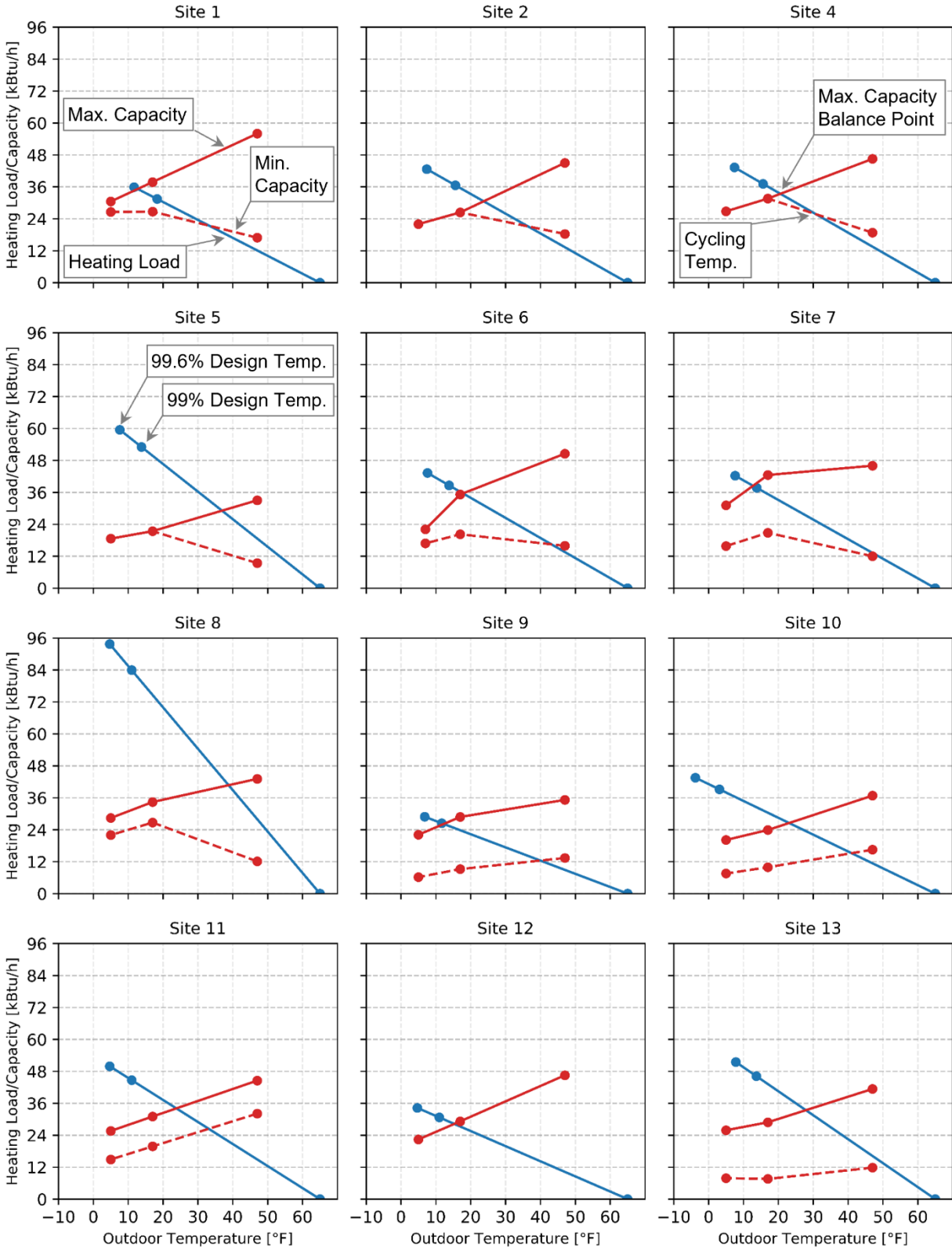


Figure 4. House heating load lines (blue) and manufacturer-reported maximum and minimum heating capacities (red solid and dashed lines, respectively).

Table 6. Heat Pump Sizing and Site Balance Temperatures

Site	99% Design Temperature [°F]	Design Heating Load [kBtu/h]	Maximum Capacity at 99% Design Temperature [kBtu/h]	Maximum Capacity/Design Load [%]	Balance Point Temperature [°F]
1	18.3	32.7	38.6	118%	13.8
2	15.6	36.6	25.9	71%	23.7
4	15.6	37.1	31.0	84%	20.6
5	13.8	53.1	20.7	39%	36.9
6	13.8	38.6	31.7	82%	17.8
7	13.8	37.7	39.5	105%	12.7
8	11	84.0	31.4	37%	38.8
9	11.7	26.4	25.8	98%	12.3
10	3.1	39.2	19.6	50%	23.1
11	11	44.7	28.3	63%	23.8
12	11	30.7	25.8	84%	15.3
13	13.7	46.2	28.0	61%	27.9

3 Field Monitoring Methodology

3.1 Field Protocol

In 2020, BNL, NREL, DOE, Oak Ridge National Laboratory, and the project subcontractors collaborated to develop a field protocol that dictated the data collection and instrumentation plan (BNL 2020). The field protocol described all the key aspects of the study—house thermal audit data collection, heating and cooling equipment information and product data, site photos, blower airflow correlation testing, data logging and measurement locations, and the commissioning process. The detailed field protocol was used to develop a series of data entry forms for subcontractors to use in the field, which can be found in Appendix A.

The field protocol was designed to answer the project’s key research questions while ensuring consistency between the NREL and BNL approaches. Air-side temperature and humidity measurements were taken to calculate heat pump capacity and COP, which relied on an airflow rate correlation developed using data collected while the field technician was onsite installing the instrumentation. The airflow rate correlation, which is further described in Section 3.3, was used in data processing to calculate the real-time indoor airflow rate as a function of the measured blower power.

The field protocol allowed for flexibility to adapt to the real-world conditions encountered by the field technician while installing the instrumentation. Most of the refrigerant-side measurements specified in the protocol were disregarded as installation was overly invasive to the equipment while in the field. However, as described in Section 4, the vapor line surface temperature measurement was critical for determining heat pump operating mode.

3.2 Data Acquisition

As mentioned in Section 1, all homes in this study utilized a centrally ducted heat pump for space conditioning. Two independent, standalone data loggers were used at each site—one located within proximity of the heat pump ODU and the other close to IDU. This approach was chosen to minimize the time spent on site, and the data collected from the ODU and IDU loggers was combined during post-processing. Each data logger was paired with a cell modem to facilitate remote downloading and a backup memory module in case of communication issues.

Figure 5 shows a schematic of the key measurements on the IDU and ODU. Three thermocouples were installed in the supply air stream to assess the temperature distribution in the supply duct, which could affect the capacity calculation. Supply and return temperature and relative humidity (RH) sensors were installed to calculate the latent cooling capacity and air density. The IDU total electrical power measurement was used to determine the auxiliary heat usage while the blower electrical power measurement was used in the airflow rate correlation. The inverter frequency, which is directly proportional to the compressor speed, was measured by placing a current transformer (CT) on one of the wires exiting the ODU inverter and connecting that directly to the pulse count channel of the data logger.

Table 7 lists the specific sensors corresponding to the measurements in Figure 5.

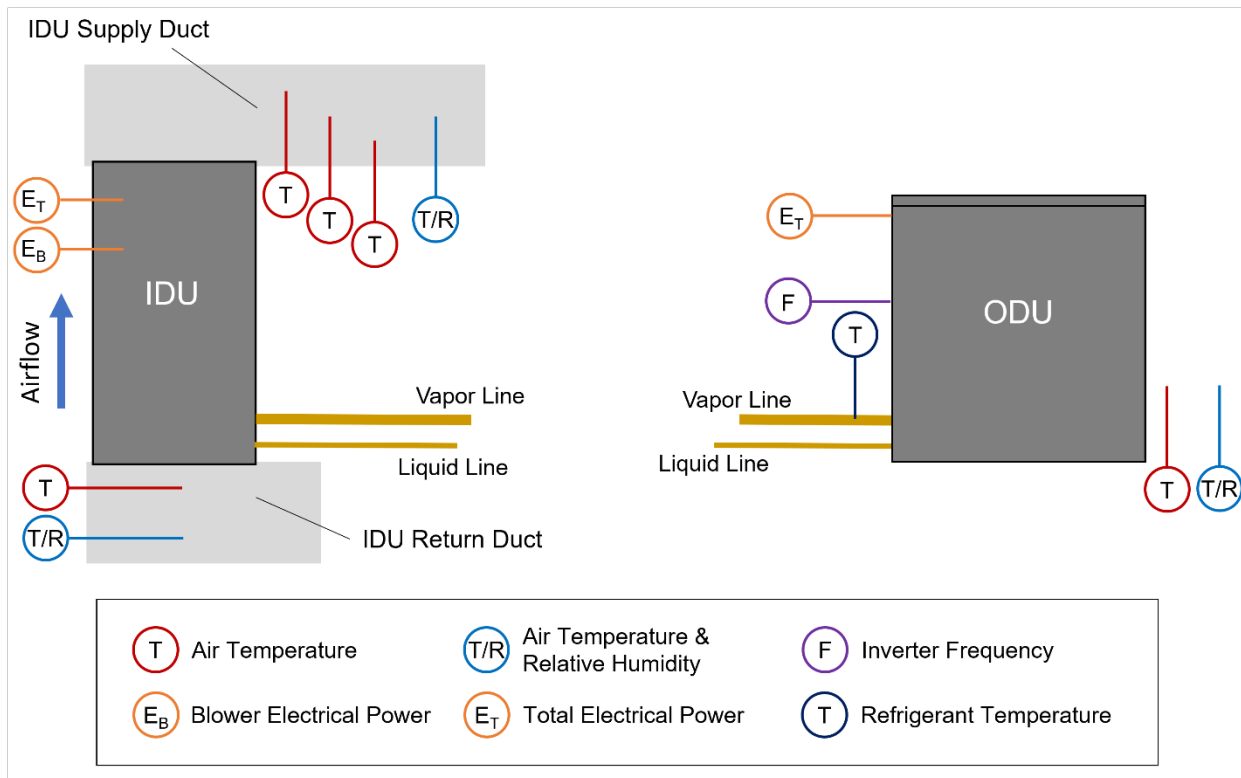


Figure 5. Schematic depicting key measurements on the IDU and ODU used to meet project objectives.

Table 7. List of Key Sensor Types

IDU		ODU	
Measurement	Sensor	Measurement	Sensor
Supply air temperature (3)	Type-T thermocouple	Outdoor air temperature (3)	Type-T thermocouple
Supply air temperature and relative humidity	Vaisala HMP110	Outdoor air temperature and relative humidity	Vaisala HMP110
Return air temperature	Type-T thermocouple	Vapor line surface temperature	Type-T thermocouple
Return air temperature and relative humidity	Vaisala HMP110	ODU total energy	WattNode WNB-3D-240-P
IDU total energy	WattNode WNB-3D-240-P	Inverter frequency	Continental Controls ACTL-0750-005 OPT 1V
IDU blower energy	WattNode WNB-3D-240-P		

3.3 Blower Airflow Data and Correlations

A correlation between IDU blower power and indoor airflow rate was used to calculate capacity and COP. During the installation of the indoor monitoring equipment, blower power and indoor airflow rate were measured at four or more blower speeds. The system was set in different operating modes using the thermostat technician checkout function. The airflow rate was

measured using a flow plate with a manufacturer-specified accuracy of $\pm 5\%$ at a minimum of four points, and the corresponding blower power measurement was taken. For Sites 4 and 7, airflow tests were reconduted following system/ductwork repairs and resolution of the blower modulation issue. Figure 6 plots the measured airflow rate versus the measured blower power (points) and the corresponding correlation (dashed line) used for data processing and analysis. The volumetric airflow rate (\dot{V}_{blower}) is proportional to the cubed root of the blower power (\dot{P}_{blower}) based on the fan laws.

$$\dot{V}_{blower} = a * \sqrt[3]{\dot{P}_{blower}} \quad (3)$$

The coefficient a from Equation 3 for each site was determined by fitting the measured fan data, and these are listed in Table 8.

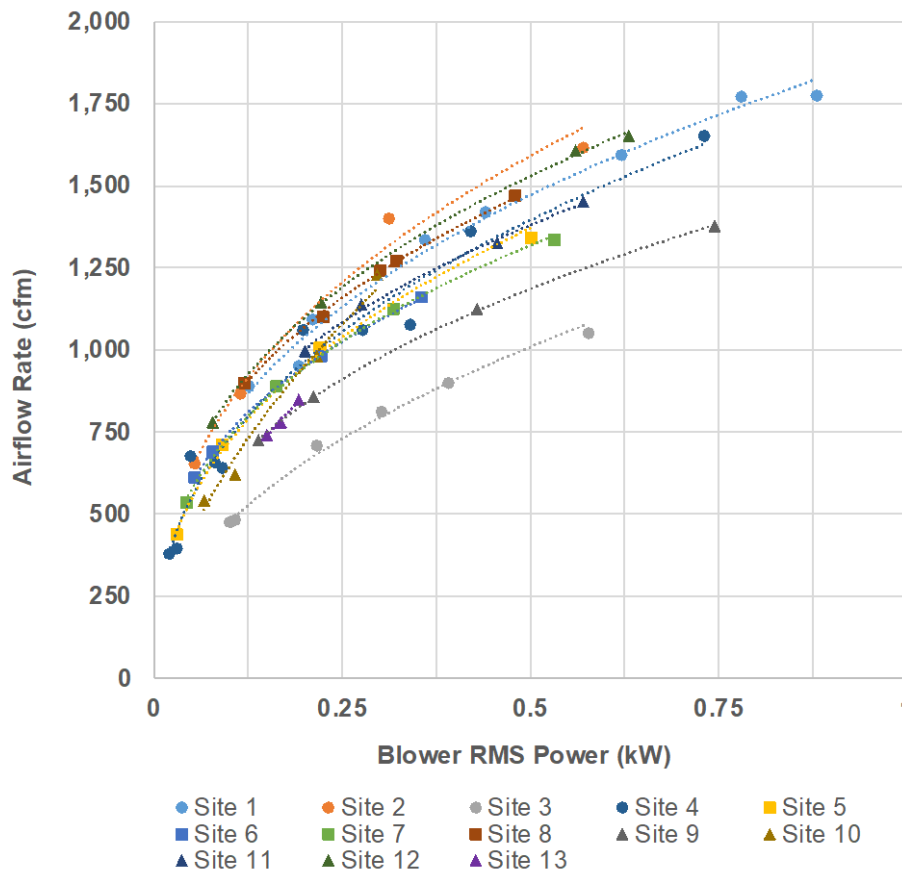


Figure 6. Measured blower airflow rate and power (points) and correlation used for performance calculations (lines).

The Site 3 blower airflow is lower than the other systems because it is located at an elevation of 5,597 feet above sea level, and lower density air results in decreased blower airflow rate. The impact of the site elevation, as listed in Table 1, is accounted for in the air mass flow rate (\dot{m}_{air}) and psychrometric calculations.

Table 8. Coefficients for the Blower Fan Curve

Site	<i>a</i>
1	1851.83
2	1935.90
3	1188.98
4	1696.72
5	1643.87
6	1624.89
7	1439.28
8	1848.41
9	2496.67
10	1608.64
11	1733.14
12	1916.93
13	1426.82

As mentioned above, the indoor airflow rate was measured using a flow plate (Figure 7), with a manufacturer-specified accuracy of $\pm 5\%$, placed in the return filter slot. The system was run in at least three operating modes set using the thermostat.



Figure 7. Flow plate used for IDU airflow measurement.

Figure 8 compares the measured airflow rate values to the manufacturer-reported cooling airflow rates in the AHRI Directory of Certified Products (AHRI 2022), which are reported in standard

cubic feet per minute (SCFM). Even though the field-measured airflow rates and the manufacturer-reported values are measured using different devices, under different operating conditions, and potentially with different control settings, comparing the two sets of values is useful to better understand the COP results presented in Section 5. Maximum measured airflow rates at 8 of the 12 sites (Sites 2, 3, 4, 5, 8, 9, 11, and 12) aligned well with the manufacturer-reported values, which is shown where the error bar, associated with the measured value, overlaps with the reported value. (Error bars are only included for the maximum airflow rate for clarity.) The remaining four sites had lower-than-expected airflow rates which could be due to control settings, operating mode, or restrictive ductwork. We could not find manufacturer-reported airflow rates for Site 13.

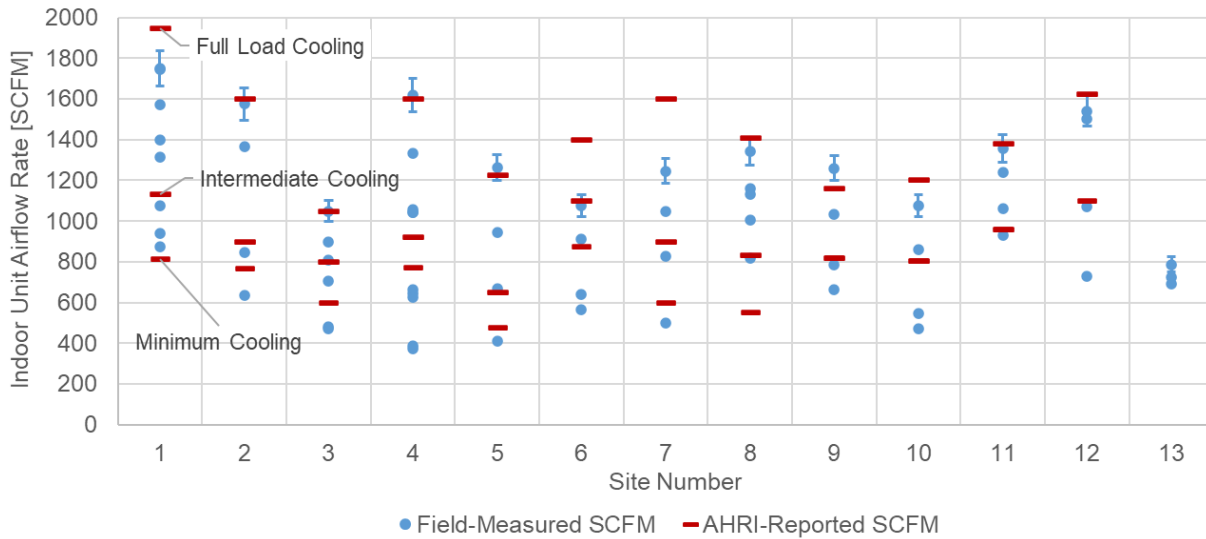


Figure 8. Comparison of field-measured indoor unit airflow rate to manufacturer-reported airflow rates listed in the AHRI Directory of Certified Products.

4 Data Analysis Approach

The overall data processing approach is outlined in Figure 9. Data processing starts with the indoor and outdoor data stream for each site, which can originate from one or more data logger files containing the raw measurements. Based on the field protocol, the measurements are collected at five-second intervals. Appendix A lists the full set of field measurements obtained from the field protocol and Table 9 lists a subset of those parameters that are used to calculate the heat pump performance. The average supply air temperature (T_{sup}) is the mean of the three supply air temperature measurements prescribed in the field protocol.

Table 9. Measurements Used for Data Processing and Calculations

Category	Description	Symbol
Air temperature and humidity	Return dry-bulb temperature	T_{ret}
	Average supply dry-bulb temperature	T_{sup}
	Return relative humidity	RH_{ret}
	Supply relative humidity	RH_{sup}
	Outdoor dry-bulb temperature	T_{out}
Refrigerant temperature	Outdoor coil, cooling mode exit	$T_{ref,vapor\ line}$
Power	IDU power	\dot{P}_{IDU}
	Blower power	\dot{P}_{blower}
	ODU power	\dot{P}_{ODU}
	Compressor inverter frequency	F_{inv}
	Total system power	\dot{P}_{total}

The data was processed using the following key steps:

1. The indoor and outdoor data logger files containing the raw measurements for each site were combined into a single data frame for data processing.
2. Measured supply and return dry-bulb temperatures and relative humidities were used to calculate the moist air properties listed in Table 10 using equations provided in the ASHRAE Handbook of Fundamentals (ASHRAE 2017).
3. The timeseries data was resampled and aggregated into 30-second frequency bins using arithmetic mean for easy data management and more reliable processing.
4. Seven different heat pump operating modes (system off, fan-only, compressor heating, auxiliary heating, compressor + auxiliary heating, defrost, and cooling) were detected by comparing temperature and power measurements with the tolerances (Section 4.1).

5. Periods of steady state operation were automatically determined using a custom steady state detector (Section 4.2). Heat pump start-up periods were also detected.
6. Heat pump indoor mass flow rate, capacity, and COP were calculated for heating and cooling modes (Section 4.3).

Table 10. Calculated Moist Air Properties

Category	Description	Symbol
Return	Humidity ratio	ω_{ret}
	Dry air density	ρ_{ret}
	Enthalpy	h_{ret}
Supply	Humidity ratio	ω_{sup}
	Dry air density	ρ_{sup}
	Specific heat	$C_{p,sup}$
	Enthalpy	h_{sup}

The data processing and calculations were implemented using a series of Python scripts, which were easily applied to each of the heat pump sites included in the study using site-specific inputs such as elevation, blower configuration, blower airflow correlation inputs, and operating mode tolerances. The Python scripts were developed using open-source numerical data processing packages and made available to all project team members through a GitHub repository. Data processing was automated to utilize the collected data efficiently and reliably.

The data was collected and processed for all the sites starting from the monitoring equipment installation date (Table 1) and ending in early August 2022.

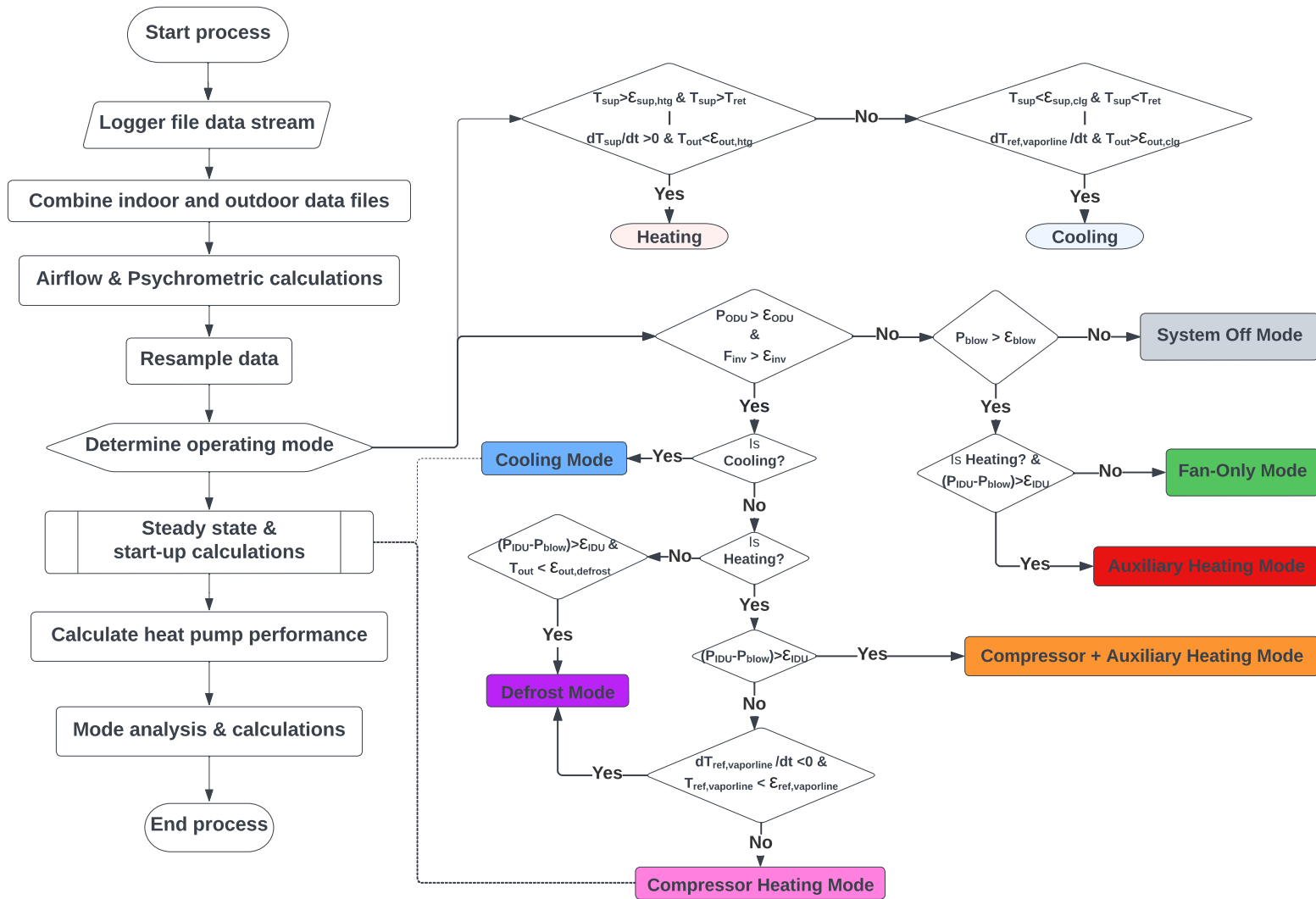


Figure 9. Flow chart outlining the data processing approach along with the decision tree for determining the heat pump operating mode.

4.1 Determining Heat Pump Operating Modes

The heat pump operating mode was automatically detected to process the large amount of data efficiently and reliably. We were able to develop algorithms to automatically detect the following seven modes:

1. System off
2. Fan-only
3. Compressor heating
4. Auxiliary heating
5. Compressor + auxiliary heating
6. Defrost
7. Cooling

The operation mode was more easily determined after the 5-second data was resampled to 30-second intervals. Figure 10 shows different heat pump operational modes detected for Site 1 during a particularly cold winter day in 2021.

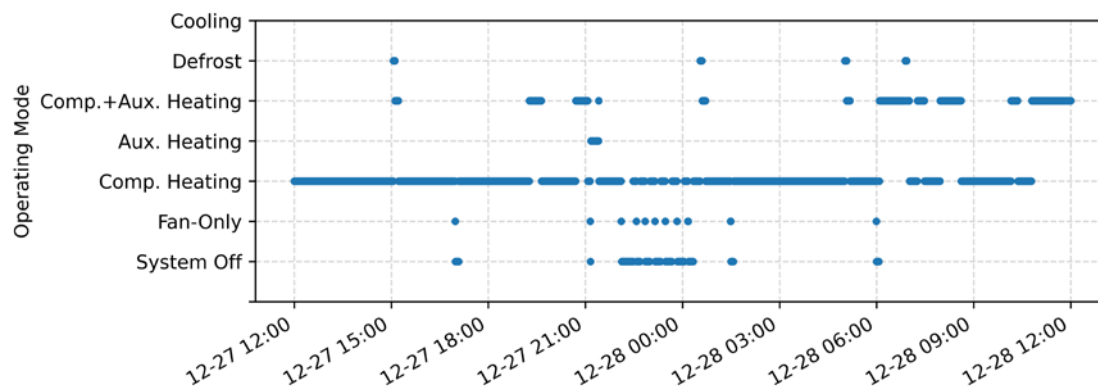


Figure 10. Automatically detected heat pump operation mode during a cold winter period.

In the following sections, different sites and different example periods are presented to demonstrate how the modes were detected automatically based on the equations.

4.1.1 System Off Mode

Detecting when the system is off is necessary to analyze the standby power consumption. The system was considered off when the ODU power (\dot{P}_{ODU}) and compressor inverter frequency (F_{inv}) measurements were less than the respective tolerances ε as shown in Equations 4 and 5:

$$F_{inv} < \varepsilon_{inv} \quad (4)$$

$$\dot{P}_{ODU} < \varepsilon_{ODU} \quad (5)$$

The specific tolerances ε for each measurement were adjusted for each heat pump. Figure 11 and Figure 12 show a snapshot of data for Site 1 from April 2021, displaying cycling and the

algorithm’s detection of when the system was *off* based on the outdoor power and inverter frequency, followed by cycling on in heating mode.

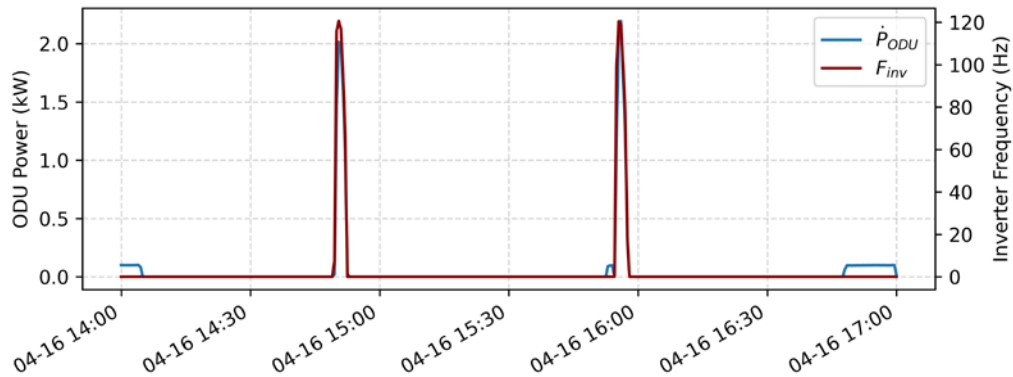


Figure 11. Outdoor power and compressor inverter frequency during a period with cycling.

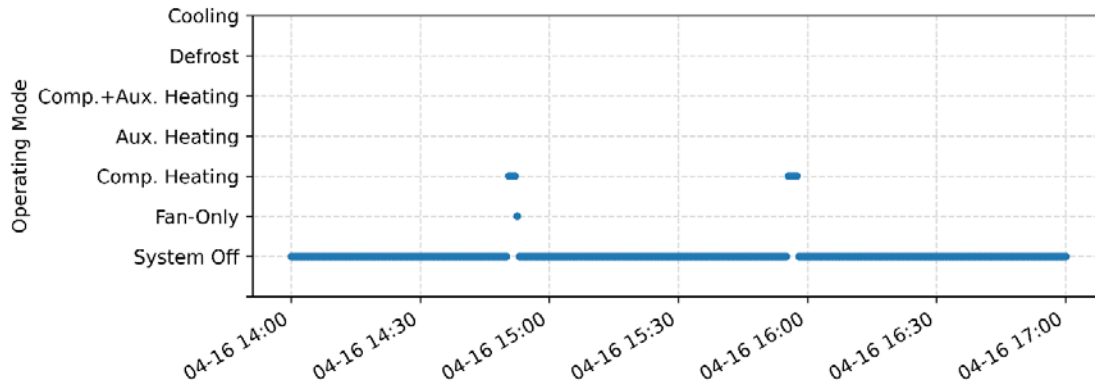


Figure 12. Automatically detected system off operation mode during a period with cycling.

4.1.2 Fan-Only Mode

The system was considered to be in fan-only mode when the compressor was *off* based on Equations 4 and 5 while the indoor blower fan was *on* based on the tolerances on blower power (ϵ_{blower}) from the following equation:

$$\dot{P}_{blower} > \epsilon_{blower} \quad (6)$$

There were several instances at each of the sites where the blower fan was running continuously or briefly turned on prior to the compressor turning on. This can be seen in Figure 13 and Figure 14 for Site 6 on a particularly cold day in November 2021 where the system cycled between off, fan-only, and compressor-based heating mode. The system was operating continuously in fan-only mode from approximately 2:15 p.m. to 10 p.m.

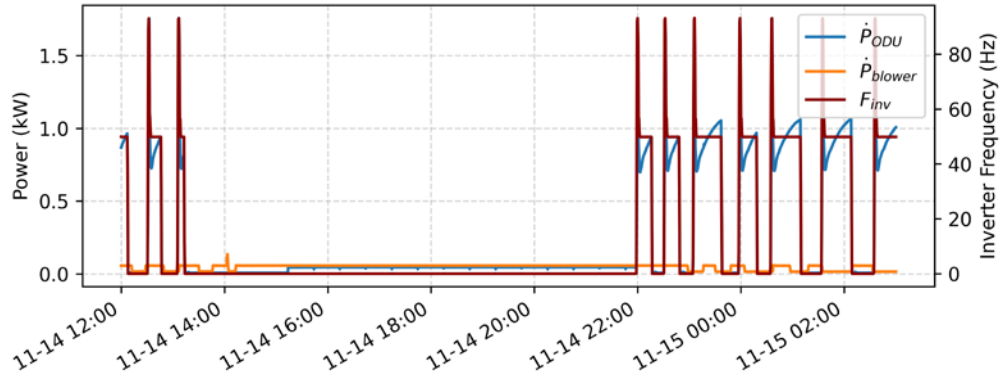


Figure 13. Blower power, outdoor power, and compressor inverter frequency during a period with fan-only operation.

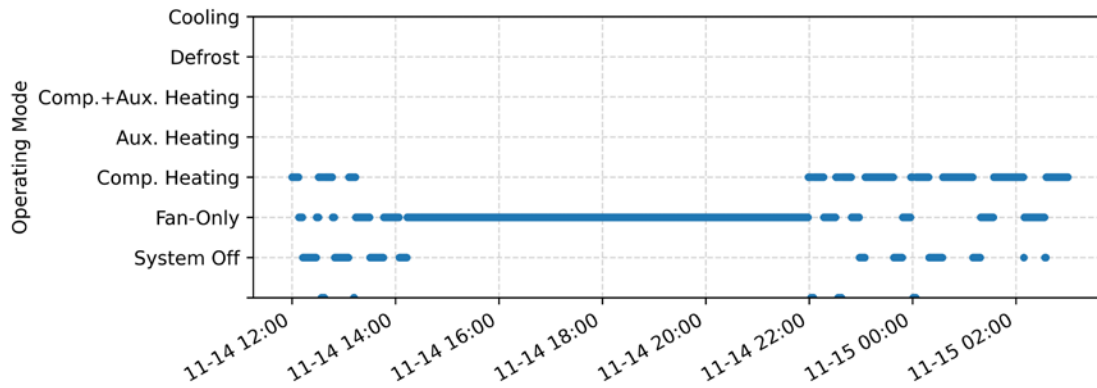


Figure 14. Automatically detected operation mode during an example period with fan-only operation.

4.1.3 Compressor Heating Mode

Heating mode performance was the focus of the study and therefore it is critical to accurately detect when the system is operating in heating mode. Heating mode can easily be detected when the system is *on*, opposite to Equations 4 and 5 and supplying warm air, based on the following equations, where $\varepsilon_{sup,htg}$ was assumed to be 20°C (68°F).

$$T_{sup} > \varepsilon_{sup,htg} \quad (7)$$

$$T_{sup} > T_{ret} \quad (8)$$

However, we are also interested in measuring the cycling performance immediately after the unit cycles on, and Equation 7 and 8 will only detect heating operation if the unit is supplying warm air. We use Equations 9 and 10 to determine if the unit has cycled on in heating mode where the supply air temperature is increasing and when the outdoor temperature is below 15°C (59°F).

$$dT_{sup}/dt > 0 \quad (9)$$

$$T_{out} < \varepsilon_{out,htg} \quad (10)$$

Figure 15 through Figure 17 shows the heat pump operation for Site 8 on a particularly cold day in November 2021, which shows that the compressor heating mode is detected immediately after the unit cycles on. This is evident based on the inverter frequency and ODU power (Figure 15) and supply and return air temperatures (Figure 16).

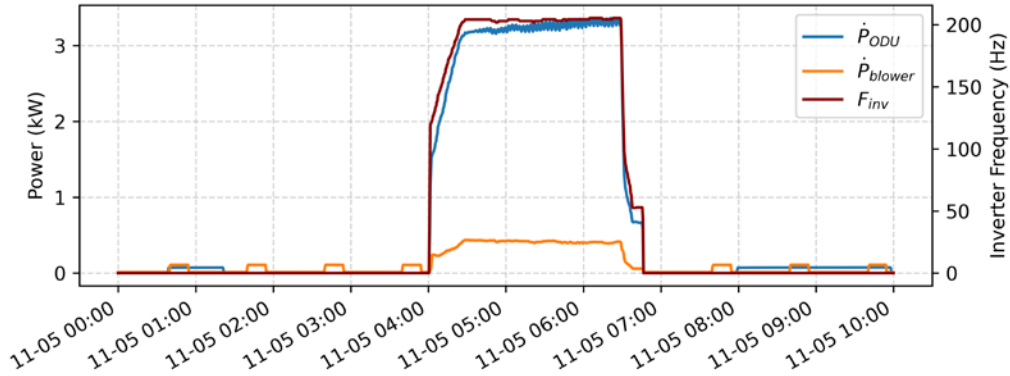


Figure 15. Blower power, outdoor power, and compressor inverter frequency during a period with heating cycle.

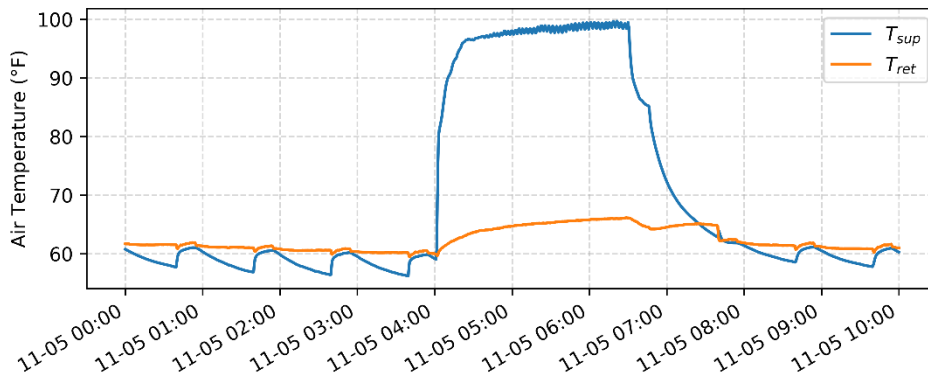


Figure 16. Supply and return air temperature during a period with heating cycle.

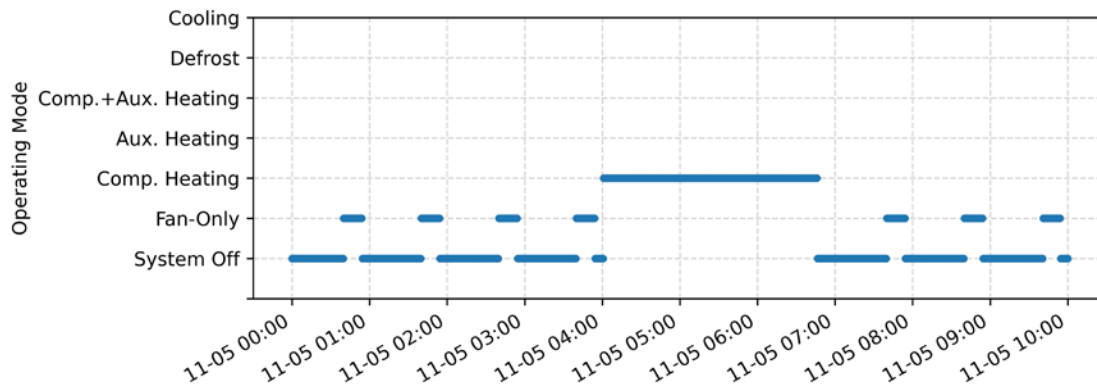


Figure 17. Automatically detected compressor heating operation mode during an example period.

4.1.4 Auxiliary Heating Mode

Because this study was particularly interested in cold temperature performance, it was important to detect auxiliary heating mode to explore how frequently the system utilizes the auxiliary heat at cold temperatures. Auxiliary heating mode occurs when the auxiliary heating system is exclusively used to heat the building and can happen when the outdoor air temperature is colder than the compressor lockout temperature. This mode was detected when the fan was running based on Equation 6, heating is detected with the compressor being *off*, and the auxiliary heater is *on*, which was found by identifying when the difference between IDU power (\dot{P}_{IDU}) and blower power (\dot{P}_{blower}) was greater than the IDU power tolerance value (ϵ_{IDU}).

$$\dot{P}_{IDU} - \dot{P}_{blower} > \epsilon_{IDU} \quad (11)$$

All systems included an auxiliary electric resistance, auxiliary heater except for Site 3, which had a natural gas backup furnace. Furnace operation was detected when the fan was *on*, heating with compressor *off*, and the supply air temperature was higher than 104°F (40°C). From Figure 18, it can be observed for Site 3 that the supply air temperature is higher and blower fan is *on* when auxiliary heating is provided on a particularly cold day in January 2022.

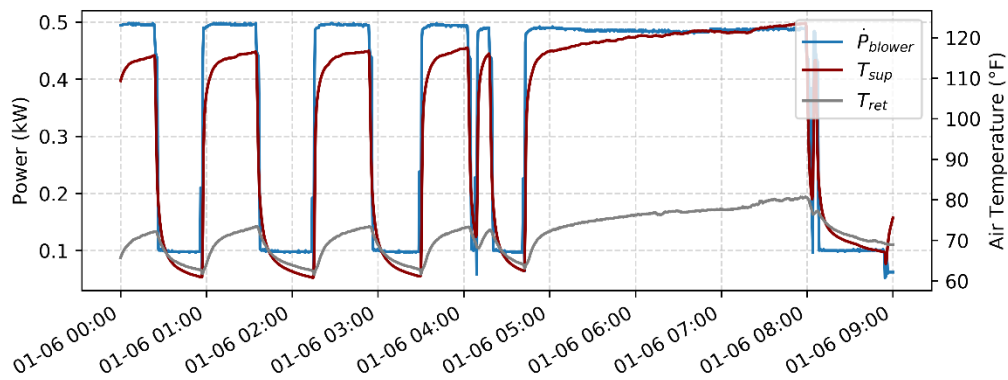


Figure 18. Blower power and supply and return air temperature during a period with auxiliary heating operation.

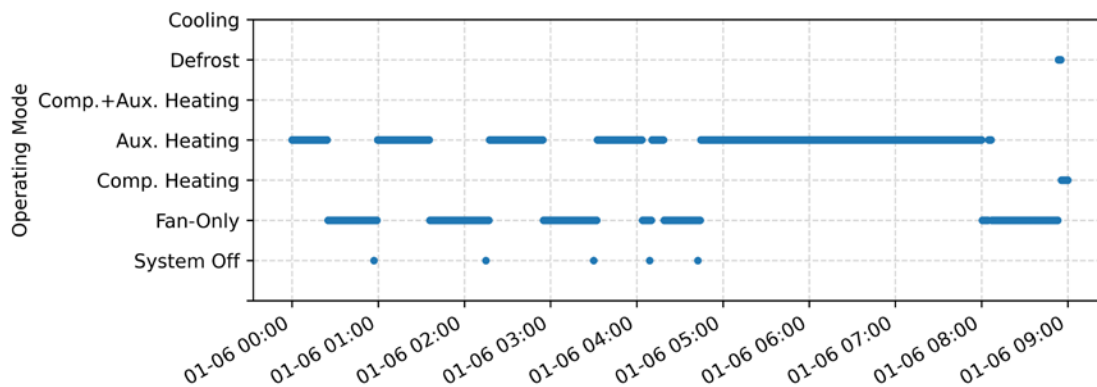


Figure 19. Automatically detected operation mode during an example period with auxiliary heating operation.

4.1.5 Compressor + Auxiliary Heating Mode

This mode was detected when both compressor and auxiliary heater were *on* to provide heating at low outdoor temperature. The equations to detect compressor heating mode and auxiliary heating mode must be satisfied. Figure 20 through Figure 22 show a cold winter day in December 2021 for Site 11 when the system operated in compressor + auxiliary heating mode continuously from 4:25 a.m. to 5:30 a.m., which was detected based on Equations 7–11.

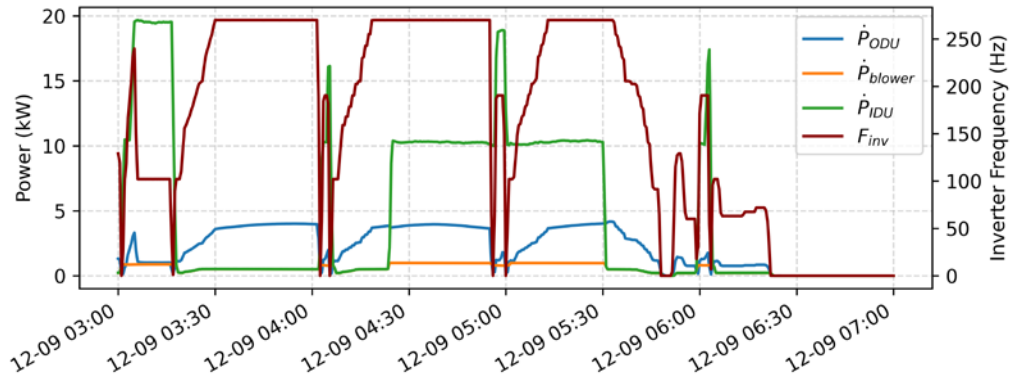


Figure 20. Blower power, outdoor and indoor power, and compressor inverter frequency during a period with compressor + auxiliary heating operation.

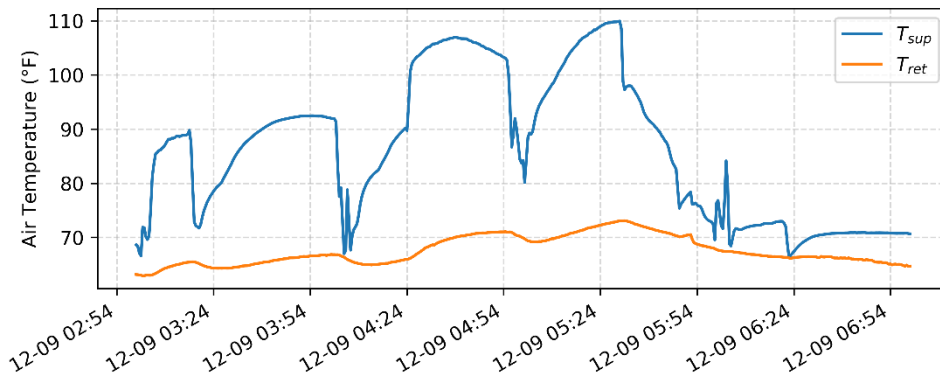


Figure 21. Supply and return air temperature during a period with compressor + auxiliary heating operation.

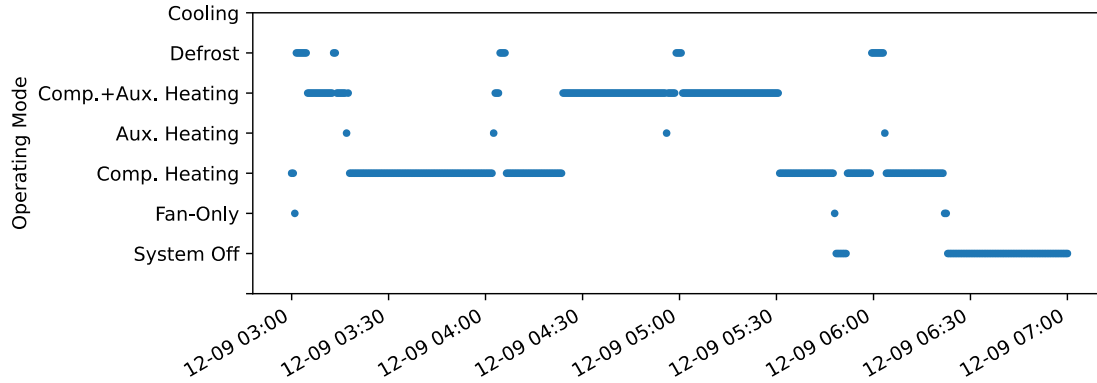


Figure 22. Automatically detected compressor + auxiliary heating operation mode during an example period.

4.1.6 Defrost Mode

Defrost mode was challenging to detect because of the transient measurements during the cycle. We found defrost mode can be automatically detected when the system and/or auxiliary heat is *on*, it is cool outside, and the refrigerant vapor line surface temperature ($T_{ref,vapor\ line}$) is decreasing and is below the set tolerance.

$$dT_{ref,vapor\ line}/dt < 0 \quad (12)$$

$$T_{ref,vapor\ line} < \varepsilon_{ref,vapor\ line} \quad (13)$$

$$T_{out} < \varepsilon_{out,defrost} \quad (14)$$

To reliably detect defrost operation, we set $\varepsilon_{out,defrost}$ to 50°F (10°C). From Figure 23, it can be observed that as $T_{ref,vapor\ line}$ decreases at outdoor temperature below 50°F (10°C), defrost mode is detected for Site 7. The defrost cycle lasted for about seven minutes. It is also interesting to note that the defrost cycle is followed by compressor + auxiliary heating mode to account for defrost recovery, which is shown in Figure 25.

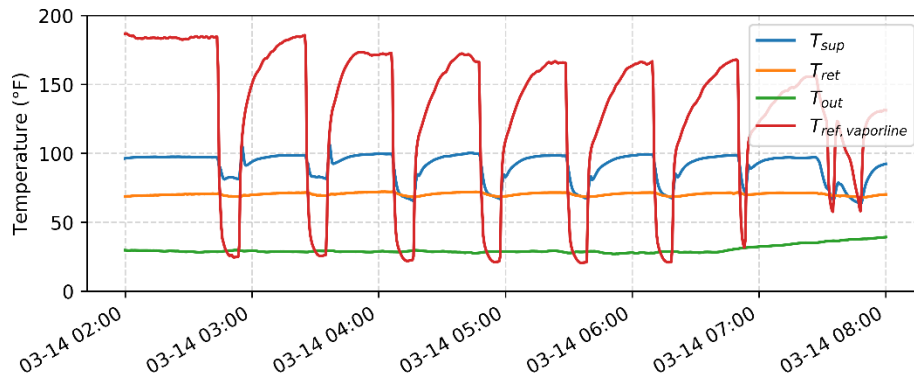


Figure 23. Air and refrigerant temperatures during a defrost cycle.

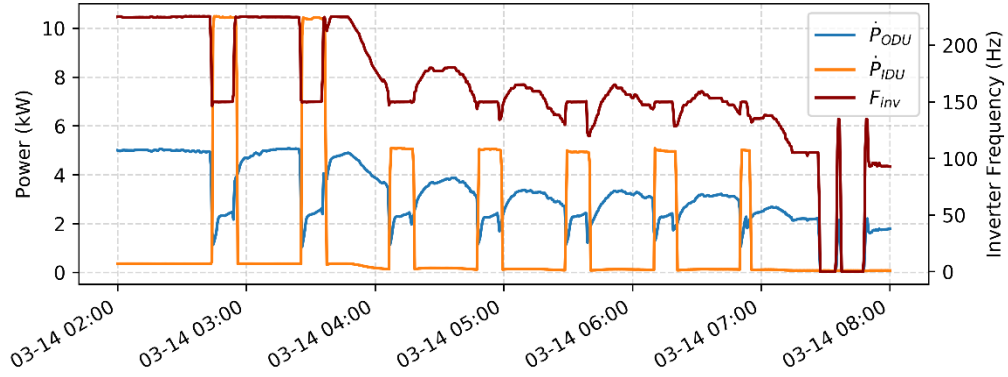


Figure 24. ODU and IDU power during a defrost cycle.

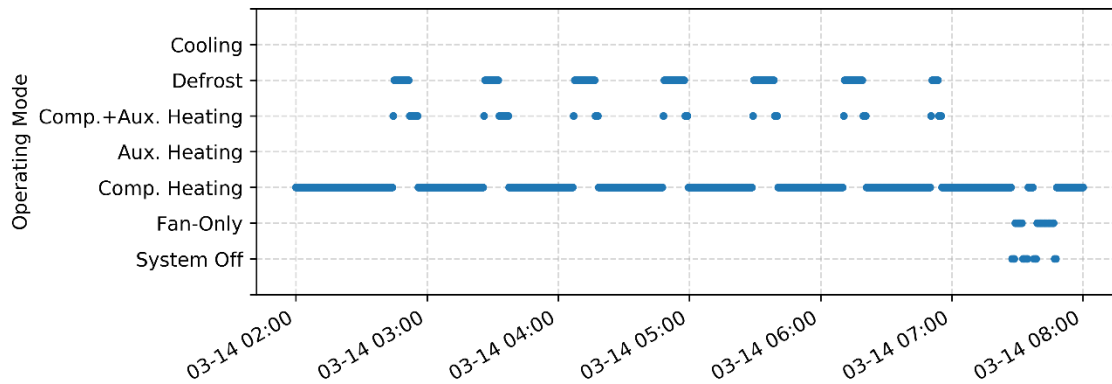


Figure 25. Automatically detected defrost cycle.

4.1.7 Cooling Mode

Cooling mode was easily detected when the system was *on* opposite to Equations 4 and 5 and supplying cold air, based on the following equations, where the supply temperature tolerance value for cooling, $\varepsilon_{sup,clg}$ was assumed to be 69.8°F (21°C).

$$T_{sup} < \varepsilon_{sup,clg} \quad (15)$$

$$T_{sup} < T_{ret} \quad (16)$$

However, we were also interested in measuring the cycling performance immediately after the unit cycles on in cooling mode. Equation 15 and 16 will only detect cooling operating if the unit is supplying cold air. We use Equations 17 and 18 to determine if the unit has cycled on in cooling mode and when the outdoor temperature is above 50°F (10°C).

$$dT_{ref,vapor\ line}/dt < 0 \quad (17)$$

$$T_{out} > \varepsilon_{out,clg} \quad (18)$$

Figure 26 through Figure 28 show relevant measurements during a period with cooling cycle for Site 7. Cooling mode was easily detected when the system was *on* and supply air temperature was less than the return temperature at higher outdoor temperature.

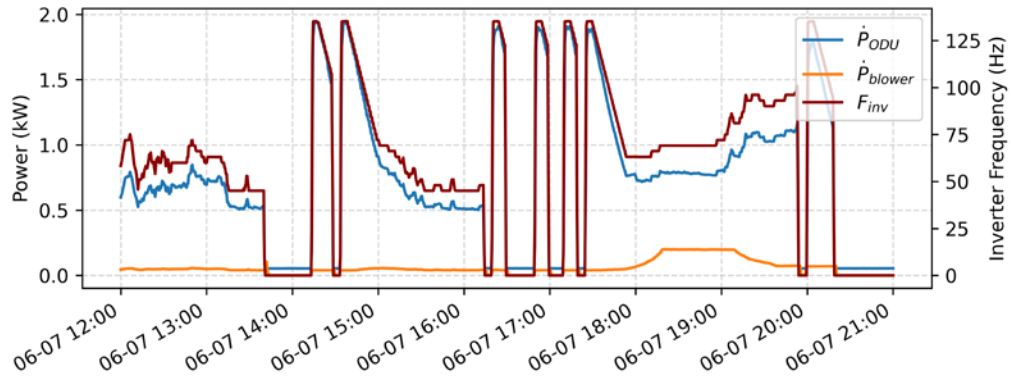


Figure 26. Blower power, outdoor power, and compressor inverter frequency during a period with cooling cycle.

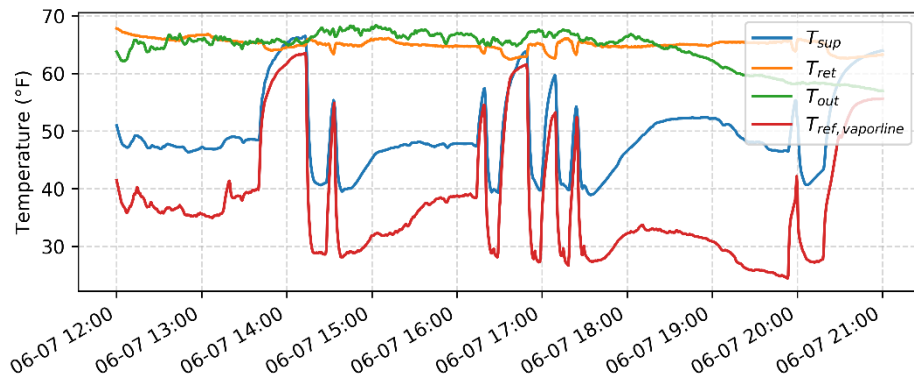


Figure 27. Air and refrigerant temperatures during a period with cooling cycle.

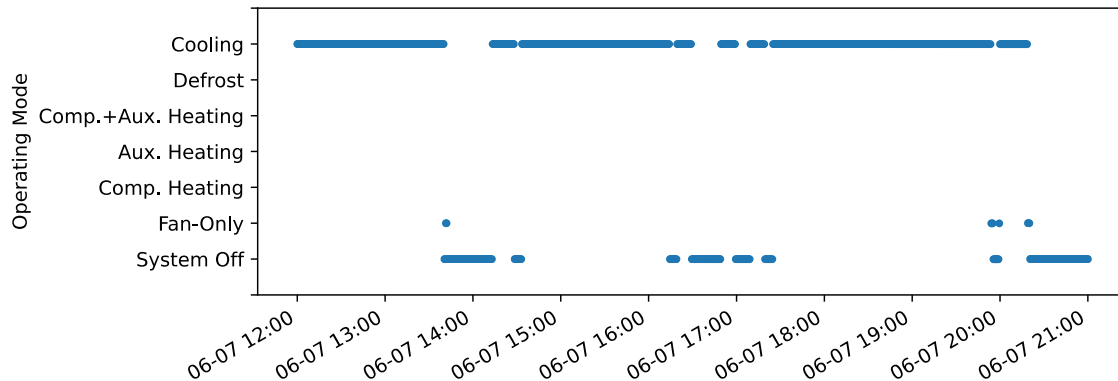


Figure 28. Automatically detected cooling operation mode during an example period.

4.2 Determining Steady State Periods

Automatic detection of steady state operation was required to assess steady state performance. We used a hybrid online steady state detection method which employs slope detection in conjunction with variance detection to identify steady state over a moving data window. Li and Braun (2003) incorporated a combination slope and variance method to determine the steady state of seven state variables in their fault detection and diagnosis research on packaged air conditioning equipment.

A linear regression is performed over a predefined moving data window and the fitted slope is monitored. When the absolute value of the slope falls below the defined threshold, the process signal is considered steady. Even though the slope method can filter out transient data, it cannot differentiate cyclic behavior of oscillating data. The variance of a moving data window is monitored to characterize random variation of the data and the steady state is detected if the variance is below a defined threshold. A large threshold for moving variance method will include some of the transient data while small thresholds carry a risk of isolating data with both deterministic and random variations. Thus, a combination of both slope detection and variance detection methods will ensure good performance.

The detection parameters, thresholds, and moving window size depend on the characteristics of data and algorithm employed. We use the average supply air temperature, T_{sup} , and inverter frequency, F_{inv} to determine if the system has reached steady state. Initial estimates of thresholds and window size were determined for each site and the detection parameters were tuned to predict steady state accurately. The slope threshold for T_{sup} is set at $0.02^{\circ}\text{C}/\text{s}$ and the variance threshold is set at 0.02°C^2 to identify good performance data. Similarly, the slope threshold for inverter frequency is 0.01 and the variance threshold is set at 0.01 Hz^2 . The length of the moving window was set at two minutes using the resampled 30-second data. If the data was continuously steady for three minutes, then the data row was identified as steady state operation condition.

Figure 29 and Figure 30 show the identification of steady state from the rolling window of supply air temperature and inverter frequency data. During this example period for Site 1, the algorithm detects multiple steady state periods. At other times, the variation in supply air temperature and inverter frequency means the system is not in steady state.

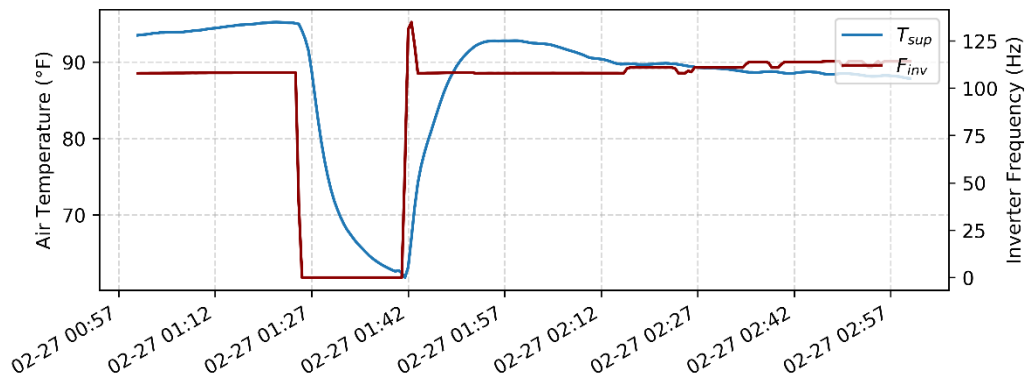


Figure 29. Supply air temperature and inverter frequency over a moving data window.

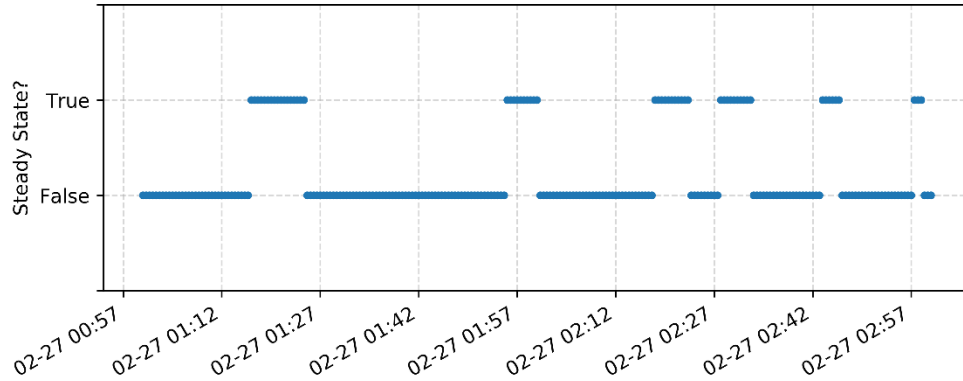


Figure 30. Steady state detection using hybrid online steady state detection method.

4.3 Performance Calculations

The following three parameters were calculated to determine the heat pump performance:

1. Indoor unit mass flow rate (\dot{m}_{air})
2. Heat pump capacity (\dot{Q})
3. Coefficient of performance (COP)

The capacity and COP were calculated for heating and cooling modes separately.

The indoor unit air mass flow rate (\dot{m}_{air}) was calculated using:

$$\dot{m}_{air} = \rho_{dry} \dot{V}_{blower} \quad (19)$$

where ρ_{dry} is either the supply or return dry air density for a draw through or push through blower, respectively, and the blower volumetric air flow rate (\dot{V}_{blower}) was calculated using a correlation derived from data collected during the initial site visit that uses the measured blower power (Equation 3).

Using the indoor unit mass flow rate, the sensible capacity ($\dot{Q}_{sensible}$) was calculated as (AHRI 2017):

$$\dot{Q}_{sensible} = \frac{\dot{m}_{air} c_p (T_{sup} - T_{ret})}{1 + \omega_{sup}} \quad (20)$$

For heating mode, the latent heating capacity (\dot{Q}_{latent}) was 0. The total heat pump capacity (\dot{Q}) is the sum of sensible and latent capacity as shown in the equation below:

$$\dot{Q} = \dot{Q}_{sensible} + \dot{Q}_{latent} \quad (21)$$

For cooling mode, the total capacity was directly calculated as:

$$\dot{Q} = \dot{m}_{air} (h_{sup} - h_{ret}) \quad (22)$$

And finally, the COP for compressor-based heating and cooling is calculated using:

$$COP = \dot{Q} / (\dot{P}_{ODU} + \dot{P}_{blower}) \quad (23)$$

The data was resampled to 30-second intervals prior to conducting the calculations to reduce noise, allowing for more consistent operating mode detection.

5 Heating Mode Performance Results and Discussion

5.1 Heating Season Summary Data

Prior to discussing detailed results from the study, we summarize the heat pump performance for each site during winter 2021–2022, as all sites were being monitored during this time. Results are listed in Table 11 (note that Site 12 had less data than the other sites due to an issue with the data logger). To ensure we captured all hours with heating operation during the winter months, we assumed winter 2021–2022 started on October 1, 2021 and ended on March 30, 2022.

Table 11 lists the percent of time a heat pump was either completely off, operating in fan-only mode, utilizing compressor-based heating, running the auxiliary heat, or in defrost mode during the six-month period. Section 5.2 goes into further detail by plotting operating mode binned by outdoor air temperature. Although all the heat pumps had some ability to modulate, the heat pumps were off for a significant fraction of the time during these months. For example, the heat pump at Site 11 was off nearly 75% of the time. This could have been partially due to a gas fireplace in the living room; however, the homeowner stated it was infrequently used on some evenings. Sites 3, 6, and 12 set their thermostats to continuous fan mode for lengthy time periods, which is why those sites had less time when the system was completely turned off.

The auxiliary heat energy use listed in Table 11 was determined by summing the auxiliary heater energy during time periods of auxiliary-only heating and compressor with auxiliary heating; meaning defrost cycles are not included in the summation. The auxiliary heat energy use for Sites 2, 5, 8, 11, and 12 exceeded nearly 40% of the compressor-based heating energy and for Sites 2 and 8 the auxiliary heat used more energy than compressor-based heating. Based on the heat pump sizing and house load lines plotted in Figure 4 from Section 2.6, we expected auxiliary heat energy use to be high for Sites 5, 8, and 11, because the heat pump balance temperature for these two sites was approximately 37°F, 39°F, and 24°F, respectively. However, based on Figure 4, it appeared that heat pump for Site 2 was more appropriately sized than for Sites 10 and 13, which had relatively little auxiliary heat runtime. Auxiliary heat energy use is further described in Section 5.4.

The defrost energy was determined by summing the total IDU and ODU energy use during the reverse cycle operation and does not consider energy consumed during defrost recovery. Though a relatively small fraction of the time was spent in defrost mode for all sites except Site 7, the defrost cycle did consume a relatively significant amount of energy for some sites. For Sites 5, 7, 8, and 11, the defrost energy use exceeded 20% of the energy used for compressor-based heating. Defrost energy is further described in Section 5.6.

The third-to-last row in Table 11 lists the compressor-based heating COP during winter 2021–2022. The seasonal heat pumping COP was calculated by summing the total heat output for each 30-second sample, i , and dividing by the total IDU and ODU energy use during compressor-based heating operation, which neglects auxiliary heat energy use.

$$COP_{HP,season} = \frac{\sum \dot{Q}_i}{\sum (\dot{P}_{ODU,i} + \dot{P}_{blower,i})} \forall i \text{ compressor only heating samples} \quad (24)$$

Site 8 had the highest compressor-based heating seasonal COP but also had the highest auxiliary heat energy use. The average seasonal COP across all twelve sites was 2.5 and varied from 1.7 (Site 6) to 3.5 (Site 8). Heat pump COP is further described in Section 5.3.

Unfortunately, the heating output could not be accurately measured when the auxiliary heat was turned on due to the proximity of the thermocouples to the heating elements. Therefore, we used the seasonal heat pump COP ($COP_{HP,season}$) to estimate the compressor-based portion of the heating output when both the compressor and auxiliary elements were turned on. This was then used to estimate the overall system COP and the fraction of the heating load served by the compressor. The following equations were used where heating output and energy consumption are summed for all samples, i , for all modes of heating operation. The overall system COP ($COP_{system,season}$) accounts for the heat delivered to the house during compressor-based heating, compressor-based heating with auxiliary heating, and auxiliary heating only.

The seasonal heating pump output ($Q_{HP,season,total}$) was estimated using Equation 25 for all samples, i , with heat pump operation (compressor-based heating and compressor with auxiliary heating).

$$Q_{HP,season,total} = COP_{HP,season} \cdot \sum(\dot{P}_{ODU,i} + \dot{P}_{blower,i}) \quad (25)$$

Because all the auxiliary heater energy is transferred to the IDU air stream, the overall system COP can be estimated using the following equation:

$$COP_{system,season} = \frac{(Q_{HP,season,total} + \sum \dot{P}_{IDU,i})}{(\sum \dot{P}_{ODU,i} + \sum \dot{P}_{IDU,i})} \quad (26)$$

Lastly, we estimate the fraction of the building heating load served by the compressor using Equation 27.

$$f_{compressor} = \frac{Q_{HP,season,total}}{(Q_{HP,season,total} + \sum \dot{P}_{IDU,i})} \quad (27)$$

The last two rows of Table 11 list the estimated fraction of the building's heating load served by the compressor and the overall system COP accounting for auxiliary heating. These two metrics could not be calculated for Site 3 because we did not measure the natural gas consumption. Sites 2, 8, and 11 utilized the vapor compression system the least amount for building heating. The sites with the highest fractions of load served by the compressor correspond to the sites with the least amount of auxiliary heating. The large amount of auxiliary heating at Site 8 effectively decreased the heat pump seasonal COP from 3.5 to 2.4.

The fraction of load served by the compressor and overall system COP were also plotted in Figure ES-1 and Figure ES-2, respectively.

Table 11. Summary of Heating Data for Winter 2021–2022

	Site 1	Site 2	Site 3	Site 4	Site 5	Site 6	Site 7	Site 8	Site 10	Site 11	Site 12	Site 13
Hours of data	4,368	4,367	4,368	4,368	4,368	4,368	4,368	4,367	4,368	4,368	2,524 ^d	4,367
Percent of time system off [%]	40.9	4.9	18.2	59.9	43.8	1.6	24.7	35.5	41.3	74.8	22.9	35.0
Percent of time with fan-only operation [%]	0.8	43.6	41.9	1.9	0.8	38.1	19.4	8.0	8.2	0.3	44.2	0.3
Percent of time with compressor operation [%]	57.4	40.4	35.5	37.0	52.7	58.6	49.3	54.6	48.4	23.4	32.0	64.1
Percent of time with auxiliary heat on [%]	2.1	9.1	3.6	1.9	6.0	2.0	8.3	11.8	2.9	4.1	5.2	0.2
Percent of time in defrost [%]	0.3	0.9	1.3	1.2	1.9	0.4	6.3	1.5	1.0	0.9	0.6	0.6
Compressor-based heating energy [kWh] ^a	4,497	3,343	2,498	2,901	3,340	4,894	5,438	4,326	3,670	2,248	1,957	5,636
Blower energy (season) [kWh]	549	614	687	170	460	274	520	799	321	485	360	348
Auxiliary heater energy (heating) [kWh]	512	3,446	N/A ^e	314	1,268	1,041	549	4,524	354	1,693	803	44
Defrost cycle [kWh] ^b	130	464	44	565	804	119	2,266	1,256	288	525	182	45
Compressor-based heating season COP ^c	2.5	2.7	2.8	3.1	2.7	1.7	2.0	3.5	2.7	2.3	2.4	1.9
Fraction of load served by compressor	0.96	0.73	N/A	0.97	0.88	0.89	0.95	0.81	0.96	0.77	0.87	0.99
System heating season COP	2.4	1.9	N/A	2.9	2.2	1.5	1.9	2.4	2.6	1.8	2.0	1.9

^a Includes ODU and IDU (blower) energy.

^b Defrost cycle energy listed here does not include periods of recovery.

^c Heating season COP was calculated by summing total heat output, then dividing ODU and IDU energy consumption.

^d Site 12 logger issue resulted in fewer hours of data collected during winter 2021–2022.

^e Natural gas consumption for Site 3 was not measured.

5.2 Heating Season Operating Modes

Because this study was particularly focused on cold temperature performance, it is interesting to explore the heat pump operating mode specifically at cold temperatures ($<28^{\circ}\text{F}$) to understand how frequently the system utilizes compressor-based and/or auxiliary heat. Figure 31 plots the hours of data collected during winter 2021–2022, colored by operating mode. We filtered the data for Figure 31 to coincide with winter 2021–2022 to have an approximately equal number of total hours for each site.

The bars shaded pink indicate hours with only compressor-based heating, meaning the auxiliary heat is turned off and the system is exclusively using the vapor compression system to heat the building. Steady-state and transient time periods are both included.

The hours shaded orange and red denote operation of the auxiliary heater, where orange refers to hours with simultaneous compressor and auxiliary heating and red corresponds to only auxiliary heat. Sites 2 and 8 are the two all-electric sites with the most auxiliary heat runtime, which is further discussed in Section 5.4. Site 2 was the only all-electric site with a significant amount of time during which the auxiliary heat was exclusively used to heat the building. This was despite the auxiliary heat lockout temperature being set to 25°F , meaning the auxiliary heat should not have turned on at temperatures above 25°F , indicating a sensor or control issue with the system. The dual fuel system at Site 3 could not run the heat pump and furnace simultaneously because the indoor coil was downstream of the furnace. Thus, we do not see any hours at Site 3 with simultaneous compressor and auxiliary heating.

Most of the all-electric sites had very few hours with outdoor temperatures below the compressor lockout temperature (listed in Table 5). Site 10 was the exception. Though the compressor lockout temperature at Site 10 was disabled, the compressor did not run at temperatures below 0°F , which was likely due to an on-board control setting that cannot be adjusted in the field. The compressor lockout temperature for Site 3 was adjusted by the homeowner during the study but it is clear the compressor does not run below 4°F .

Times when the system is either off or in fan-only mode are denoted by gray and green, respectively. Notably, the variable-capacity heat pumps spent large portions of time during which they did not provide space heating at cold temperatures. Most sites utilized thermostat temperature setbacks (Table 5), which could explain time periods without system operation; however detailed setpoint schedules were not collected during the homeowner survey. Section 5.5 further explores the measured heat pump runtime fractions and capacity modulation.

Lastly, defrost is denoted in Figure 31 by the purple bars. Except for Site 7, a relatively low proportion of time was spent in defrost mode. The algorithm for determining defrost mode was presented in Section 4.1.6 and did not include the time spent recovering from the reverse cycle. The heat pump systems included in the study are all premium products that likely utilize on-board sensors to initiate demand-based defrost and the need to defrost the outdoor heat exchanger generally decreases at cold temperatures because of the low moisture content. Additionally, all the sites were in dry climate zones where the need to defrost the outdoor coil would be much less than that of heat pumps installed in humid or marine climate zones.

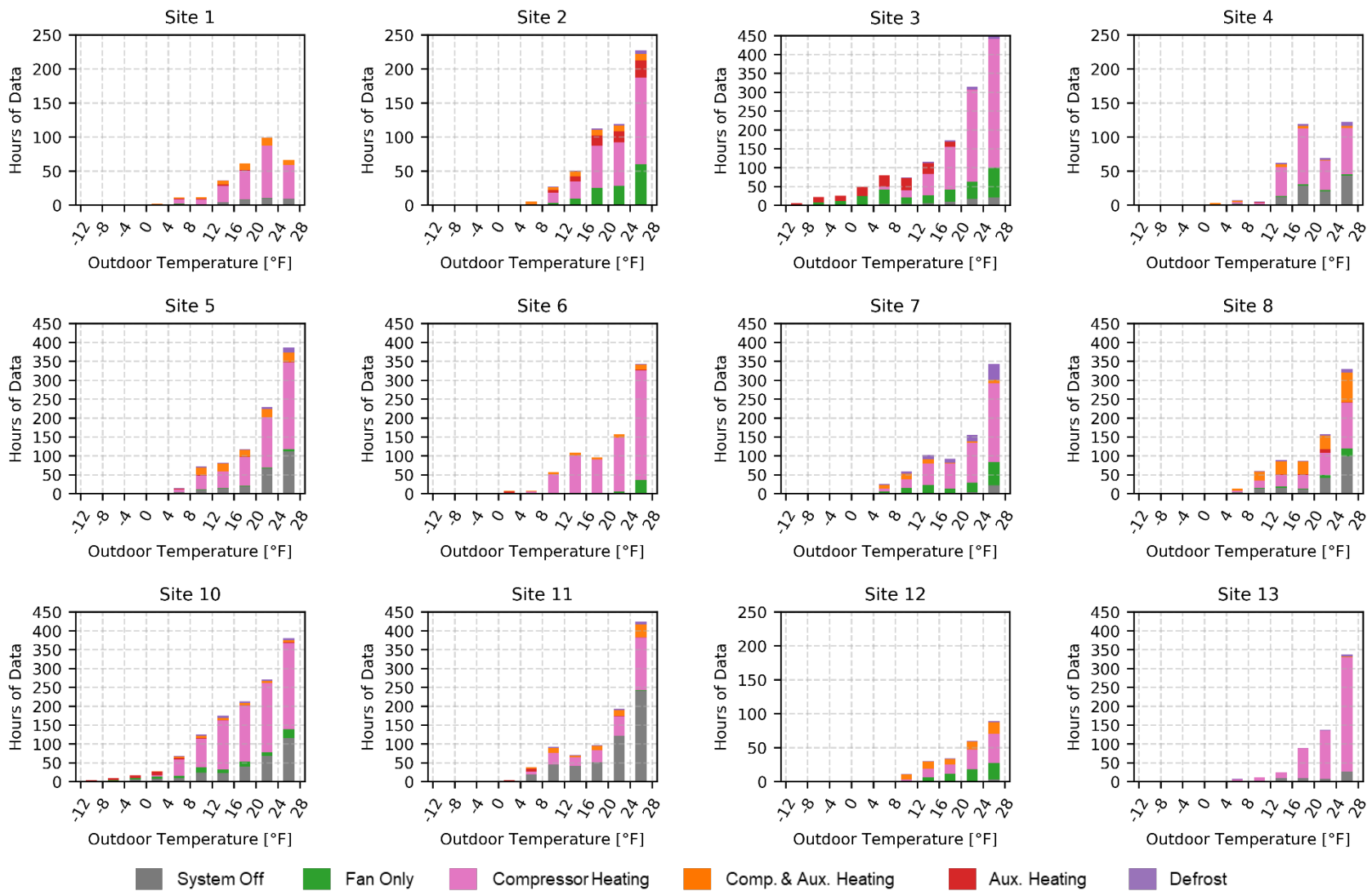


Figure 31. Heat pump operational modes at cold temperatures during winter 2021–2022.

5.3 Compressor-Based Heating COP and Capacity

The compressor-based heating COP is a measure of heat pumping efficiency and neglects auxiliary heat energy consumption and distribution system losses. Figure 32 and Figure 33 plot the steady-state compressor-based heating COP. Figure 32 plots 30-second down-sampled data using a box and whisker plot; whereas Figure 33 plots the capacity-weighted mean COP calculated by summing total heat output within a temperature bin and dividing it by the total energy consumption. The blue boxes or bars are the field-measured results, which account for the blower power (e.g., net COP), and the red lines are manufacturer-reported values at minimum and maximum compressor speeds. The higher manufacturer-reported COPs in Figure 32 and Figure 33 are at the minimum compressor speed and lower COPs are at the maximum compressor speed. Figure 34 and Figure 35 are similar to Figure 32 and Figure 33, plotting compressor-based heating capacity rather than COP.

The variation in steady-state COP and capacity in Figure 32 and Figure 34, respectively, can be explained by variations in compressor speed and return air temperature. Site 12 was the only site without a variable-capacity compressor, which explains why there was little variation in the 30-second steady state data.

The four COP and capacity plots compare the field-measured results to manufacturer-reported values to approximate the expected performance, which were either sourced from the NEEP product list or manufacturer expanded performance tables. The three points correspond to the three outdoor temperatures listed in the NEEP product list: 5°F, 17°F, and 47°F.

Manufacturer-reported COPs and capacities may be from laboratory measurements or heat pump system models, and certain control settings and operating conditions, such as indoor airflow rate, return air temperature and compressor speed, may be different between the field-collected data and manufacturer-reported values. These potential sources of discrepancy are important to consider when viewing Figure 32 through Figure 35. Despite the potential sources of discrepancy, comparing the field-measured performance to expected values is useful to estimate the expected performance.

From Figure 32, the steady-state heating COPs at 7 of the 12 sites (Sites 2, 3, 4, 5, 8, 10, and 13) agreed reasonably well with manufacturer-reported values, indicated by the box and whisker plots that span the manufacturer-reported COP range at most temperature bins. For the remaining sites (Sites 1, 6, 7, 11, and 12), the measured COPs were lower than the manufacturer-reported values. Though the heat pump at Site 8 had the highest compressor-based heating COP, the site also had the highest auxiliary heat energy consumption which decreases the overall system COP.

In Figure 34 and Figure 35, the manufacturer-reported capacity increases as the outdoor air temperature gets warmer, which is the expected trend. However, modulating systems vary the compressor capacity based on the building load, which decreases as the outdoor air temperature get warmer. Thus, it is not surprising that the field-measured capacity for some sites exhibit opposite trends with respect to outdoor air temperature. Site 12 is one of the exceptions where the measured capacity increases as the outdoor air temperature gets warmer. Recall that Site 12 is a two-stage system with limited modulating capability.

The measured capacity tends to be closer to the minimum manufacturer-reported capacity rather than the maximum. From Figure 34, the measured capacity is close to the maximum manufacturer-reported capacity at cold outdoor air temperatures for Sites 3, 8, 10, 11, and 13. Even though Site 8 had the most auxiliary heat runtime, the heat pump capacity does align well with manufacturer-reported values, underscoring that the auxiliary heat runtime is due to equipment under-sizing.

Figure 36 plots the steady state compressor heating indoor airflow rate, calculated using the blower airflow correlation, and compares it to manufacturer-reported values listed in the AHRI Product Directory (AHRI 2022). Figure 6 plotted the measured IDU airflow rates collected during the site visit. Sites with lower-than-expected COPs (Sites 1, 6, 7, 11, and 12) did not consistently have lower-than-expected IDU airflow rates. Additionally, out of the sites with COPs that aligned most closely with manufacturer-reported values (Sites 3, 4, 5, 8, and 10), some had lower than expected IDU airflow (Sites 3, 4, and 10). Thus, lower-than-expected IDU airflow does not consistently explain the lower-than-expected COP.

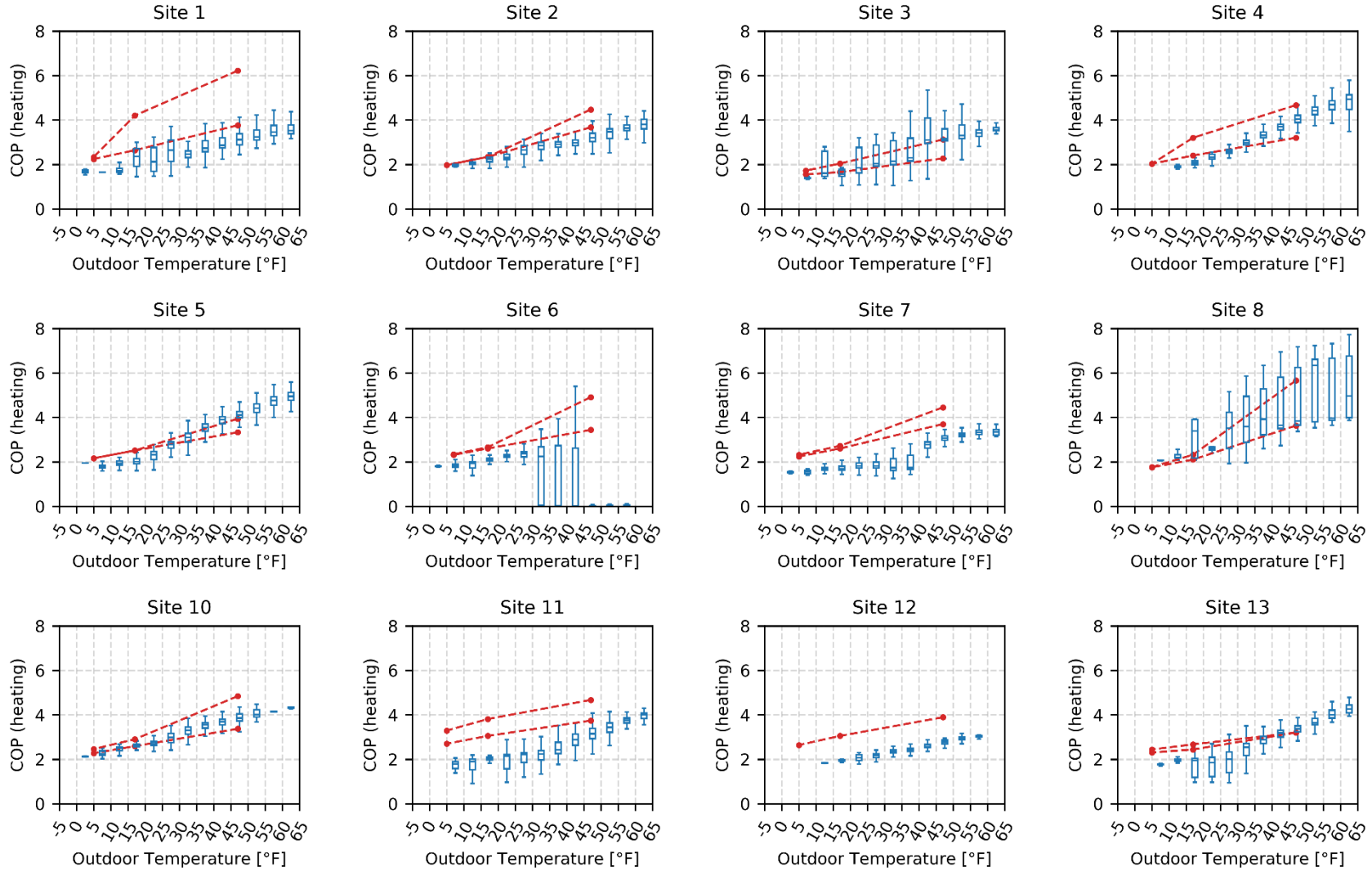


Figure 32. Box and whisker plot of steady-state compressor-based heating COPs (blue boxes) and manufacturer-reported COPs at minimum and maximum speeds (red lines).

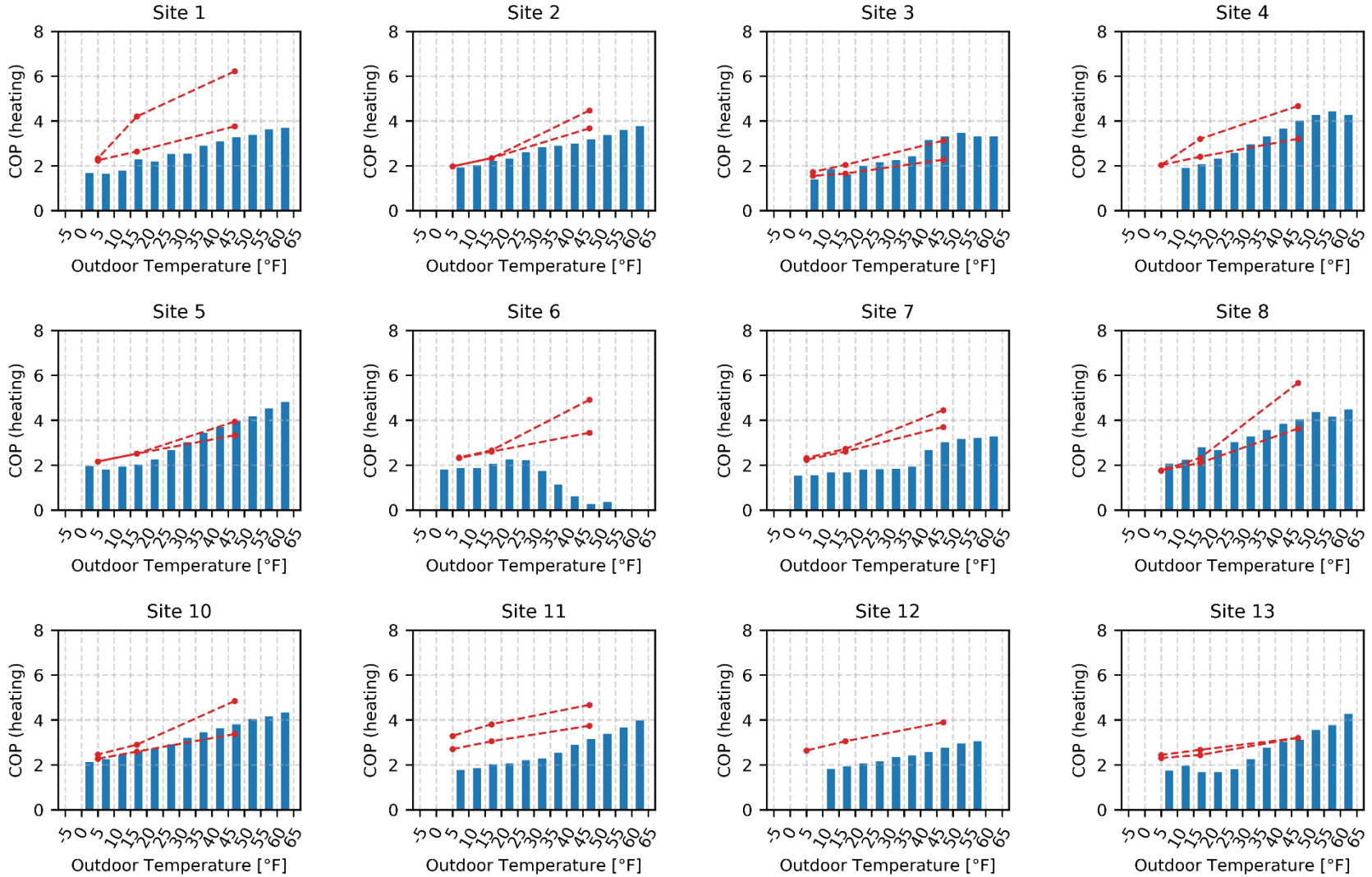


Figure 33. Mean steady-state compressor-based heating COPs (blue bars) and manufacturer-reported COPs at minimum and maximum speeds (red lines).

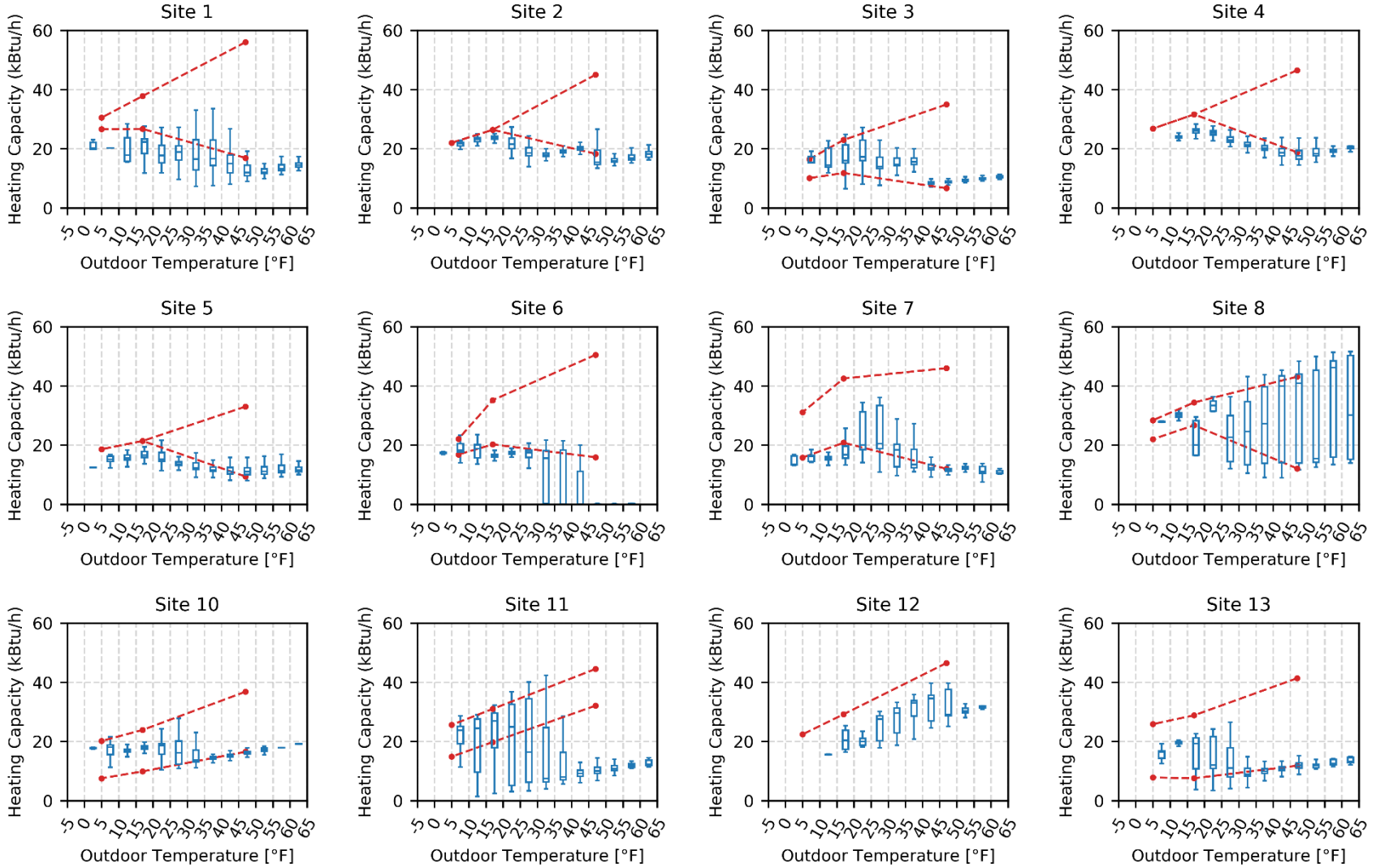


Figure 34. Box and whisker plot of steady-state compressor-based heating capacity (blue boxes) and manufacturer-reported capacities at minimum and maximum speeds (red lines).

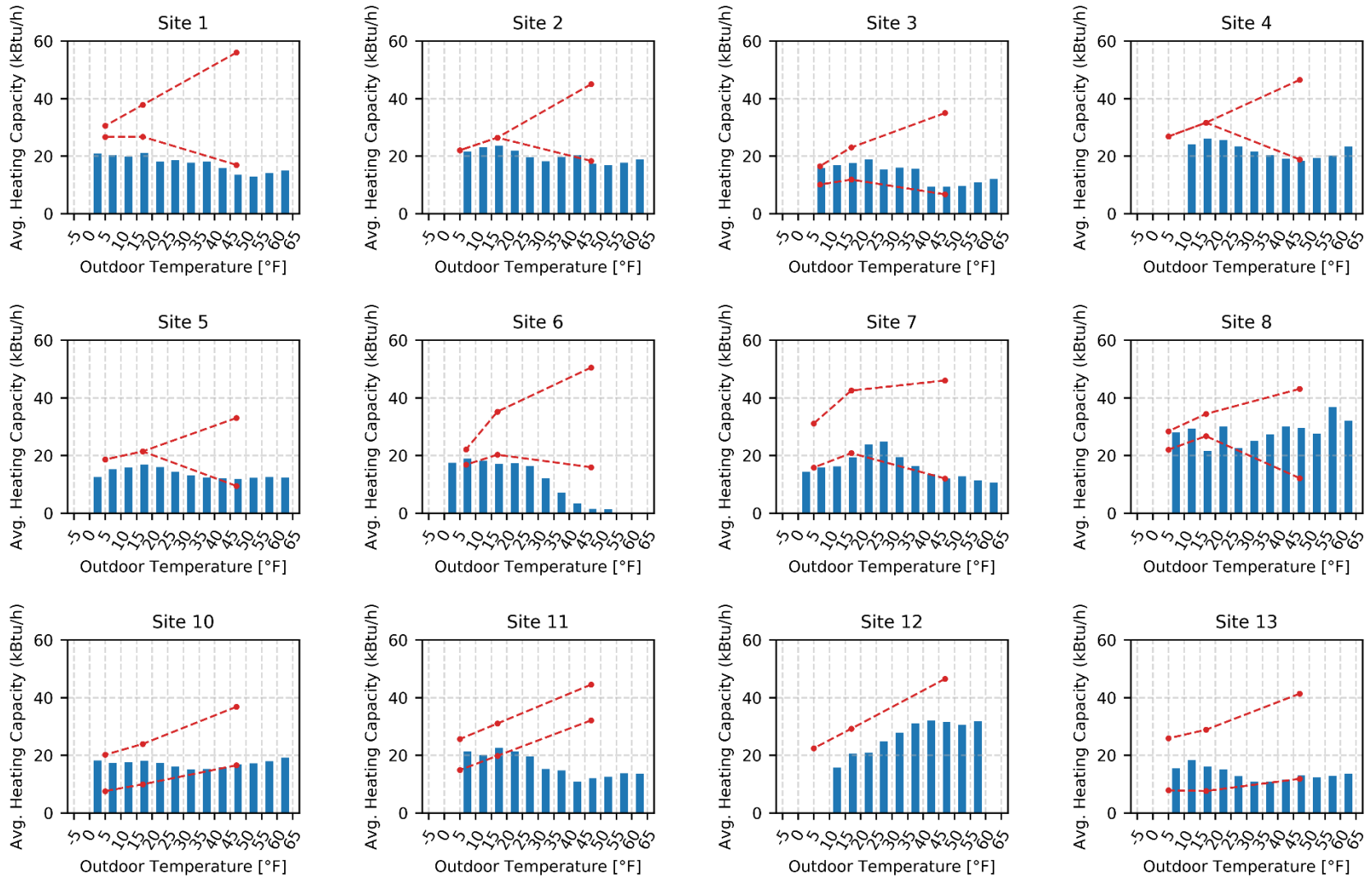


Figure 35. Mean steady-state compressor-based heating capacity binned by outdoor temperature (blue bars) and manufacturer-reported capacities at minimum and maximum speeds (red lines).

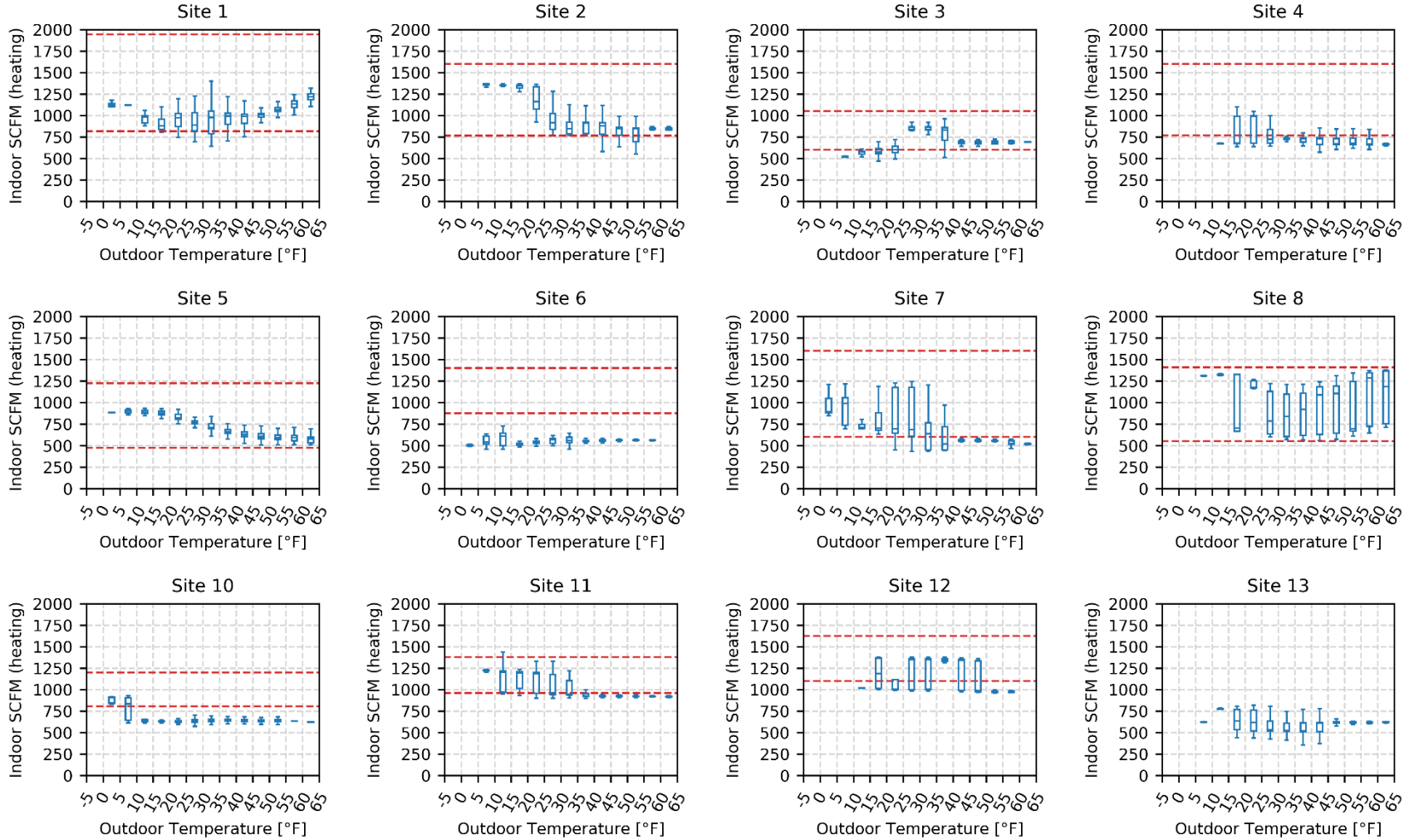


Figure 36. Box and whisker plot of steady-state compressor-based heating IDU airflow rate (blue boxes) and manufacturer-reported full load and minimum speed airflow rates (red lines).

5.4 Auxiliary Heater Use

For all-electric homes that utilize electric resistance auxiliary heating elements, excessive auxiliary heater runtime can be costly and lead to significant energy waste. Thus, efforts should be taken to minimize auxiliary usage by proper heat pump sizing and control settings.

Figure 41 plots the auxiliary heater energy consumed during winter 2021–2022 for the all-electric sites, binned by outdoor air temperature, and differentiates the energy consumed during heating modes (compressor with auxiliary and auxiliary-only) and defrost operation. The auxiliary heater energy use was calculated by subtracting the blower energy from the IDU total energy use. As previously mentioned, the natural gas used by the furnace at Site 3 was not directly monitored. In Figure 41, it is important to observe that the y-axis scale is different for Site 8 due to the high auxiliary heat usage at this one site.

Section 5.6 elaborates further on defrost energy use. However, auxiliary heater energy is linked to defrost as all the heat pumps ran the auxiliary heater during, and sometimes after, defrost cycles. In Figure 41, we see the auxiliary heater energy for Site 4 was primarily consumed during defrost.

The auxiliary heater energy use plotted in Figure 41 largely corresponds to the auxiliary heat lockout temperatures listed in Table 5. This indicates there is little energy consumed in the warmer bin adjacent to the lockout temperature. The exceptions are Sites 2 and 8, which are elaborated on below.

Sites 2 and 8 consumed the most auxiliary heating energy. From Table 11, the auxiliary heater energy consumption for Sites 2 and 8 was greater than the energy consumed during compressor-based heating operation. The reason for the excessive auxiliary heat energy appears to be different for each of the sites.

The high auxiliary heat use at Site 2 appears to be caused by a fault with the controls or the onboard outdoor temperature sensor. From Figure 38, we see the auxiliary heat turned on at outdoor air temperatures well above the specified auxiliary heat lockout temperature, which was 25°F for Site 2 (Table 5). Additionally, there were many hours at relatively warm outdoor temperatures (40°–50°F) when the auxiliary heater was the only heat source and the compressor was not running despite the compressor lockout temperature being disabled (Table 5). The fault started on February 16, which is evident when plotting the daily ODU and auxiliary heater energy use in Figure 37. The heat pump at Site 2 did not utilize the compressor from February 16 through April 11 and exclusively used the electric resistance auxiliary heater to heat the home. It is worth noting that the homeowner did not notice the change in heat pump behavior during this time.

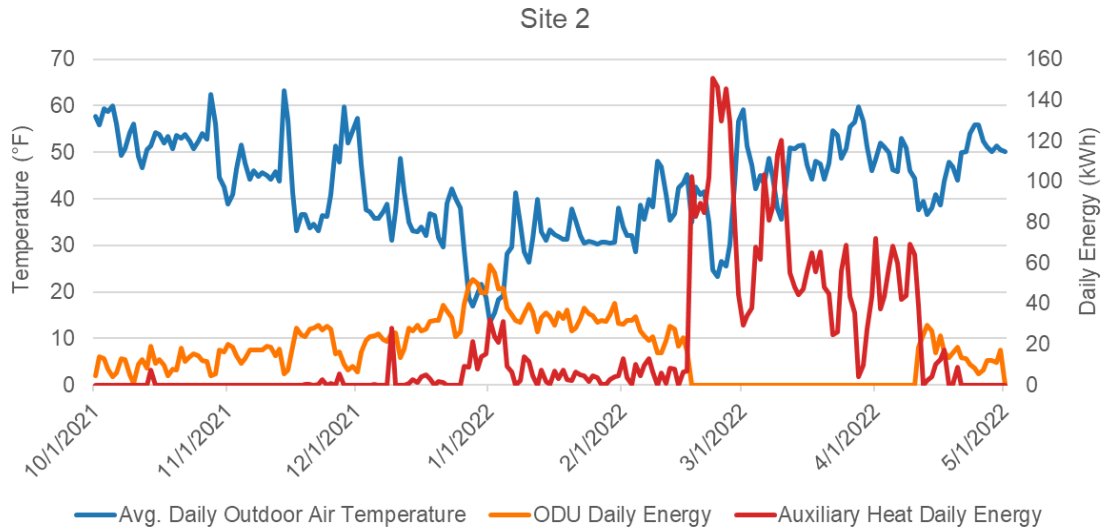


Figure 37. Site 2 daily ODU and auxiliary heater energy use during winter 2021–2022.

As previously mentioned, the heat pump installed at Site 8 was undersized for the house load with a balance point temperature of $\sim 39^{\circ}\text{F}$, and in Figure 38, the orange bars indicate the auxiliary heat at Site 8 was used extensively at outdoor air temperatures below 40°F . Thus, the heating load calculations predicted the excessive auxiliary heat energy use at Site 8. Based on Figure 4, the heat pump at Site 5 was also identified as undersized for the heating load, and the heat pumps at Sites 10, 11, and 13 were potentially undersized. Out of the eleven reported-on homes in the Northwest, Sites 11 and 5 consumed the third- and fourth-most auxiliary heat energy, respectively. The auxiliary heat at Sites 10 and 13 consumed a relatively small amount of energy. Despite having the coldest weather in the study, Site 10 was able to utilize compressor-based heating for nearly all the heating load except at outdoor temperatures below $0^{\circ}\text{--}4^{\circ}\text{F}$, when the system relied exclusively on the auxiliary heat. The auxiliary heat at Site 13 was primarily used during defrost cycles and the following recovery period.

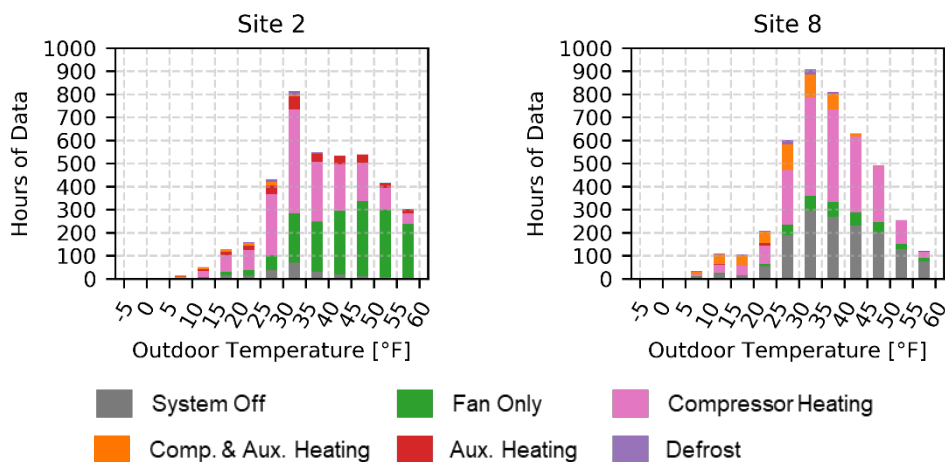


Figure 38. Operating modes for Sites 2 and 8 to highlight auxiliary heat use.

Table 12 shows the auxiliary heat runtime, in hours, during winter 2021–2022, binned by outdoor air temperature. The hours of auxiliary operation in Table 12 include operating modes of compressor plus auxiliary heating and auxiliary heating only; thus, time spent in defrost mode is not included here. The percentages in Table 12 are calculated as the amount of time the auxiliary heat is turned on divided by the total amount of time the system is providing heating. For example, a value of 50% would indicate the auxiliary heat is on for half the time when the system is providing space heating. In general, the auxiliary heater usage increases at colder temperature bins. The odd trend for Site 1 could be due to the small amount of data in the coldest three temperature bins.

The dual fuel heat pump at Site 3 could not run the natural gas furnace and heat pump simultaneously. The homeowner tweaked the heat pump and furnace lockout temperatures slightly during the study; however, the compressor lockout temperature hovered around 5°F and natural gas furnace lockout temperature was around 24°F. When the outdoor temperature was in between the two lockout temperatures, the system would assign heating priority to the heat pump, treating the natural gas furnace as an additional stage of heating. From Table 12, we see the heat pump was primarily used at outdoor air temperatures above 8°F. Below 8°F, the furnace was utilized more.

Table 12. Auxiliary Heat Runtime at Cold Temperatures During Winter 2022–2023

Site ID	Total Hours of Data	Auxiliary Heating Runtime [hours] (Percent of Total Heating Time)								
		≤0°F	0°–4°F	4°–8°F	8°–12°F	12°–16°F	16°–20°F	20°–24°F	24°–28°F	28°–32°F
1	605	0.2 (20.0%)	0.3 (17.0%)	2.4 (26.0%)	3.7 (32.2%)	7.7 (24.3%)	11 (20.8%)	11.2 (12.7%)	7.2 (12.7%)	21.5 (8.2%)
2	1135	0 N/A	0 N/A	3.4 (69.7%)	7.4 (32.4%)	14.6 (36.7%)	23.4 (27.6%)	24.9 (28.1%)	34.6 (21.3%)	52 (12.1%)
3	1119	12.5 (100.0%)	20.2 (96.2%)	21.3 (64.3%)	24.4 (46.1%)	12.4 (23.1%)	8.3 (8.8%)	0.6 (0.5%)	0.3 (0.2%)	0 (0.0%)
4	844	0 N/A	2.4 (86.7%)	2.4 (58.3%)	0.5 (16.1%)	4.1 (8.8%)	3.7 (4.4%)	1.2 (2.7%)	3.1 (4.4%)	7.8 (3.3%)
5	1712	0 N/A	0 (0.0%)	3.4 (35.4%)	21.4 (36.5%)	21.6 (32.6%)	18.2 (19.1%)	20.9 (13.6%)	25.4 (9.9%)	39.6 (9.1%)
6	1401	0 N/A	5.3 (87.2%)	2.6 (32.8%)	6.1 (10.6%)	7.4 (6.9%)	5.4 (5.7%)	8.3 (5.5%)	15.8 (5.2%)	20.4 (4.0%)
7	1369	0 N/A	0.1 (100.0%)	9.8 (54.9%)	14.6 (39.5%)	11.2 (16.5%)	2.7 (3.9%)	3.5 (3.2%)	7.9 (3.6%)	11.1 (3.2%)
8	1386	0 N/A	0.3 (51.4%)	5 (54.9%)	23 (55.2%)	36 (53.3%)	34.6 (48.7%)	46.1 (44.1%)	79.5 (39.6%)	83.1 (22.0%)
10	1819	14.5 (100.0%)	11.4 (84.4%)	8.2 (15.9%)	6.6 (7.9%)	6.6 (4.8%)	6 (3.9%)	5.2 (2.8%)	6.8 (2.9%)	6.1 (1.9%)
11	1594	0 N/A	1.2 (100.0%)	11.3 (61.5%)	13.2 (30.1%)	4.6 (17.4%)	11 (25.3%)	16.7 (24.2%)	35.4 (20.3%)	29.1 (14.1%)
12	409	0 N/A	0 N/A	0 N/A	7.6 (75.7%)	10.4 (46.1%)	8.5 (39.8%)	11.9 (29.5%)	16.7 (28.0%)	24.5 (24.5%)
13	1252	0 N/A	0 N/A	0 (0.0%)	0 (0.0%)	0 (0.0%)	0 (0.0%)	0 (0.0%)	1.6 (0.5%)	1.7 (0.3%)

5.5 Cycling and Capacity Modulation

Variable-capacity equipment adjusts the compressor speed to match the building load which should lead to lower cycling rates compared to single-stage and two-speed equipment, thereby improving efficiency and occupant thermal comfort. Thus, equipment runtime is expected to be higher than non-variable-capacity equipment; however, the equipment operates at higher COPs at lower compressor speeds.

Figure 42 plots the mean compressor heating runtime fraction binned by outdoor temperature, which was calculated by summing the fraction of time the compressor was operating in compressor-based heating, compressor plus backup, or defrost modes and dividing it by the total number of hours in the bin. Thus, a runtime fraction of 0.5 indicates the compressor was operating for 50% of the time. Figure 43 plots the number of cycles per hour binned by outdoor

air temperature, which was determined by counting the number of times the system cycled from off to heating (compressor-based heating, compressor with auxiliary heating, and auxiliary heating only) during a given hour. In general, we expect equipment with high runtime fractions to have low cycling rates because if the equipment is running for a large fraction of the time, it will not be cycling on and off.

We generally see the compressor runtime fraction increase as the outdoor air temperature drops because the compressor operates longer to meet the building heating load. However, the monitored runtime fractions are generally lower than expected based on the heating capacity and building load lines plotted in Figure 4, which could be due to solar gains or occupant thermostat heating setpoint adjustments. Site 6 had the highest runtime fraction, and the compressor ran nearly 100% of the time when outdoor air temperatures were between 5°F and 25°F. At Sites 3, 5, 8, and 10, the compressor runtime fraction decreases at the coldest temperature bins because the equipment has switched to using exclusively auxiliary heat. This trend is most pronounced at Site 3 due to the binary operation of the either the compressor or furnace in the dual fuel system. An occupant's thermostat temperature setback schedule can also explain lower-than-expected runtime fractions, such as at Site 8 where we expected compressor runtime fractions to be higher as the heat pump was undersized. Site 11 had the lowest mean runtime fractions, which was due to long time spans where the equipment did not operate and thus the runtime fraction was zero for many hours. This also explains the trends in Figure 43 for Site 11. The heat pump at Site 11 often had one on-cycle during a 24-hour period; thus there were many hours with zero on/off cycles.

The cycling rate for most sites was approximately 1–2 cycles per hour. However, the heat pump at Site 13 cycled notably more than the other sites and exhibited higher than normal cycling rates at outdoor air temperatures above 40°F. Figure 39 plots an eight-hour period from Site 13 showing the ODU and IDU power consumption for a mild day in November 2021 where outdoor air temperature ranged from 40°–45°F. During this time, the equipment exhibited short cycling with ~7–8 cycles per hour. It is possible the issue was resolved with a service call because the short cycling issue appears to have been resolved starting in early January (Figure 40).

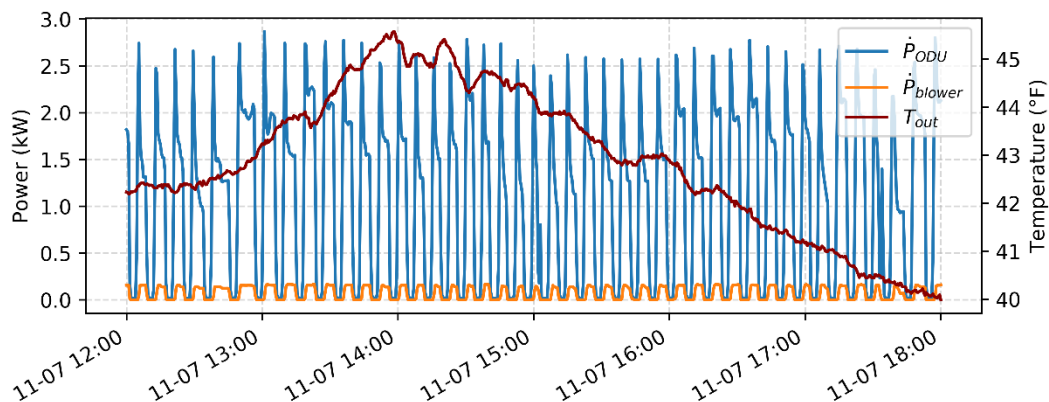


Figure 39. High cycling rate at Site 13 during mild temperatures.

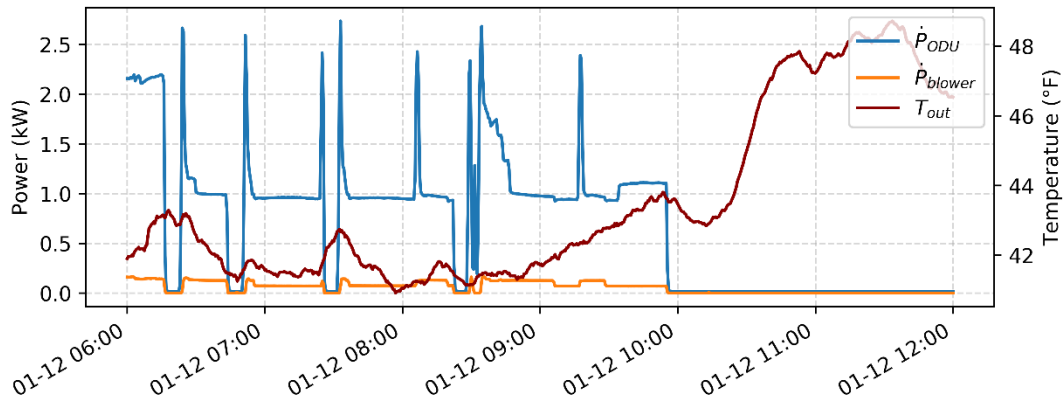


Figure 40. High cycling rate resolved at Site 13.

Figure 44 plots the compressor inverter frequency during steady state heat operation, which is proportional to the compressor speed, and Figure 45 plots a histogram of the fraction of time spent in each inverter frequency bin during winter 2021–2022. There was a measurement error with the inverter frequency at Site 13, so plots for Site 13 are not included in Figure 44 and Figure 45.

During steady-state heating, we expect the inverter frequency to be higher at colder outdoor air temperatures because the system will increase the compressor speed to match higher building heating loads. However, the onboard controls for some systems, such as the heat pumps at Sites 3 and 6, decrease the compressor speed at very cold temperatures, which is observable in Figure 44. Additionally, because a variable-capacity heat pump should adjust the compressor speed to match the heating load, we expect a narrow range of steady state inverter frequencies at each outdoor air temperature bin, which is clear at Sites 1–6 and 10. The plot for Site 8 in Figure 44 indicates the system operated at a broad range of compressor speeds for most outdoor air temperature bins; however, Figure 45 shows the compressor operated primarily at low and high speeds. The heat pump at Site 10 was the only noncommunicating system in the study, which explains why there was less variation in the inverter frequency with respect to outdoor air temperature compared to other systems.

From Figure 45 we see that systems operated for a relatively small amount of time at maximum compressor speed and Sites 1, 3, 4, 7, 8, 10, and 11 operated at minimum compressor speed for the greatest amount of time. The inverter frequency for the heat pump at Site 5 was more evenly spread across the range of speeds compared to the other sites. The heat pump at Site 3 was not a fully variable system with five discrete compressor speeds, which is evident in the histogram.

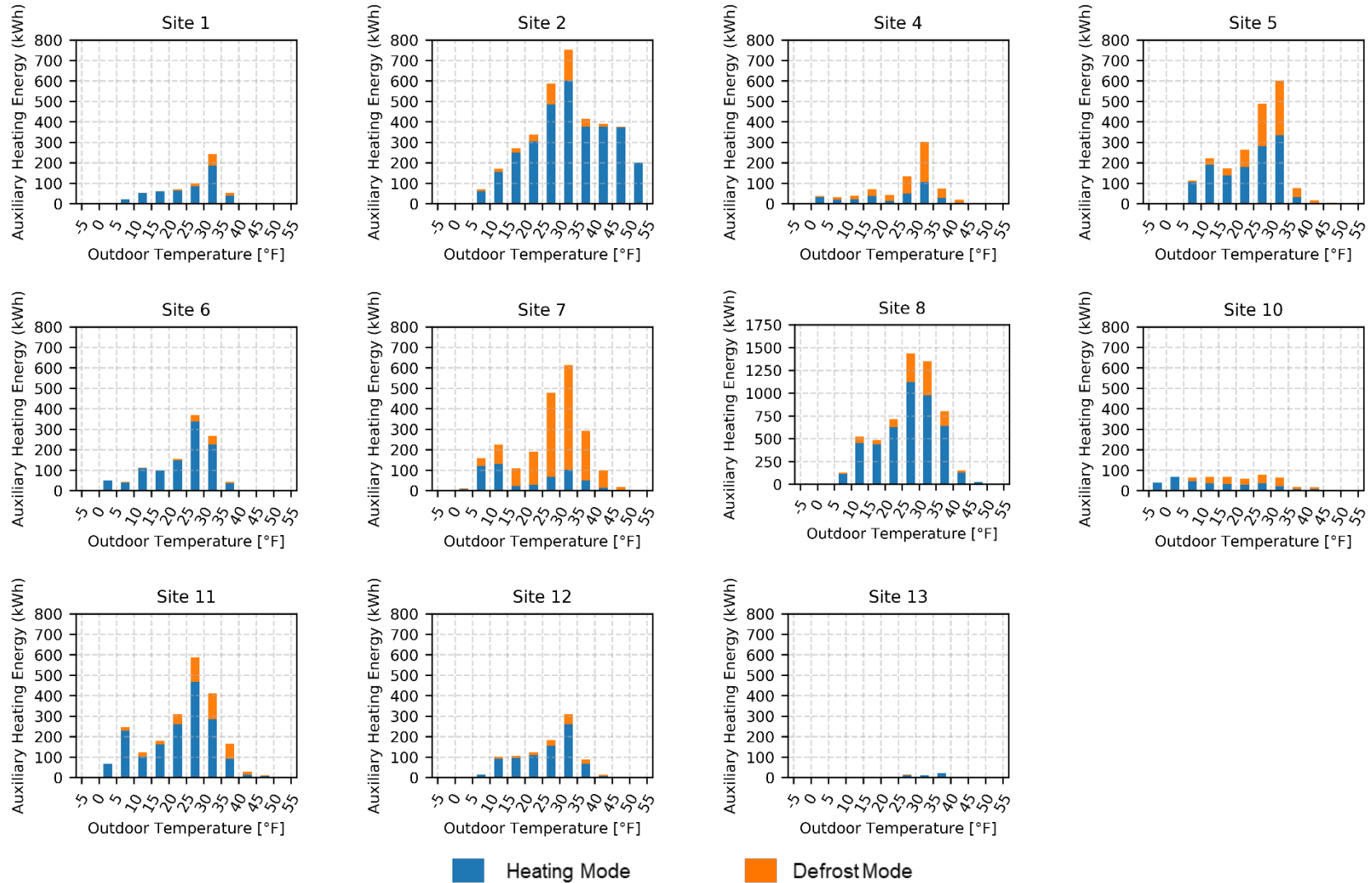


Figure 41. Auxiliary heater energy in heating (blue) and defrost (orange) modes during winter 2021–2022.

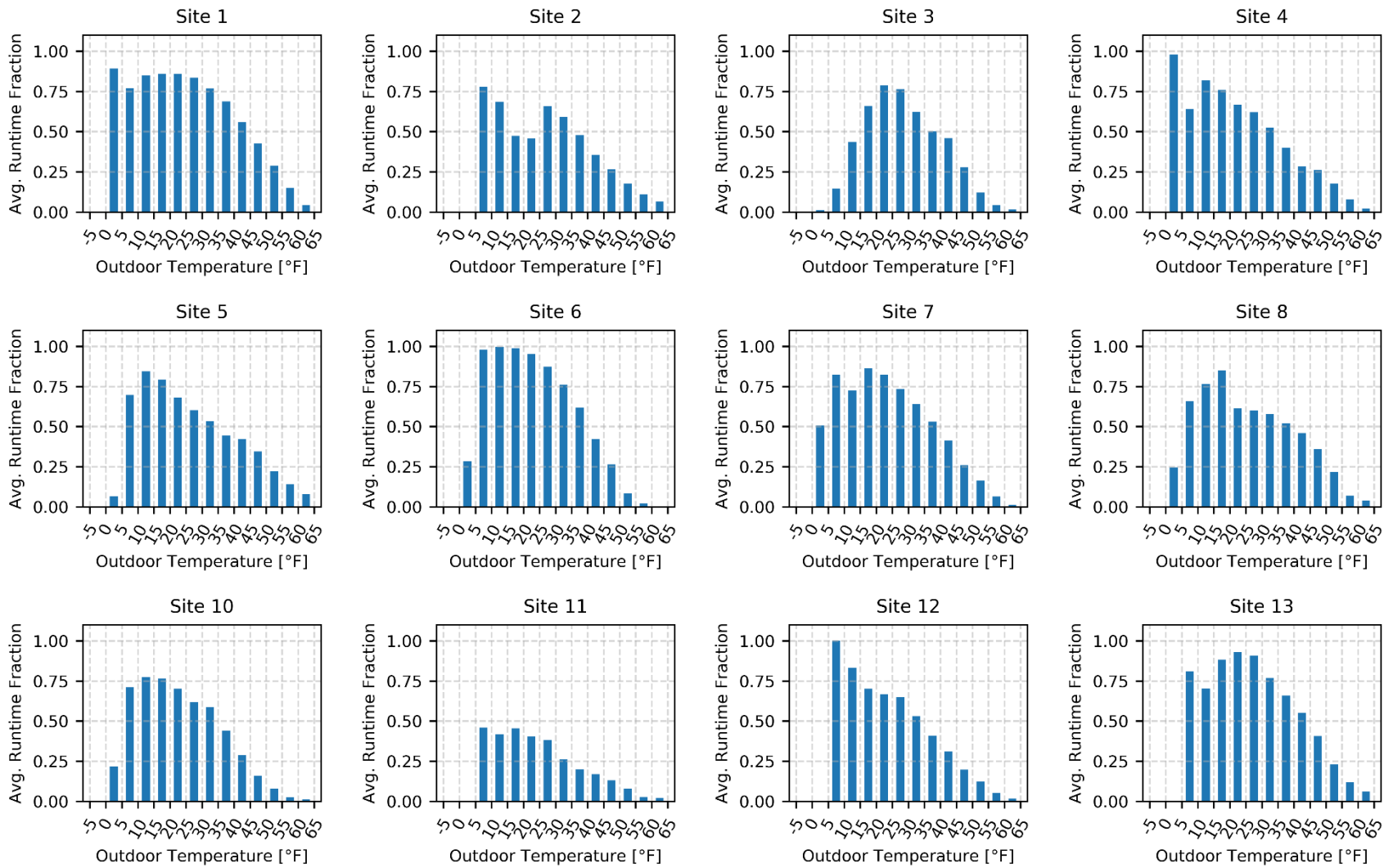


Figure 42. Mean compressor heating runtime fraction.

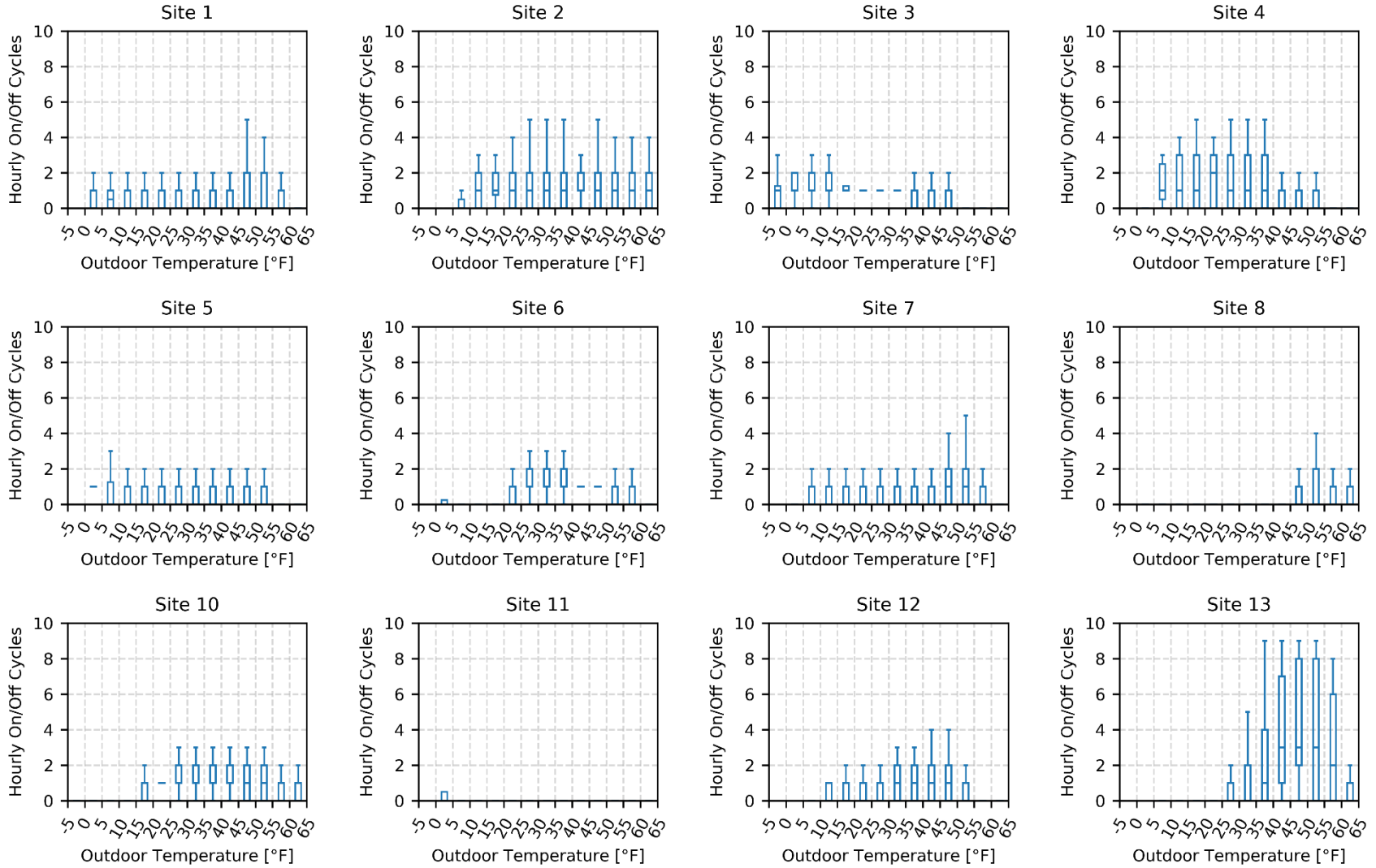


Figure 43. Box and whisker plot of compressor cycles per hour during winter 2021–2022.

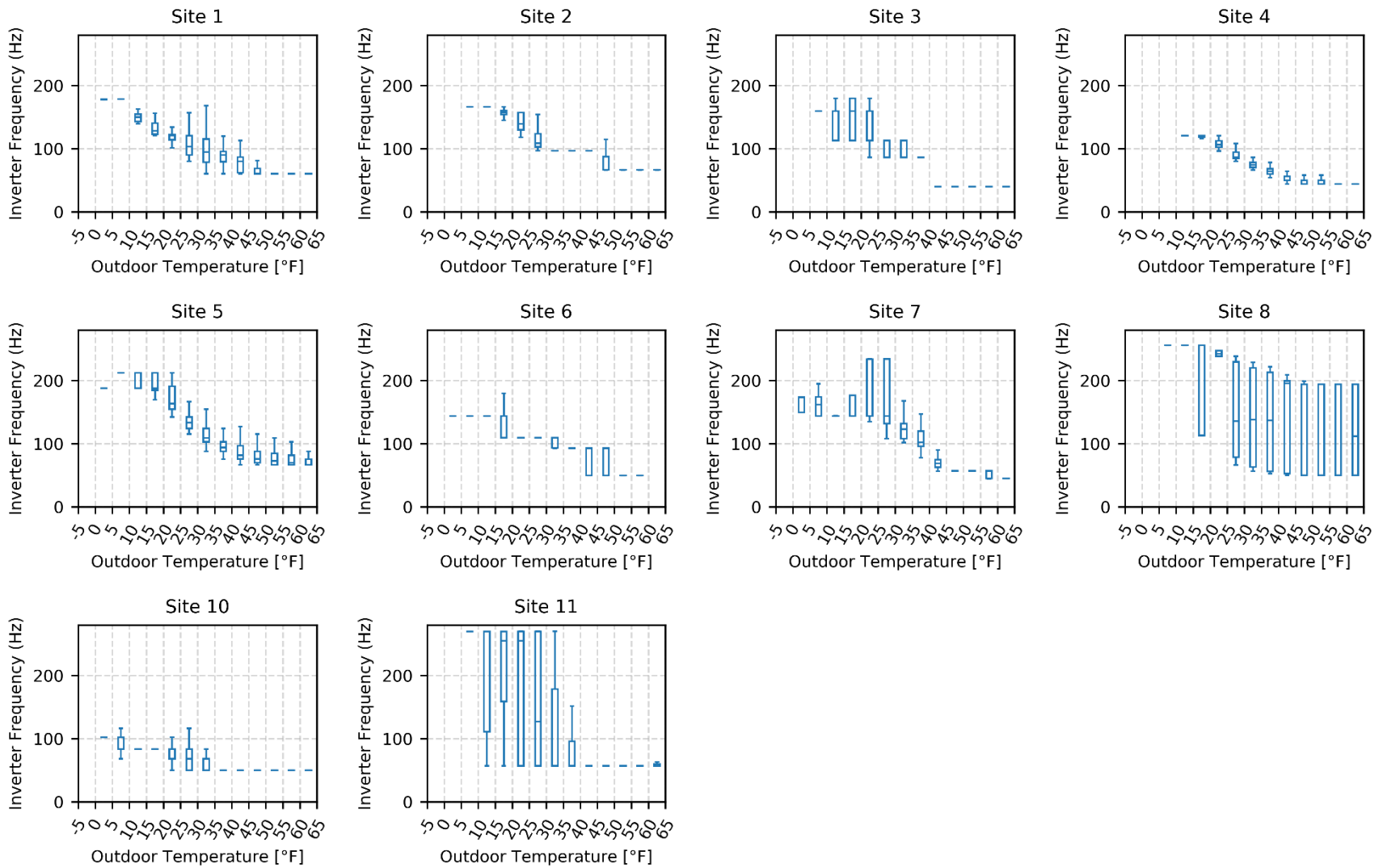


Figure 44. Box and whisker plot of inverter frequency during steady-state compressor-based heating operation.

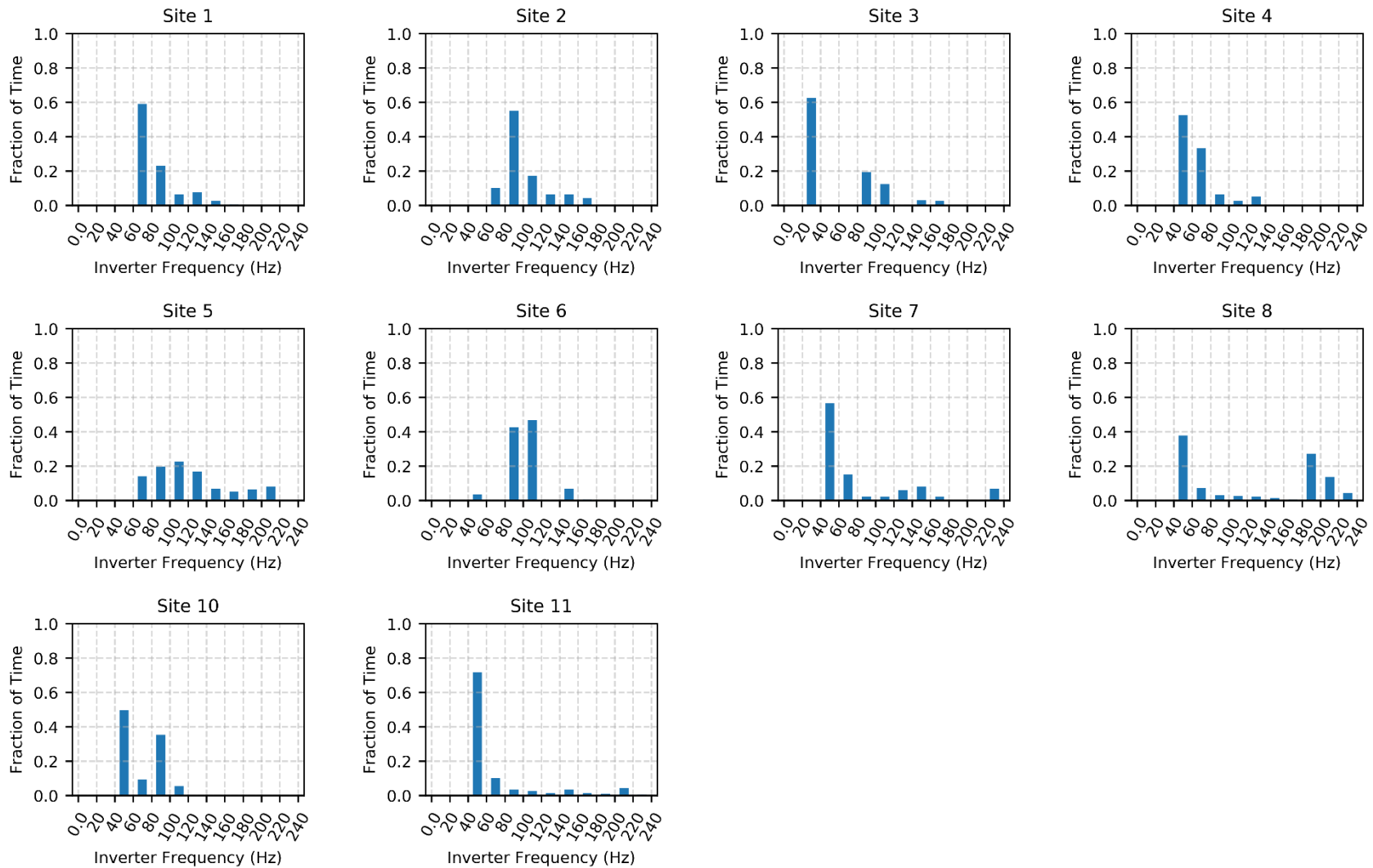


Figure 45. Fraction of time spent at a given inverter frequency during steady-state compressor-based heating operation during winter 2021–2022.

5.6 Defrost

During heating operation at cool outdoor air temperatures, frost can accumulate on the outdoor coil when the coil surface temperature is colder than the outdoor dewpoint temperature. Excessive frost formation will reduce the ODU airflow rate and overall heat transfer and thus must be periodically melted to maintain performance. Defrosting the outdoor coil is accomplished by using the compressor to send hot refrigerant to the coil, which is the same as cooling mode operation. Defrost operation is important to investigate because it can consume a significant amount of energy.

Figure 52 shows the total amount of time spent in defrost mode with respect to the outdoor wet-bulb temperature (WBT) during winter 2021–2022. We see that a relatively small fraction of the time was spent in defrost mode for all sites except Site 7. However, the amount of energy consumed by defrost mode was significant for Sites 5, 7, 8, and 11, shown in Table 11, where defrost mode consumed more than 20% of the energy used to provide compressor-based heating. Figure 53 shows the total number of defrost cycles during winter 2021–2022, which was determined by counting the total number of defrost cycles in an outdoor WBT bin. The number of defrost cycles was highest between 20° and 40°F outdoor WBT, which is expected as defrost isn't necessary at warm outdoor air temperatures, and at cold outdoor temperatures the air moisture content is low.

From Figure 53, we see the heat pump at Site 7 had the most defrost cycles, which warrants additional discussion. Figure 46 shows a particular day with frequent defrost cycles, occurring as frequently as every 30 minutes between midnight and 10 a.m. with an average length of approximately seven minutes. Figure 47 and Figure 48 show the corresponding power and temperature measurements during this period. The outdoor air temperature was consistently around 32°F (0°C). We see that the refrigerant vapor line surface temperature ($T_{ref,out,clg,exit}$) decreases while the compressor operates during the reverse cycle and the auxiliary heater is turned on, which indicates a defrost cycle is occurring. It appears the system operates at a particular speed during defrost. During the early morning hours shortly after midnight, we see the compressor speed increase during the defrost cycle. However, during the hours of 4 a.m. to 6 p.m., we see the system decrease the compressor speed during defrost. It is unclear why the heat pump at Site 7 controlled the defrost operation in this manner.

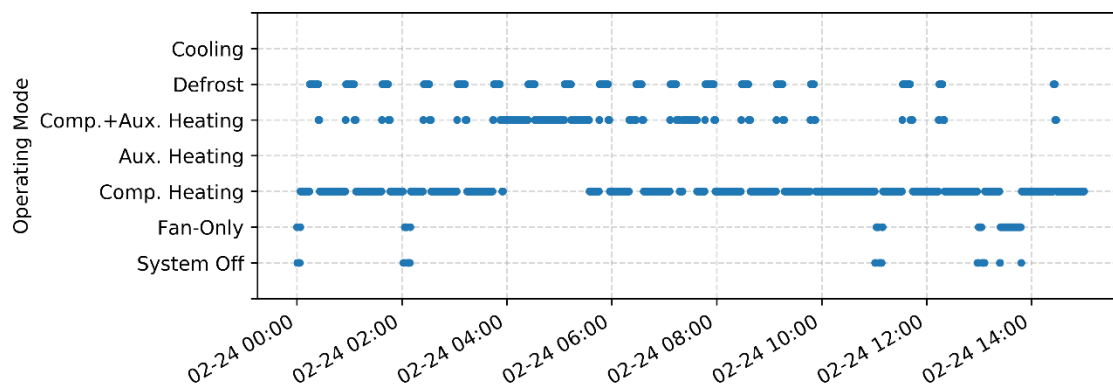


Figure 46. An example day with frequent defrost cycles for the heat pump at Site 7.

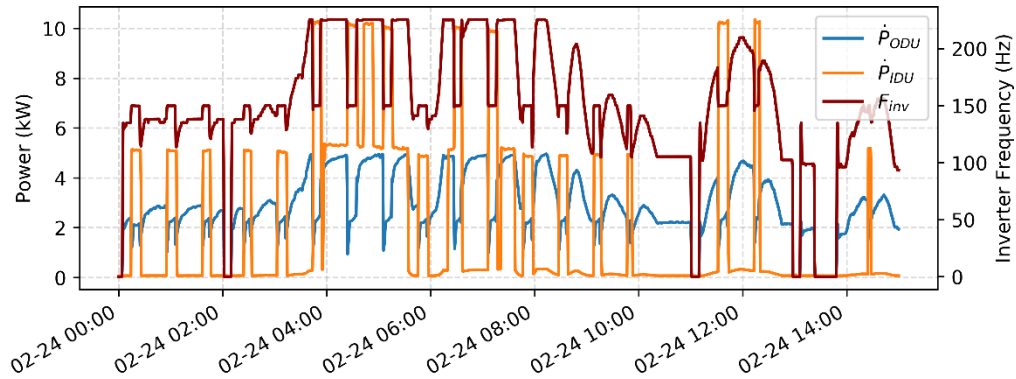


Figure 47. ODU, IDU, and blower power and compressor inverter frequency during a day with frequent defrost cycles at Site 7.

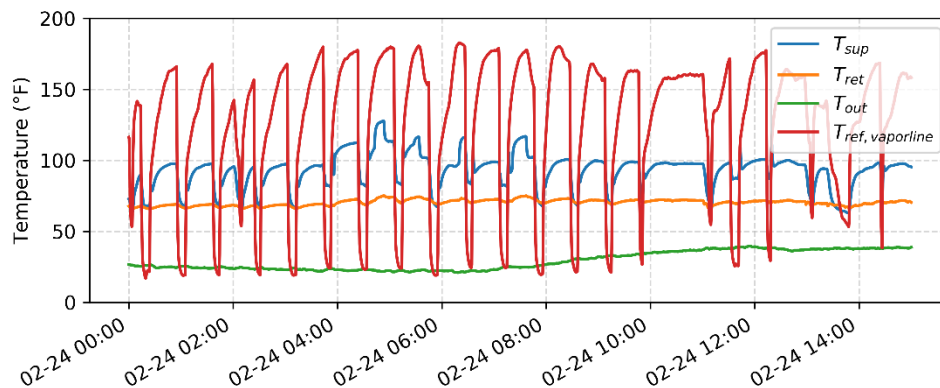


Figure 48. Air and refrigerant temperatures during a day with frequent defrost cycles at Site 7.

Figure 54 plots the defrost cycle lengths for each site. For most of the sites, we see the length of the defrost cycle was longer at lower outdoor WBT, which is expected as demand-based defrost control is typically terminated using an outdoor coil surface temperature sensor. A few sites (Sites 1, 3, and 13) had defrost cycles lasting less than five minutes while most of the sites had average cycle lengths of 3–7 minutes. The exceptions were Sites 4, 7, and 8 which had longer defrost cycles. The long defrost cycles for Site 4 were at cold outdoor WBTs and from Figure 53 we see there were a relatively small amount of defrost cycles in this temperature bin.

Figure 49 shows an example winter day for Site 7 with a long defrost cycle lasting for about 16 minutes between 4:28 a.m. and 4:43 a.m. where each point represents the operating mode for each 30-second sample. Figure 50 and Figure 51 show the corresponding power and temperature measurements during this defrost cycle. Despite the first stage of the auxiliary heater being on for the defrost cycle, the supply air temperature is lower than the return temperature, which means the defrost cycle will cool the house when the outdoor temperature is approximately 10.4°F (-12°C). Utilizing more than 5 kW of the 20-kW auxiliary heater could have potentially mitigated the cooling effect.

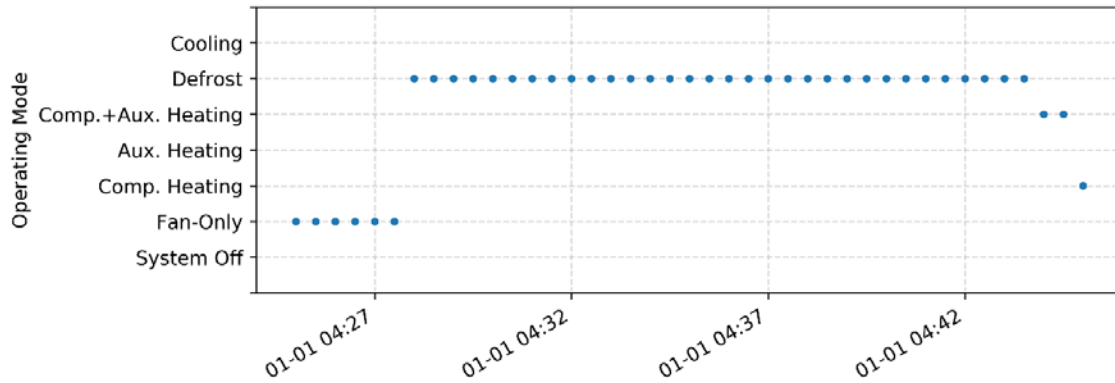


Figure 49. An example day with a long defrost cycle at Site 7.

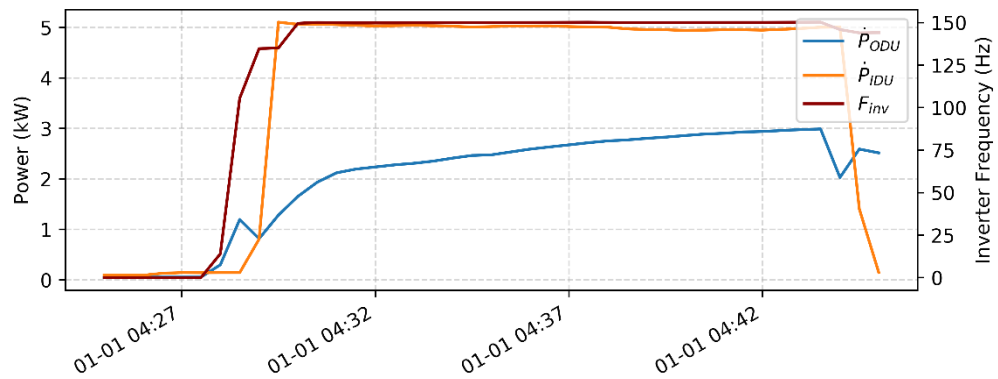


Figure 50. ODU power, IDU power, and compressor inverter frequency during a long defrost cycle at Site 7.

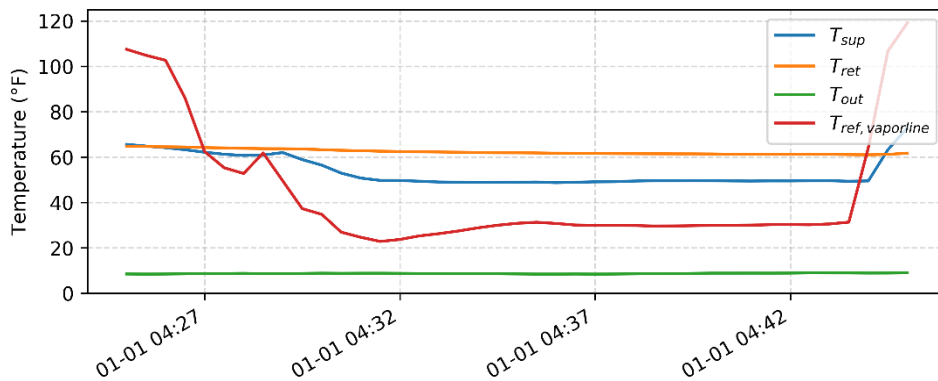


Figure 51. Air and refrigerant temperatures during a long defrost cycle at Site 7.

The defrost energy listed in Table 11 was calculated during the reverse cycle operation and did not include energy consumed during the defrost recovery period. For all the sites, the auxiliary heater operated during and/or immediately following the defrost cycle. The dual fuel system at Site 3 ran the gas furnace during the defrost cycle, which essentially transfers furnace heat to the

heat pump refrigeration system to melt the frost as the furnace was downstream of the indoor coil. Table 13 lists the auxiliary heater average runtime and power following the reverse defrost cycle. Sites 1, 8, and 13 ran auxiliary heat following the defrost cycle while most of the other sites only ran the auxiliary heat during the defrost cycle. The heat pumps at Sites 1 and 8 had the same manufacturer. In some instances, the auxiliary heat ran for longer time periods following a defrost cycle depending on the building heating load. To differentiate and account for auxiliary heat during defrost recovery, we took the statistical mode of the auxiliary heat runtime following a defrost cycle to calculate the auxiliary heating cycle runtime and corresponding average power.

Table 13. Auxiliary Heat Use Following a Defrost Cycle During Winter 2021–2022

Site ID	Auxiliary Heater Runtime Following Defrost [min.]	Average Auxiliary Heater Cycle Power Following Defrost [kW]
1	6.5	11.9
2	0.5	8.1
4	0.5	10.6
5	0.5	8.0
6	0.5	13.3
7	0.5	6.6
8	5.5	18.3
10	1.0	4.5
11	0.5	13.8
12	0.5	10.0
13	2.5	6.1

5.7 Heating Supply Air Temperature

Central forced air heat pumps have a reputation for supplying cooler air compared natural gas furnaces, which could lead to thermal comfort issues for occupants accustomed to furnaces. Additionally, the supply air temperature is proportional to the heating capacity, which decreases as the outdoor temperature gets colder.

Figure 55 plots the steady-state compressor-based heating supply temperature binned by outdoor air temperature. In general, the supply air temperature for all sites rarely exceeded 100°F, whereas fossil-fuel furnaces typically supply air close to 120°F. Some sites maintained a relatively constant supply air temperature independent of outdoor air temperature (Sites 1, 4, 5, 6, and 13), while the supply air temperature decreased at colder outdoor air temperatures for others (Sites 2, 7, 8, 10, 11, and 12). The supply air temperature at Site 6 had a notable step change between the 40°–45°F and 45°–50°F temperature bins, which appears to be due to the compressor speed control, shown in Figure 44, which exhibited a similar trend.

5.8 Standby Power Consumption

Booten, Christensen, and Winkler (2014) showed that crankcase heater energy use can be significant in oversized heat pumps. Though most of the heat pumps in this study were estimated

to be undersized (Table 6), we briefly discuss the standby energy use, which was calculated when the systems were off.

Figure 56 plots the ODU and IDU power consumption when the systems were off. All heat pumps in the study included a compressor crankcase heater in the ODU but the type (internal or bellyband), wattage, and control algorithm varied across the sites. Site 7 had the highest standby power of the all-electric sites, consistently consuming ~80 Watts. The ODU standby power for the heat pump at Site 5 was dependent on the outdoor air temperature indicating the crankcase heater was turned off at temperatures above ~45°F. The ODU standby power for the other sites was not dependent upon the outdoor air temperature. The increase in the IDU standby power for Site 3 at cold temperatures could be due to the furnace inducer motor turning on prior to the blower during the furnace startup sequence.

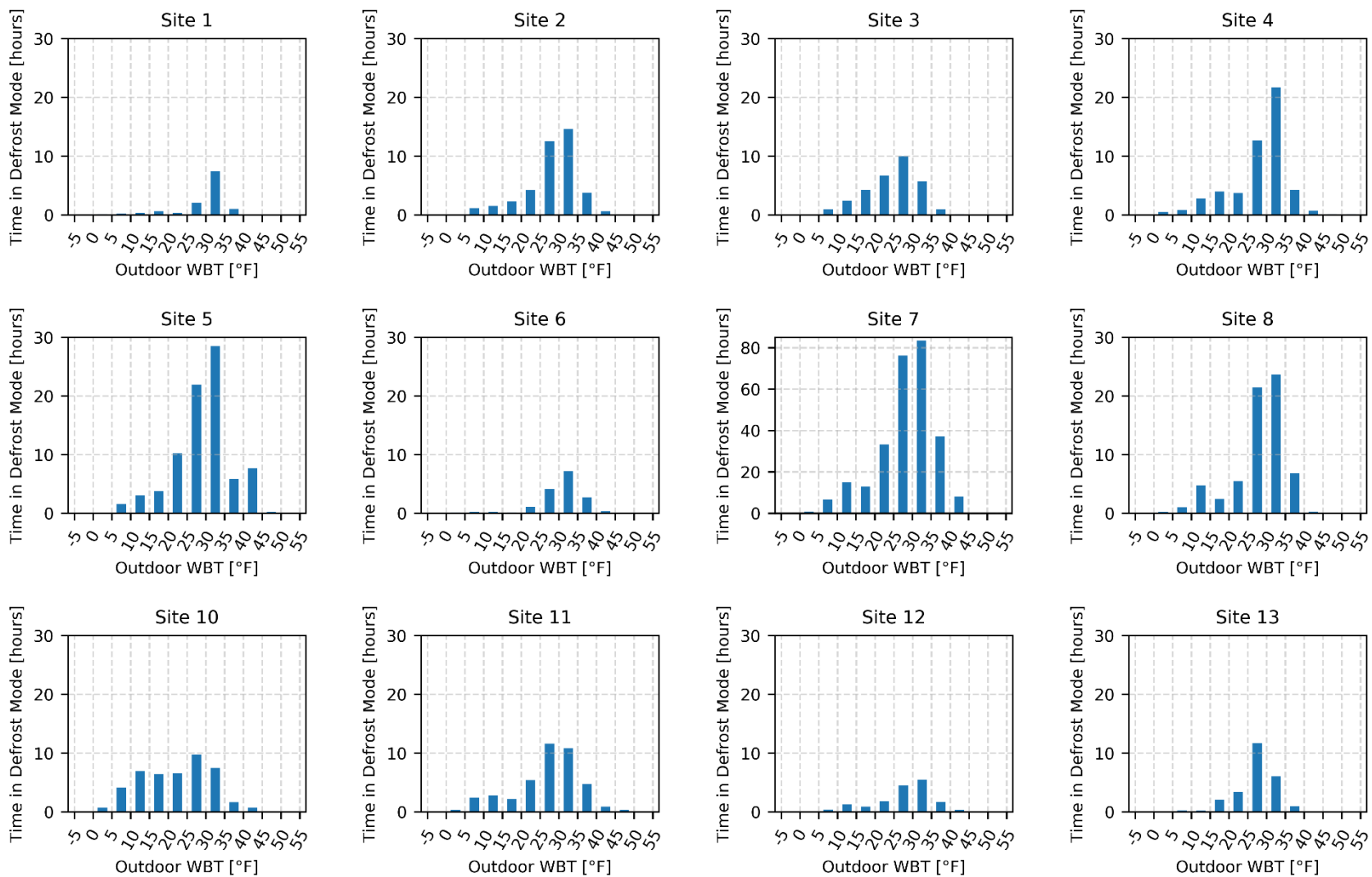


Figure 52. Time spent in defrost mode during winter 2021–2022.

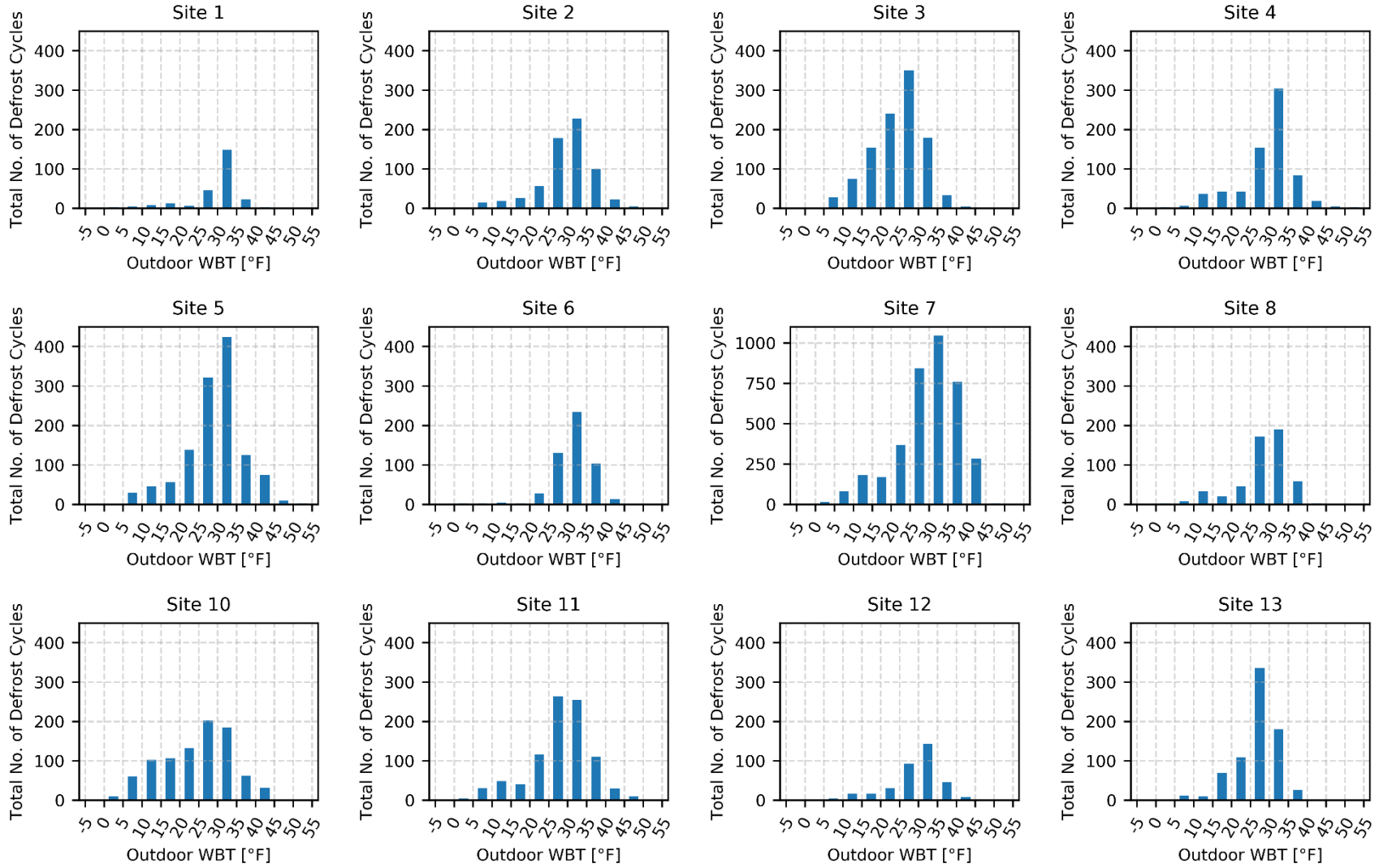


Figure 53. Total number of defrost cycles during winter 2021–2022.

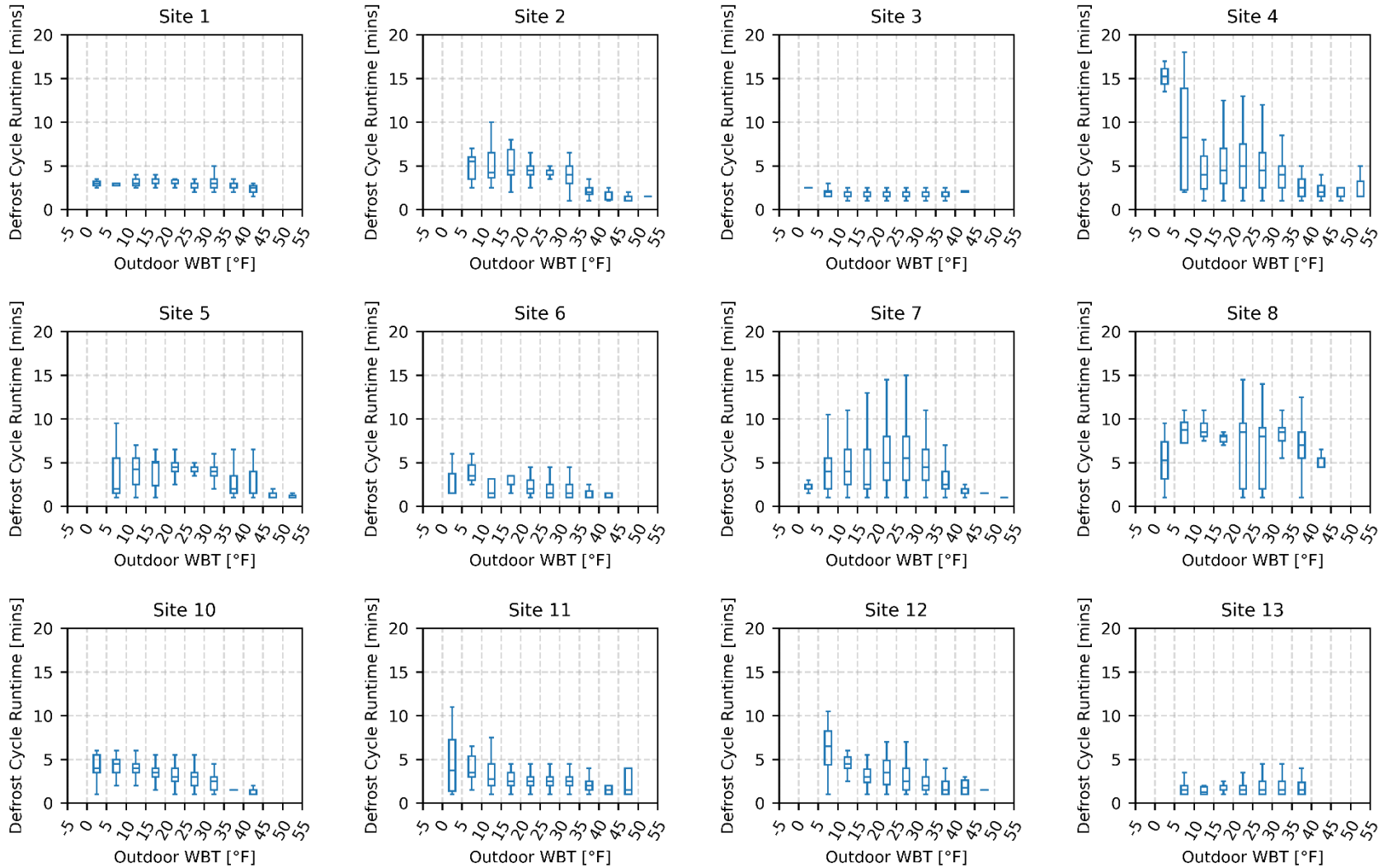


Figure 54. Box and whisker plot showing the defrost cycle length during winter 2021–2022.

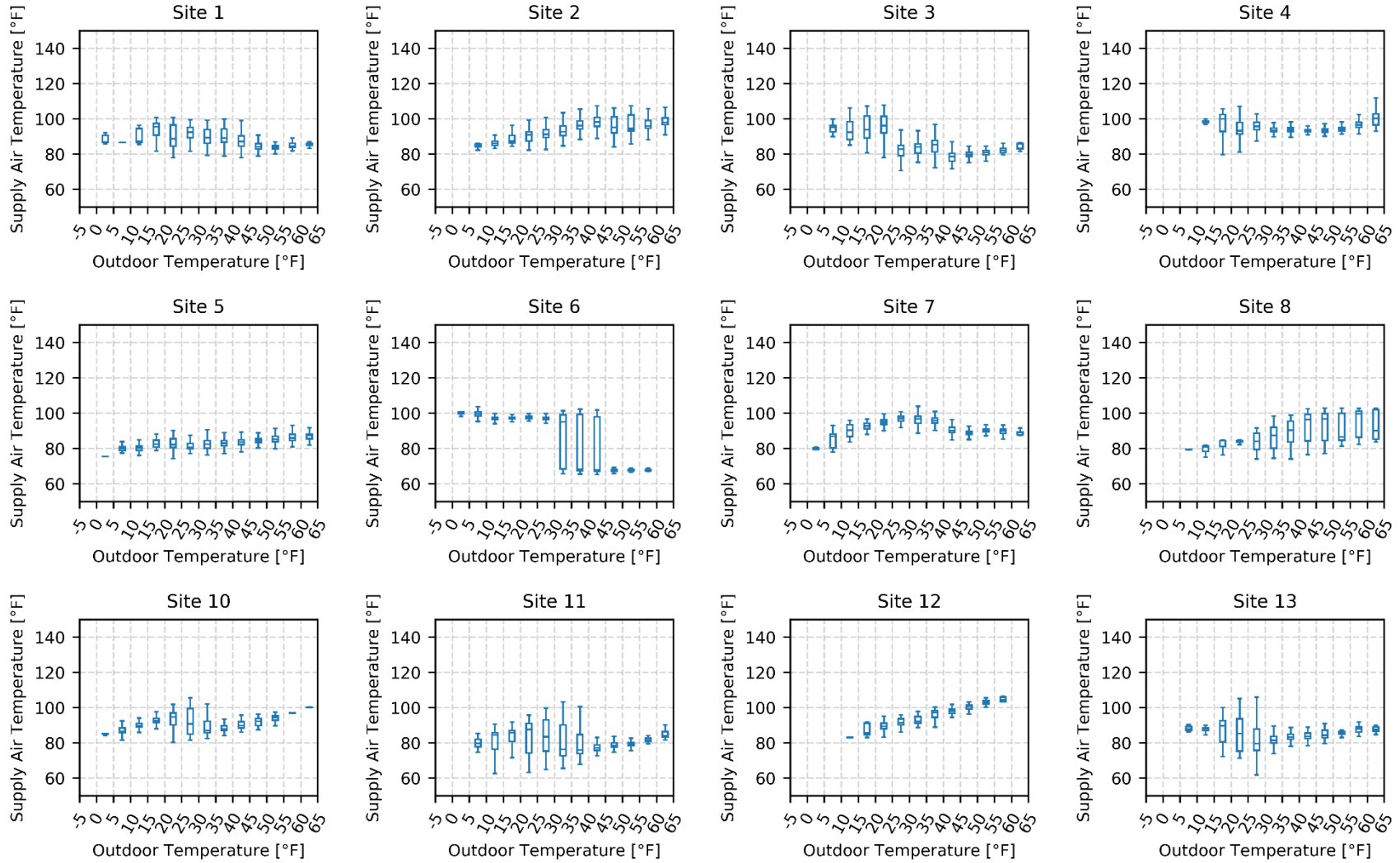


Figure 55. Box and whisker plot showing heat pump supply air temperature during periods of steady-state compressor-based heating.

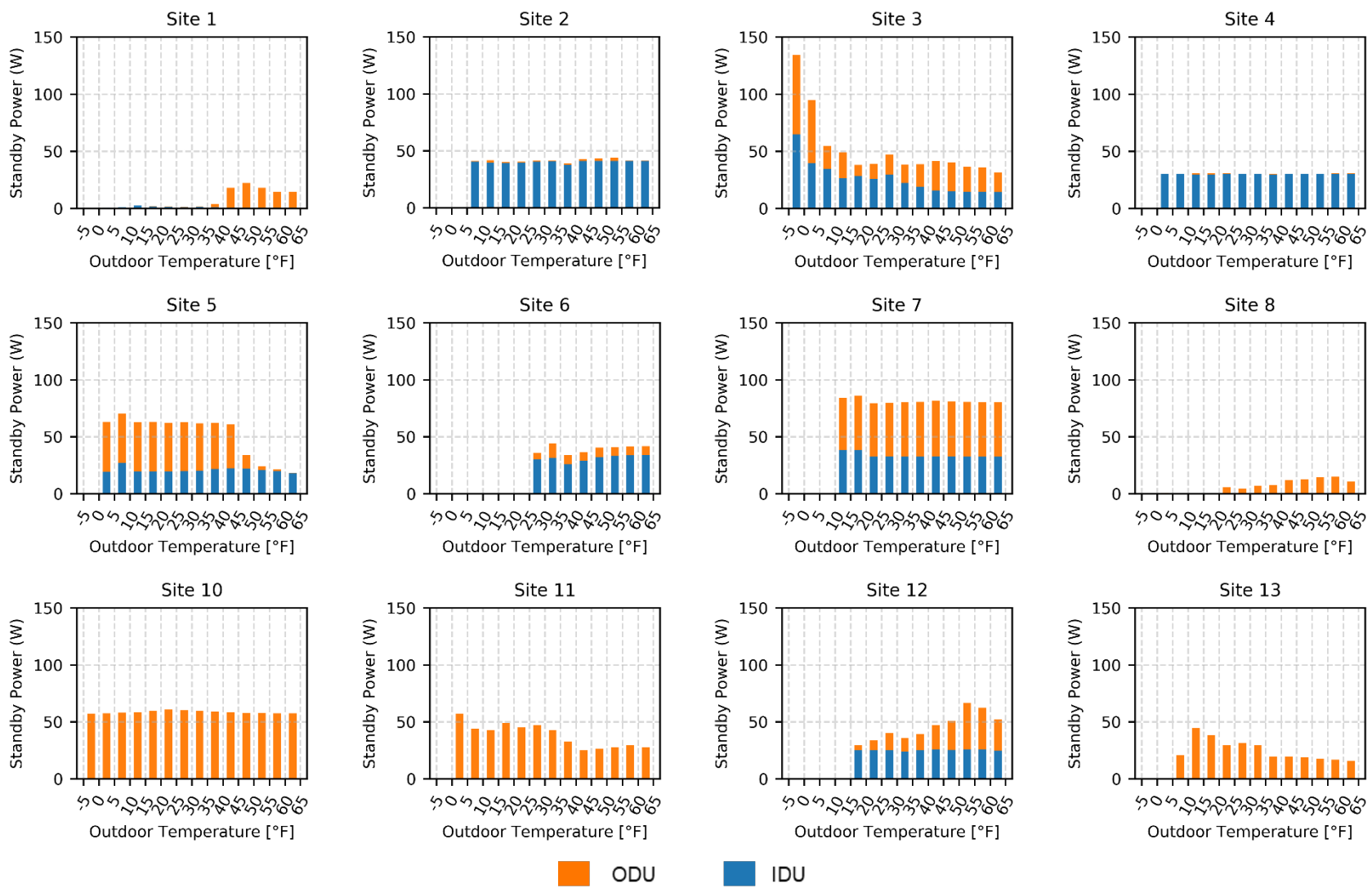


Figure 56. Average ODU (orange) and IDU (blue) standby power during winter 2021–2022.

6 Cooling Mode Performance Results and Discussion

Though the focus of the study was on assessing heating mode performance specifically at cold outdoor temperatures, the conditions at most sites also reached hot outdoor temperatures and cooling data was collected. This section briefly summarizes the observed cooling mode performance.

6.1 Cooling Season Operating Modes

During the cooling season the heat pumps are either off, in fan-only mode, or in cooling mode. Figure 57 shows a histogram of operating modes binned by outdoor temperatures ranging from 75°–115°F. The outdoor temperature exceeded 110°F for several hours at some sites, which is unusually warm for these locations. For reference, the ASHRAE 1% summer dry-bulb temperature for Spokane, Washington is 88.9°F, which means the outdoor temperature exceeds 88.9°F for approximately 88 hours per year, on average. Some sites had a few hundred hours above 90°F, as shown in Figure 57.

Despite the unusually warm summer conditions, several heat pumps did not operate for many hours in cooling mode. The heat pumps at Sites 4, 8, 10, 12, and 13 were off for most of the summer. The lack of heat pump cooling operation could have been due to occupant thermostat schedules or diurnal temperature changes precooling the building. The heat pump at Site 7 operated in cooling mode for the greatest amount of time. It is interesting to note that the return plenum issue (mentioned in Section 2.2.1) was confirmed and resolved by the installation contractor during the summer because the occupants were uncomfortable.

Similar to the winter season, the heat pumps at Sites 3, 6, and 12 ran for a significant amount of time in fan-only mode. Sites 2 and 8 also ran the heat pump in fan-only mode during the summer.

6.2 Cooling Capacity and Coefficient of Performance

Figure 58 and Figure 59 plot the steady-state cooling COP. Figure 58 plots 30-second down-sampled data using a box and whisker plot, whereas Figure 59 plots the capacity-weighted mean COP calculated by summing total cooling output within a temperature bin and dividing it by the total energy consumption. IDU blower power is accounted for in the COP calculation (e.g., net COP). Figure 60 is similar to Figure 58, plotting cooling capacity rather than COP. In general, we see the cooling COP decrease as the outdoor air temperature increases, as expected. For several sites we see the steady state capacity increase as the outdoor air temperature rises because the heat pump increases the compressor speed to meet higher building cooling loads. The heat pump at Site 13 did not operate for many hours in cooling mode, particularly at outdoor temperatures below 100°F, which explains the lack of steady state COP data in Figure 58 through Figure 60.

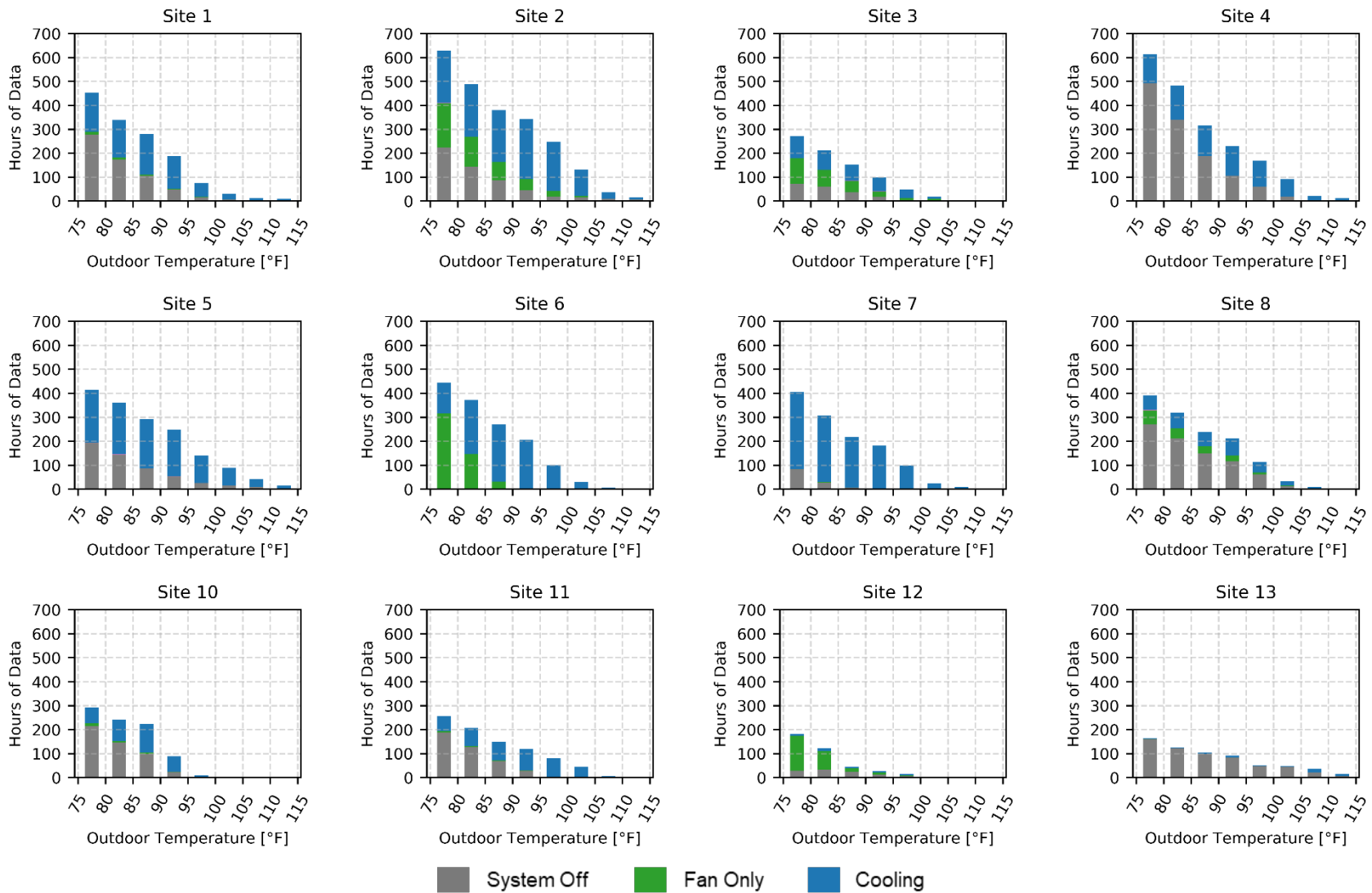


Figure 57. Heat pump operational modes at warm outdoor air temperatures.

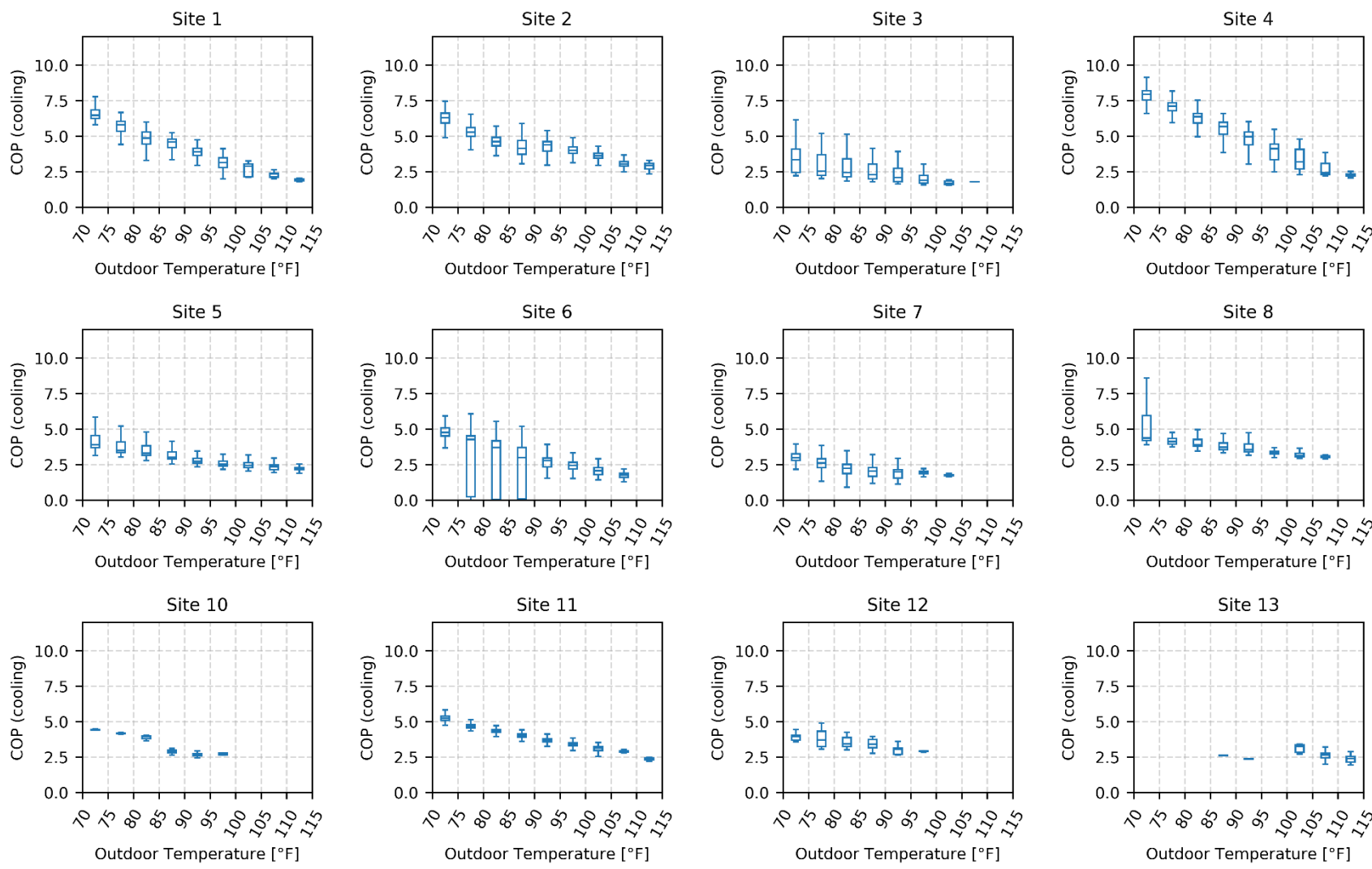


Figure 58. Box and whisker plot of steady-state cooling COPs.

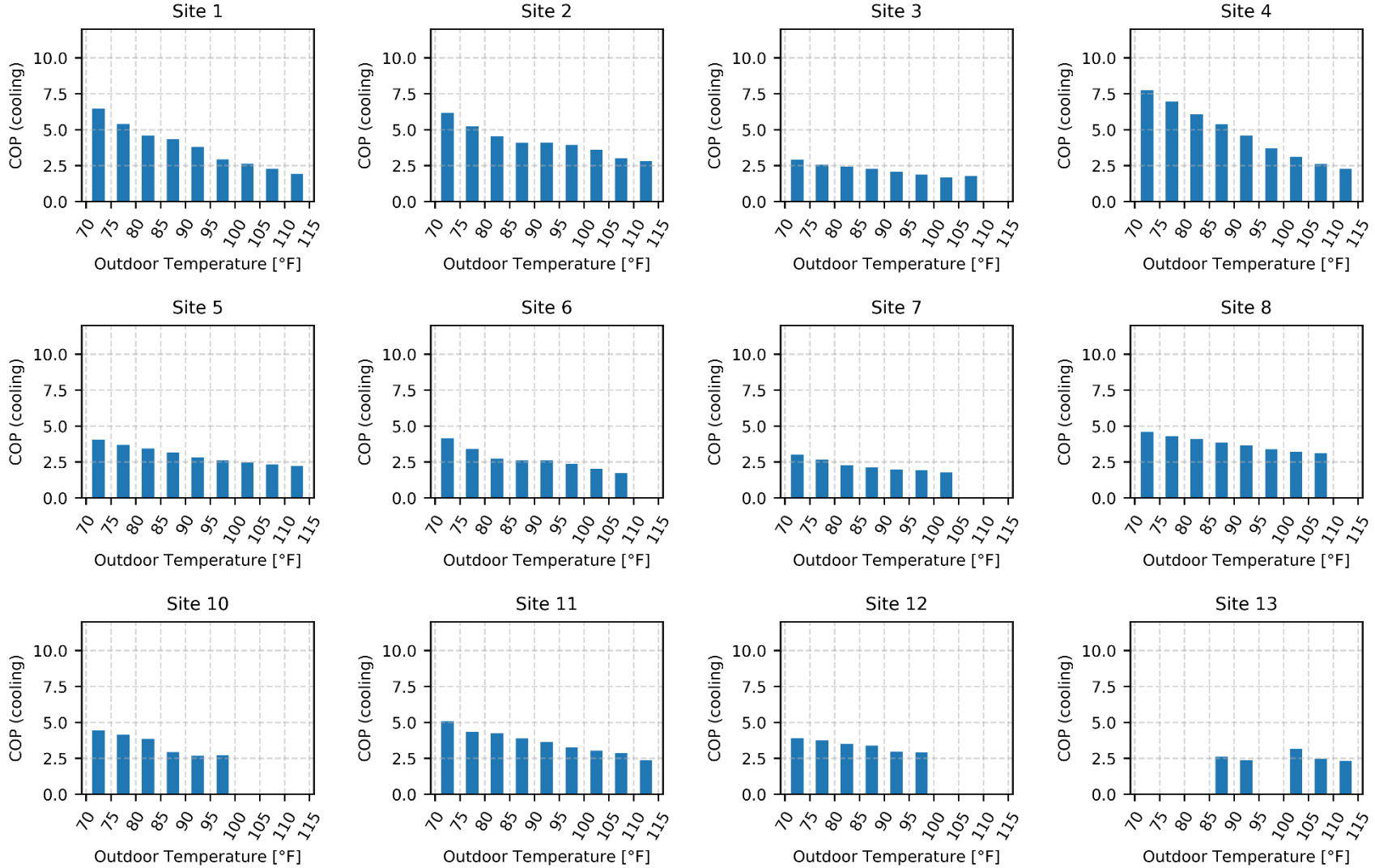


Figure 59. Mean steady-state cooling COPs.

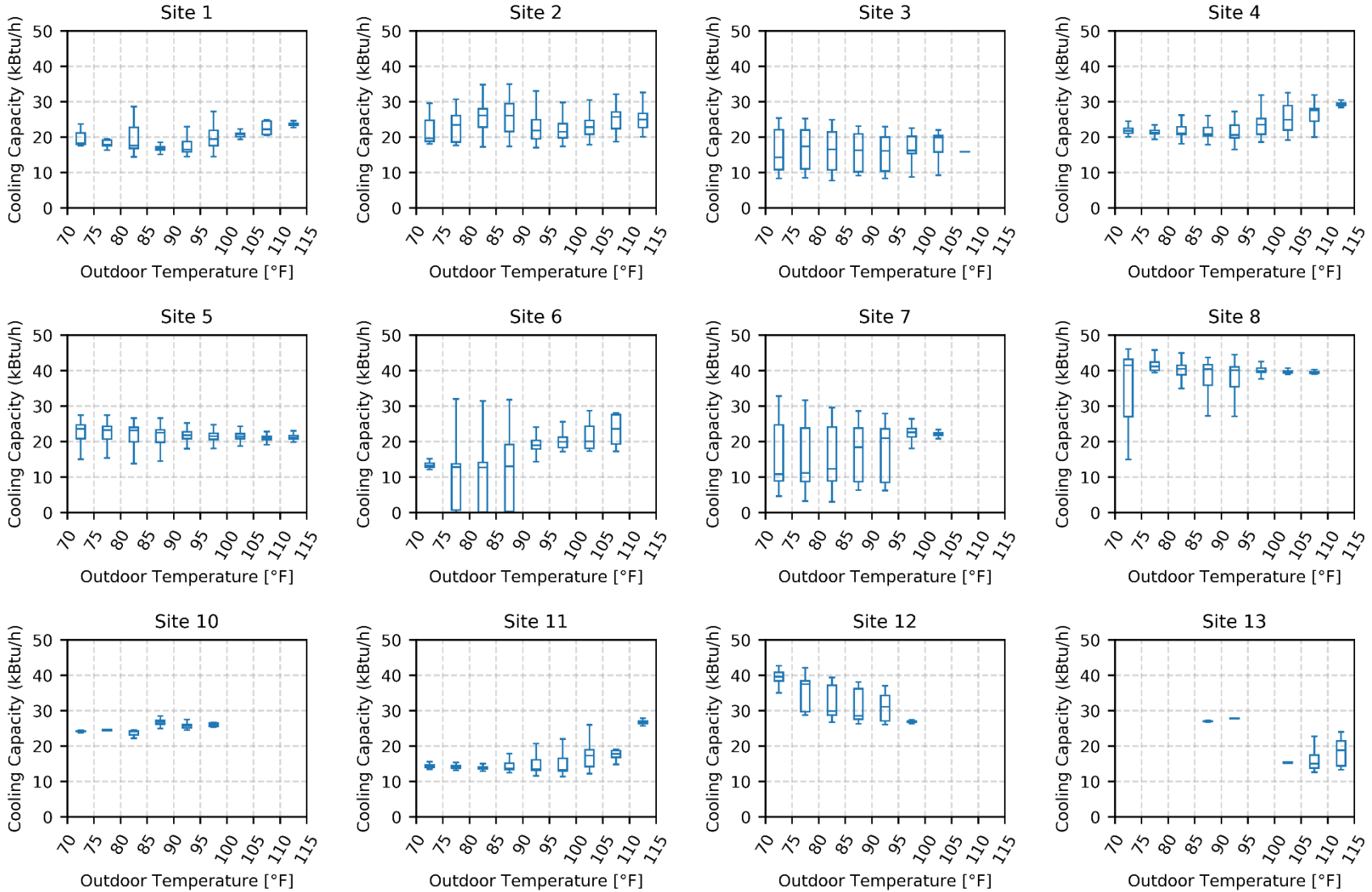


Figure 60. Box and whisker plot of steady-state cooling total capacity.

6.3 Capacity Modulation and Cycling

Figure 62 plots the mean cooling runtime fraction binned by outdoor temperature, which was calculated by summing the fraction of time the system was operating in cooling mode and dividing it by the total number of hours in the bin. The trends in Figure 62 are similar to the data plotted in Figure 57, and in general, we see the compressor runtime fraction increase as the outdoor air temperature gets hotter because the compressor operates longer to meet the building cooling load. The heat pumps at Sites 3, 8, 12, and 13 rarely operated for more than 75% of the time at any outdoor temperature bin. The heat pumps at Sites 6 and 11 ran continuously at outdoor temperatures above 90°F and 95°F, respectively. The cooling runtime fraction for the heat pump at Site 7 equaled one for most of the summer. As the focus of the study was on heating mode performance, design cooling load calculations were not conducted. Thus, it is difficult to assess the heat pump sizing for cooling operation.

The heat pumps at all but four sites operated at very low cycling rates. Figure 61 plots the number of cycles per hour binned by outdoor air temperature for Sites 1, 2, 3, and 10, which was determined by counting the number of times the system cycled from off to cooling. The other sites are not plotted because there were zero on/off cycles for most of the hours, similar to the 75°–80°F temperature bin for Site 3 in Figure 61. The cooling mode cycling rates for Sites 1 and 2 were higher compared to heating mode cycling, whereas cooling and heating cycling rates were similar for Sites 3 and 10.

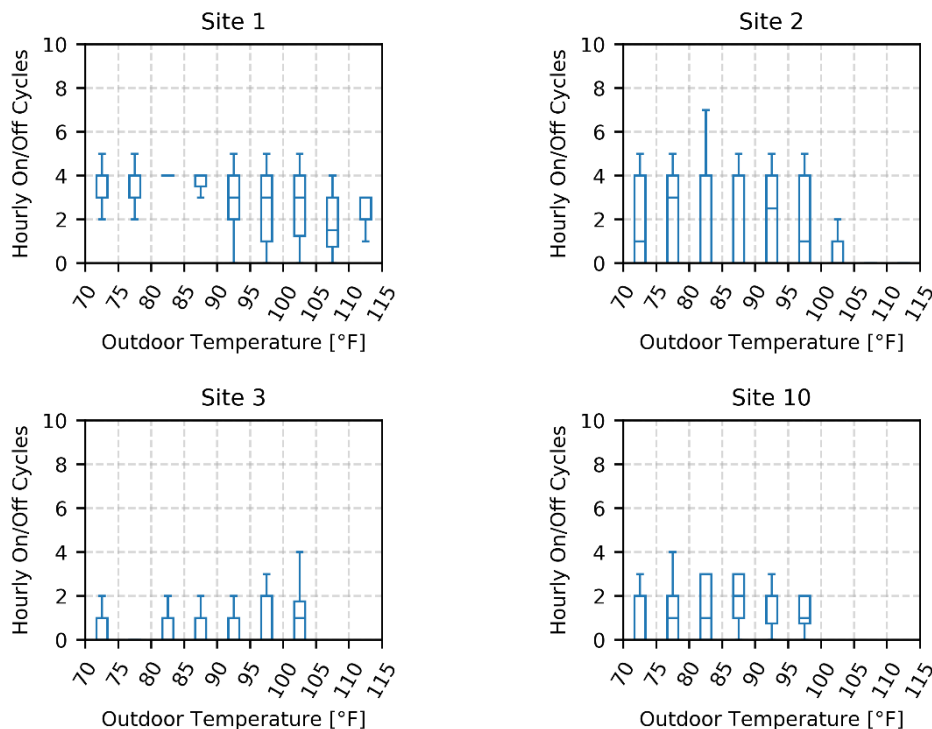


Figure 61. Box and whisker plot of compressor cycles per hour during cooling mode operation for Sites 1, 2, 3, and 10.

Figure 63 plots the steady state cooling compressor inverter frequency, which is proportional to the compressor speed. There was a measurement error with the inverter frequency at Site 13, so plots for Site 13 are not included in Figure 63. In general, the inverter frequencies were similar for cooling and heating for most sites.

During steady-state cooling, we expect the inverter frequency to be higher at warmer outdoor air temperatures as the system will increase the compressor speed to match higher building cooling loads. Additionally, because a variable-capacity heat pump should adjust the compressor speed to match the cooling load, we expect a narrow range of steady state inverter frequencies at each outdoor air temperature bin, which is clear at Sites 1, 5, 6, 8, and 10. Variation in steady state inverter frequency within a temperature bin could be due to variation in solar loads.

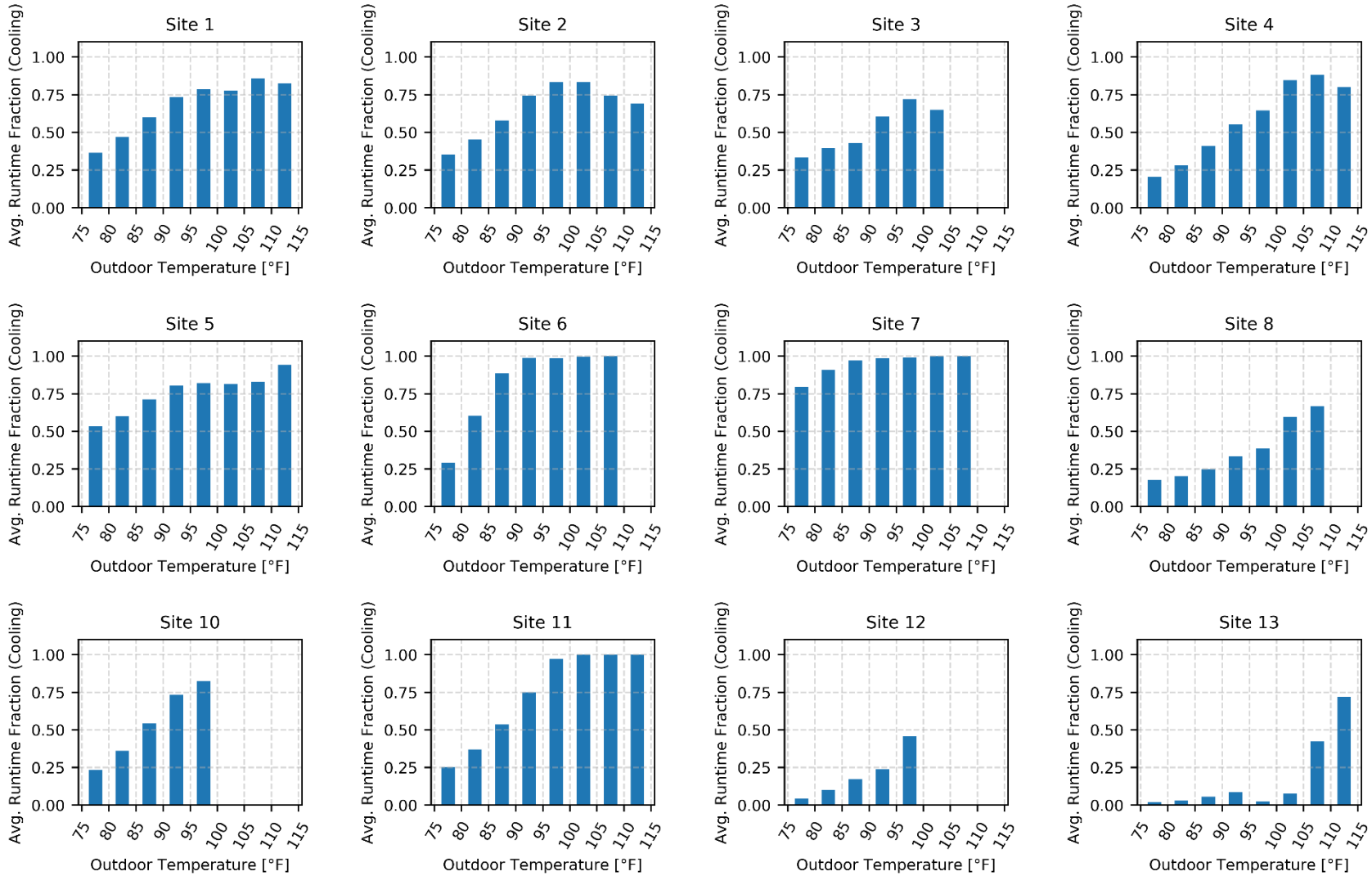


Figure 62. Mean cooling runtime fraction.

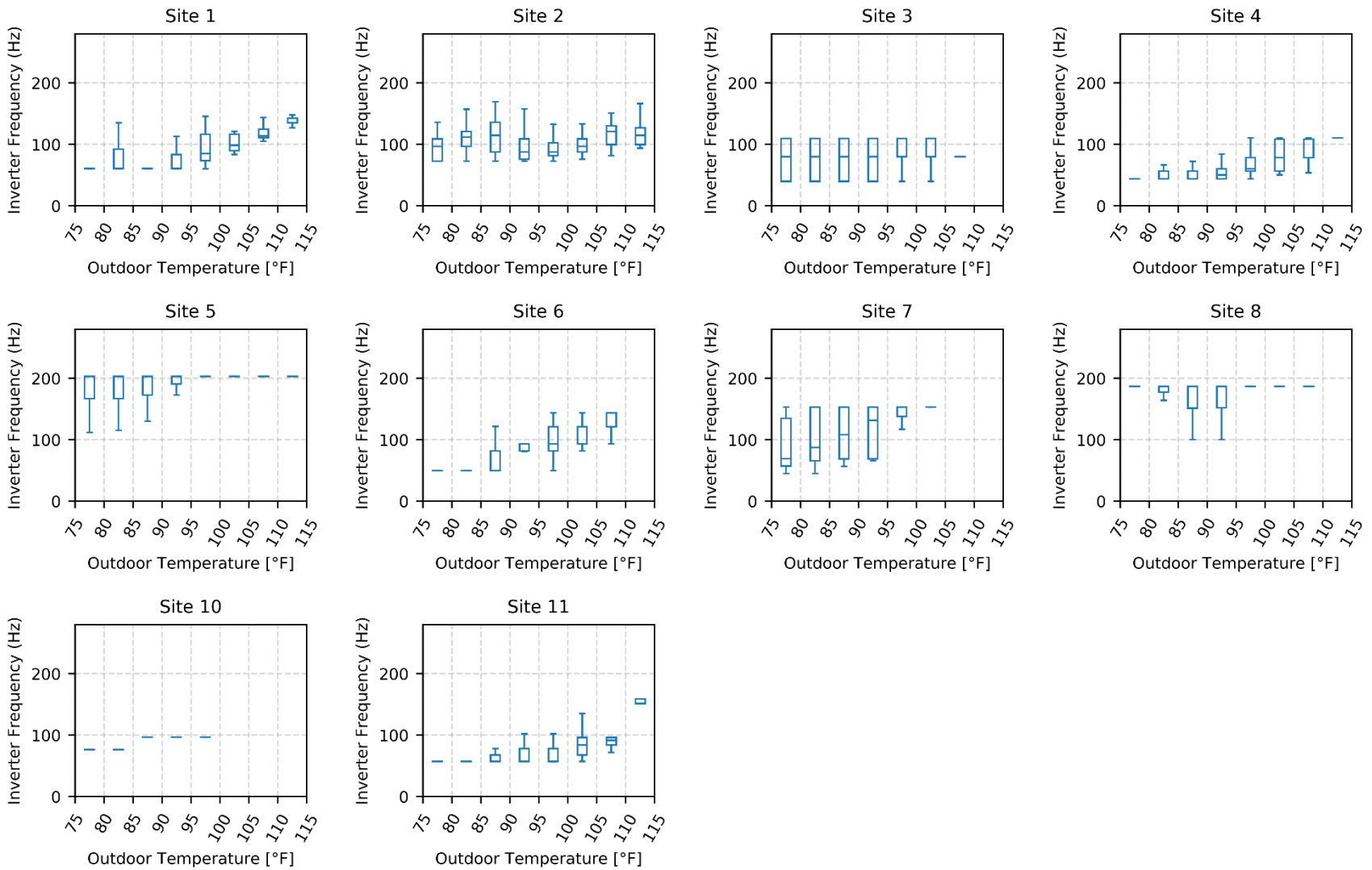


Figure 63. Box and whisker plot of inverter frequency during steady-state cooling operation.

7 Summary and Conclusions

NREL monitored 13 central heat pump systems installed in single-family residential buildings located in a cold climate for at least one full winter season. This report described the house characteristics and heat pump specifications, field monitoring and data analysis methodologies, and measured heating and cooling field performance. Due to an instrumentation issue, this report included data on 12 of the 13 monitored heat pumps.

The primary objective of this project was to measure in-field performance of centrally ducted, variable-capacity air-source heat pumps in cold climates to validate performance and develop field-based performance maps. The project focused on quantifying heat pump performance at cold temperatures.

The sites identified for the study were primarily located in the northwestern United States as homes in the region tend to have all-electric space heating systems and high-efficiency heat pumps have been incentivized for several years. NREL partnered with Ecotope, Inc., a small energy consulting firm located in Seattle, for site recruitment and monitoring equipment installation. All the sites included in the study had previously installed a high-efficiency central heat pump system. One site, located in a Denver suburb, had the only dual fuel heat pump in the study.

Conclusions include:

- **Heating COP:** Heating COPs were compared to manufacturer-reported values attained from either the NEEP Cold-Climate Air Source Heat Pump Product Listing (NEEP 2022) or manufacturer-published expanded performance tables. Steady state COPs at 7 of the 12 sites agreed well with expected performance. For the remaining sites, the measured COPs were lower than expected. One potential cause for low COP is a low indoor airflow rate. However, sites with lower-than-expected COPs did not consistently have low indoor unit airflow rates. Nor were the heat pumps with lower-than-expected COPs consistently from certain manufacturers.
- **Heating capacity:** The measured capacity was closer to the minimum manufacturer-reported capacity rather than the maximum most of the time. For 5 of the 12 sites, the measured capacity aligned well with maximum manufacturer-reported capacity at cold outdoor air temperatures. Four of the sites with lower-than-expected COP also had lower-than-expected capacity.
- **Capacity Modulation:** Heat pumps at 11 of the reported-on sites included variable-capacity compressors. However, despite having modulation capabilities, the heat pumps were off for a significant fraction of the time at outdoor temperatures at which we expected the system to run continuously. This could be due to occupant thermostat setpoint schedules or the equipment controls.
- **Auxiliary Heat Use:** The electric resistance, auxiliary heating energy use exceeded 40% of the compressor-based heating energy at 5 of the 11 reported-on all-electric sites. At two of those five sites, the auxiliary heating consumed more energy than compressor-

based heating, which was caused by one system being undersized and one system having control and/or sensor issues.

- **Defrost Operation:** All systems spent a relatively small fraction of the operating hours in defrost mode. However, the energy consumed by defrost operation exceeded 20% of the compressor-based heating energy at 4 of 12 sites due to operation of the auxiliary heater during defrost. Two sites ran the auxiliary heater for more than five minutes following the defrost cycle. Defrost operation was the primary consumer of auxiliary heating at 3 of 11 sites. Defrost energy use was not fully accounted for at the dual fuel site because natural gas consumption was not directly measured.
- **Heating Supply Air Temperature:** The supply air temperature for all sites rarely exceeded 100°F. Five sites maintained a relatively constant supply air temperature independent of outdoor air temperature, while the supply air temperature decreased at colder outdoor air temperatures for six of the sites.

7.1 Recommendations to Improve Installed Performance

Installation, sizing, commissioning, and control issues impacted the heating season energy consumption at several sites in our study. Based on these findings, we recommend the following:

- **Conduct Proper Commissioning:** All heat pump systems should be properly commissioned to ensure quality installation. Three of the heat pumps in our study were operating with faults at the time monitoring equipment was installed and required technician service calls to resolve the faults. All the heat pumps in our study were initially installed by qualified contractors participating in a utility rebate program. One heat pump had faulty auxiliary heat control, which could be challenging for a technician to diagnose during a site visit.
- **Avoid Under-Sizing:** Our results showed that under-sizing the heat pump can lead to unnecessary auxiliary heat energy consumption, but this was not consistent across all sites. Thus, sizing heat pumps based on the 99% heating design temperature may not be necessary in all cases depending on the house characteristics, heat pump capacity retention, and auxiliary heater control. Recent work published by the Northwest Energy Efficiency Alliance showed that calculating building loads using an outdoor temperature warmer than the design temperature for use in sizing heat pumps resulted in the lowest levelized cost of ownership (NEEA 2022).
- **Maximize Heat Pump Utilization to Maximize COP:** As expected, sites that utilized the compressor to meet the building's heat load for much of the heating season achieved higher seasonal COPs. Underutilization of the heat pump at some sites was due to undersized heat pumps and faulty auxiliary heater controls.
- **Avoid Auxiliary Heat Operation During and After Defrost:** As mentioned above, all systems spent a relatively small fraction of the operating hours in defrost mode. However, the auxiliary heater consumed a significant amount of energy during defrost and defrost recovery. Control options should be investigated to avoid turning on the auxiliary heater during defrost. Though this approach is used to temper the cold supply

air and avoid occupant discomfort, turning off the IDU blower could mitigate the comfort impact, which is an approach utilized in MSHP systems. Extending the auxiliary heat runtime after the defrost cycle is likely not necessary as only 2 of the 12 all-electric sites controlled the auxiliary heat this way.

- Improve Demand-Based Defrost Control Algorithms: The defrost runtime varied significantly across sites experiencing similar weather conditions. Though the variable-capacity systems in this study used demand-based defrost control utilizing embedded sensors, improvements to control algorithms could mitigate unneeded defrost operation.

7.2 Recommendations to Improve the Field Protocol

We recommend the following improvements to the field protocol for future studies:

- Monitor Reversing Valve Status: We were able to detect the operating mode, specifically defrost cycles, by analyzing the vapor line surface temperature measurement. However, operating mode detection would have been simpler, and potentially more reliable, had we measured the status of the reversing valve. This could have been implemented by wiring a relay in parallel to the reversing valve and detecting the opened/closed state of the relay.
- Avoid Locations with Limited Cell Phone Signal Strength (if possible): Remote data downloading is key to ensure data quality and for routine processing of the data. This is best accomplished using cell modems because relying on building occupant's wireless internet is problematic for several reasons. The primary cause of data loss during our study was unreliable cell modem connections, onboard memory filling up, and back-up memory proving unreliable.
- Data Loggers with Sufficient Onboard Memory: As indicated above, we did lose data due to unreliable back-up memory devices. This problem could have been resolved had we used newer, more expensive data loggers with sufficient onboard memory to collect five-second data for the duration of the study.

References

10 CFR Part 430. 2022. *Appendix M to Subpart B of Part 430 – Uniform Test Method for Measuring the Energy Consumption of Central Air Conditioners and Heat Pumps.*

Air-Conditioning Contractors of America (ACCA). 2016. *Manual J – Residential Load Calculations (8th Edition).* Arlington, VA: Air-Conditioning Contractors of America.

Air-Conditioning, Heating, and Refrigeration Institute (AHRI). 2017. *AHRI Standard 210/240 – 2017 Standard for Performance Rating of Unitary Air-Conditioning and Air-Source Heat Pump Equipment.* Arlington, VA: Air-Conditioning, Heating, and Refrigeration Institute.

Air-Conditioning, Heating, and Refrigeration Institute (AHRI). 2020. *AHRI Standard 210/240 – 2023 Standard for Performance Rating of Unitary Air-Conditioning and Air-Source Heat Pump Equipment.* Arlington, VA: Air-Conditioning, Heating, and Refrigeration Institute.

Air-Conditioning, Heating, and Refrigeration Institute (AHRI). 2022. *AHRI Directory of Certified Product Performance.*

<https://www.ahridirectory.org/Search/SearchHome?ReturnUrl=%2f>

ASHRAE. 2017. *ASHRAE Handbook of Fundamentals.* Atlanta, GA: ASHRAE.

Booten, Chuck, Craig Christensen, and Jon Winkler. 2014. *Energy Impacts of Oversized Residential Air Conditioners--Simulation Study of Retrofit Sequence Impacts.* Golden, CO: National Renewable Energy Laboratory. NREL/TP- 5500-60801.
<https://www.nrel.gov/docs/fy15osti/60801.pdf>.

Brookhaven National Laboratory (BNL). 2020. Air-Source Heat Pumps Cold-Climate Field Performance Project – Testing Protocol. Unpublished document. Upton, NY: Brookhaven National Laboratory.

CADMUS. 2016. *Ductless Mini-Split Heat Pump Impact Evaluation.* Waltham, MA: CADMUS.
<https://ma-eeac.org/wp-content/uploads/Ductless-Mini-Split-Heat-Pump-Impact-Evaluation.pdf>.

CADMUS. 2017. *Evaluation of Cold Climate Heat Pumps in Vermont.* Waltham, MA: CADMUS.
https://publicservice.vermont.gov/sites/dps/files/documents/Energy_Efficiency/Reports/Evaluation%20of%20Cold%20Climate%20Heat%20Pumps%20in%20Vermont.pdf.

Energy Information Agency (EIA). 2020. “2020 Residential Energy Consumption Survey Data, End-Use Consumption Tables.” Accessed December 12, 2022.
<https://www.eia.gov/consumption/residential/data/2020/>.

Energy Information Agency (EIA). 2021. “Annual Energy Outlook 2021.” Accessed December 12, 2022. https://www.eia.gov/outlooks/aeo/tables_side.php.

Larson, Ben, Benjamin Hannas, Poppy Storm, and David Baylon. 2013. *Ductless Heat Pump Cold Climate Performance Evaluation.* Portland, OR: Bonneville Power Administration.

Li, Haorong and James E. Braun. 2003. “An improved method for fault detection and diagnosis applied to packaged air conditioners.” *ASHRAE Transactions* 109 (2003): 683.
<https://www.proquest.com/docview/192535031>.

Northeast Energy Efficiency Partnerships (NEEP). 2021. *Cold Climate Air-Source Heat Pump Specification Version 3.1*. Lexington, MA: Northeast Energy Efficiency Partnerships.
https://neep.org/sites/default/files/media-files/cold_climate_air-source_heat_pump_specification-version_3.1_update_.pdf.

Northeast Energy Efficiency Partnerships (NEEP). 2022. *Cold Climate Air-Source Heat Pump Specification Version 4.0*. Lexington, MA: Northeast Energy Efficiency Partnerships.
https://neep.org/sites/default/files/media-files/cold_climate_air_source_heat_pump_specification_-_version_4.0_final_1.pdf

Northwest Energy Efficiency Alliance (NEEA). 2022. *Variable Speed Heat Pump Product Assessment and Analysis*. Portland, OR: Northwest Energy Efficiency Alliance.
<https://neea.org/resources/variable-speed-heat-pump-product-assessment-and-analysis>.

Salmonsens, Mary. 2018. “Seven New AC Units with Variable-Speed Compressors.” *Builder*. July 14, 2018. https://www.builderonline.com/products/hvac/seven-new-ac-units-with-variable-speed-compressors_o.

Pacific Northwest National Laboratory (PNNL). 2022. *Building America Solution Center*.
<https://basc.pnnl.gov/images/climate-zone-map-iecc-2021>

U.S. Department of Energy (DOE). 2021. *Residential Cold-Climate Heat Pump Technology Challenge Specification and Supporting Documents, Version 1.2*. Washington, DC: U.S. Department of Energy. <https://www.energy.gov/sites/default/files/2021-10/bto-cchp-tech-challenge-spec-102521.pdf>.

Appendix A. Field Protocol Data Entry Forms

Checklist (Condensed Protocol) and Data Entry Form for Air-Source Heat Pumps Cold-Climate Field Performance Project

Note: The purpose of this form is to supplement the Air-Source Heat Pumps Cold-Climate Field Performance Project Testing Protocol developed by DOE, BNL, and NREL. The testing protocol document shall dictate data collection methods and hardware requirements. This short form is intended to be used by the field engineers or Site-Responsible Team Member (SRTM) to ensure the testing protocol is accurately followed.

Name:	Date(s):
Address:	Field Engineer(s):
Phone/email:	Organization:

Data Collection/Order of Tests	Data Logging Equipment	
<input type="checkbox"/> IRB Consent Documents (HRP-502) (<i>separate document</i>)	Item	Qty
<input type="checkbox"/> Form 1a: House Information	<input type="checkbox"/> Campbell CR1000	2
<input type="checkbox"/> Form 2a: Heating Energy Use	<input type="checkbox"/> Campbell RF401	2
<input type="checkbox"/> Form 2b: Cooling Energy Use	<input type="checkbox"/> Campbell Cell210 w/ Antenna	1
<input type="checkbox"/> Form 3: Site Photos	<input type="checkbox"/> WattNode WNB-3D-240-P	3
<input type="checkbox"/> Form 4: Heat Pump Information Data	<input type="checkbox"/> CR1000 Backup Battery	2
<input type="checkbox"/> Form 5: Commissioning Data	Sensors	
<input type="checkbox"/> Form 6: Blower Airflow Correlation Test	Item	Qty
<input type="checkbox"/> Form 7: Data Logging Channel Checklist	<input type="checkbox"/> T-type thermocouples (20 ft)	9
<input type="checkbox"/> Form 8: Home Thermal Audit Data	<input type="checkbox"/> Vaisala HMP110 T&RH Sensor	3
	<input type="checkbox"/> 50 A CTs - ACTL-0750-050	4
	<input type="checkbox"/> 20 A CTs - ACTL-0750-020	2
	<input type="checkbox"/> 5 A CT - ACCT-0750-005	1
	<input type="checkbox"/> JD Metering - JC10F-50A-V	2
	<input type="checkbox"/> JD Metering - JC10F-5A-V	2
	Miscellaneous	
	Item	Qty
	<input type="checkbox"/> CR1000 Enclosures	2
	<input type="checkbox"/> Radiation Shield	1
	<input type="checkbox"/> Surge Protector	2
	<input type="checkbox"/> Extension Cords	2
	<input type="checkbox"/> Sensor Extension Wire	400 ft.
	<input type="checkbox"/> Duct Blaster Rig	
	<input type="checkbox"/> Blower Door Rig	
	<input type="checkbox"/> Flow Plate w/ Pressure Gauge	

Form 1a: Ducted Systems: House Information Table

Information elements below are identical to the Air-Source Heat Pumps Cold-Climate Field Performance Project Testing Protocol Form 1 for homes with a ducted, central heat pump system.

Building Type (circle):	Mobile/Manufactured Home	Apartment (2-4 units in bldg.)
	Single-family, detached	Apartment (≥ 5 units in bldg.)
	Single-family, attached	
	Other:	
House Information:	Conditioned floor area (sq. ft.):	
	Number of stories:	
	<input type="checkbox"/> Home is a split level	
Heat Pump Service Area (circle):	Whole-house*	Dining room
	Bedroom	Office
	Living room	Laundry room
	Other:	
Additional Information:	Is there an apartment or other finished space located in the building?	
	<input type="checkbox"/> Yes	<input type="checkbox"/> No
	If yes, is there a separate heating/cooling source from the rest of the home with its own thermostat/controls?	
	<input type="checkbox"/> Yes (specify in notes)	<input type="checkbox"/> No
Use this space to describe any additional relevant general information about the home. Such information may include energy-efficiency updates, if the home is well shaded, close to the water, or unique home characteristics.		
House Pictures:	<input type="checkbox"/> Front	
	<input type="checkbox"/> Left side	
	<input type="checkbox"/> Right side	
	<input type="checkbox"/> Back	

*Note: If the heat pump does not service the entire home, this document does not apply and form 1b should be used.

Form 2a: Home's Heating Energy Use

Auxiliary Heat: *	Is there another source of <u>auxiliary heating</u> that may be used during the test period?		
	<input type="checkbox"/> Yes		<input type="checkbox"/> No
	If yes, what is the <u>auxiliary heating</u> source?		
	Central hot-air furnace	Steam or hot-water system with radiators or baseboard	Built-in electric units installed in walls, ceilings, baseboards, or floors
	Built-in room heater burning gas, oil, or kerosene	Heating stove burning cordwood, wood pellets, coal, or coke	Portable electric heaters
	Wood or gas fireplace or hearth product (describe in notes)	Secondary heat pump (ducted or ductless)	Back-up electric resistance heating element (centrally ducted heat pump systems)
	Other:		
	If yes, what fuel type is used by the <u>auxiliary heating</u> equipment: (circle all that apply)		
	Electricity	Natural gas from underground pipes	
	Propane (bottled gas)	Fuel oil	
	Wood	Other:	
	Provide available information about the <u>auxiliary heating</u> equipment:		
	Make:		Model
	Approximate age of <u>auxiliary heating</u> equipment: (circle one)		
	Less than 2 years old	2 to 4 years old	5 to 9 years old
	10 to 14 years old	15 to 19 years old	20 or more years old
	20 or more years old	Unknown	
Notes (additional relevant information):			
Explain the use patterns of the <u>auxiliary heat</u> . Be sure to mention if the thermostat setting is altered when using the secondary source.			

Thermostat Information:	Will the heat pump being monitored be tied to a central thermostat or have its own independent control?		
	<input type="checkbox"/> Central thermostat		<input type="checkbox"/> Independent control
	Is the thermostat/control that controls the heat pump programmable, meaning can it be set to automatically adjust the temperature at certain times?		
	<input type="checkbox"/> Yes		<input type="checkbox"/> No
	Which of the following describes how the household controls the temperature most of the time: (circle one)		
	Set one temperature and leave it there most of the time	Manually adjust the temperature at night or when no one is home	Program the thermostat to automatically adjust the temperature during the day and night at certain times
	A “Smart” thermostat is used with autotuned temperature settings	Turn equipment on or off as needed	The household does not have control over the equipment
	Other:		
	Winter heating setpoint information:		
	What is the typical temperature when someone is home during the day?		
	What is the typical temperature when no one is inside the home during the day?		
	What is the typical temperature inside the home at night?		
	Use this space to provide any additional relevant information about the homeowner’s heating practices and thermostat settings throughout the winter . Be sure to indicate whether nighttime setback practices are used or what homeowners may do when they leave for work/vacation.		
	Is a humidifier used in the home?		
<input type="checkbox"/> Yes		<input type="checkbox"/> No	

Form 2b: Home's Cooling Energy Use

Auxiliary Cooling: *	Is there another source of <u>auxiliary cooling</u> that may be used during the test period?			
	<input type="checkbox"/> Yes		<input type="checkbox"/> No	
	If yes, what is the <u>auxiliary cooling</u> source? (circle one)			
	Central air conditioner	Portable or window/wall units	Ductless heat pump	Other:
	Provide available information about the <u>auxiliary cooling</u> equipment:			
	Make:		Model:	
	Approximate age of <u>auxiliary cooling</u> equipment: (circle one)			
	Less than 2 years old	2 to 4 years old	5 to 9 years old	
	10 to 14 years old	15 to 19 years old	20 or more years old	
	20 or more years old	Unknown		
	Notes (additional relevant information):			
	<p>Explain the use patterns of the <u>auxiliary cooling</u>. Be sure to mention if the thermostat setting is changed when using the auxiliary source. Consider all the individual window, wall or portable air conditioning unit(s) used in the home during the summer months. Comment on their use pattern (are they only turned on when outdoor temperatures are extreme, special occasions, shoulder seasons and then the main thermostat is idle). Be sure to include the location of the unit(s) as well.</p>			

Thermostat Information:	<u>Summer Cooling Setpoint Information</u>	
	What is the typical temperature when someone is home during the day?	
	What is the typical temperature when no one is inside the home during the day?	
	What is the typical temperature inside the home at night?	
	Use this space to provide any additional relevant information about the homeowner's cooling practices and thermostat settings throughout the summer .	
Other:	Is a dehumidifier used in the home?	
	<input type="checkbox"/> Yes	<input type="checkbox"/> No
	If yes, where is the dehumidifier located?	
	In the case of ductless units, document the indoor unit vane settings:	

Form 3: Site Photos of Heat Pump

Outdoor Unit:	<input type="checkbox"/> Front/side view (> 6 ft from unit)
	<input type="checkbox"/> Front/side view with nameplate (< 3 ft from unit)
	<input type="checkbox"/> Front view of inside of jacket (removing the cover and capturing the essential components: compressor, fan, coils, refrigerant lines, control board)
	<input type="checkbox"/> Side view of inside of jacket (removing the cover and capturing the essential components: compressor, fan, coils, refrigerant, control board)
	<input type="checkbox"/> Backside of unit detailing connections (capturing the refrigerant lines/pipes)
	<input type="checkbox"/> Provide a brief description of the location of the outdoor unit (be sure to include the wall direction the heat pump sits on and if there are any notable features such as an enclosure, overhang, plants) <u>Notes:</u>
Indoor Unit:	<input type="checkbox"/> Front/side view of unit capturing location in basement or utility room and connected duct work (> 6 ft from unit)
	<input type="checkbox"/> Front/side view of indoor unit capturing make/model information (< 3 ft from unit)
	<input type="checkbox"/> Front view of inside of jacket (removing the cover and capturing the essential components: evaporator coils, blower fan)
	<input type="checkbox"/> Side view of inside of jacket (removing the cover and capturing the essential components: evaporator coils, blower fan)
	<input type="checkbox"/> View capturing size of electric resistance elements and/or gas furnace nameplate information
	<input type="checkbox"/> Ducts on the supply and return size of the air handler
Thermostat:	<input type="checkbox"/> Central thermostat (capturing the make and/or model in addition to the setpoint information captured above)
Additional:	<input type="checkbox"/> Auxiliary heating source* (> 6 ft)
	<input type="checkbox"/> Auxiliary heating source* capturing make and model (< 3 ft)

* Auxiliary heating source photos should include heat sources other than electric resistance elements present in a central heat pump system.

Form 4: Heat Pump Information and Product Data

Install Date (approximate):			
Heat Pump Information			
<u>Outdoor Unit Brand and Model Number</u>	<u>Indoor Unit Brand and Model Number</u>	<u>Aux. Heating Model Number</u>	
Is the heat pump a zoned system?	<input type="checkbox"/> Yes	<input type="checkbox"/> No	
Number of zones:	Is there a bypass damper:	Yes / No	
Notes (indicate how zone setpoints are typically set, etc.):			
Factory Refrigerant Charge:	lb	oz	
Line set length/Standard line length	/		
Thermostat Make and Model:			
Thermostat Location Description:			
Auxiliary Heat Lockout Temp. (°F):			
Compressor Cut-Out Temp. (pre/post): *	/		
Crankcase Heater Details:	Present?	<input type="checkbox"/> Yes	<input type="checkbox"/> No
Wattage and Control Details (if known):			
Pan Heater Details:	Present?	<input type="checkbox"/> Yes	<input type="checkbox"/> No
Wattage and Control Details (if known):			
Indoor Unit Location Description:			
Metering Device Type	Indoor	<input type="checkbox"/> TXV	<input type="checkbox"/> EXV
	Outdoor	<input type="checkbox"/> TXV	<input type="checkbox"/> EXV
Has accumulator? (circle)	Yes / No		
Has filter drier? (circle)	Yes / No		

Form 5: Commissioning Data*

Service Company Information		Manufacturer Literature	
Name:		<input type="checkbox"/> Service and/or installation manual	
Phone Number:		<input type="checkbox"/> Homeowner/operation manual	
Commissioning Date:		<input type="checkbox"/> Product data manual	
Additional Commissioning Details Attached:		<input type="checkbox"/> Yes	<input type="checkbox"/> No
Tech's Evaluation of Refrigerant Charge:		<input type="checkbox"/> Over	<input type="checkbox"/> Under <input type="checkbox"/> OK
System Checks			
Reversing valve OK (cooling)?	Y / N	Reversing valve OK (heating)?	Y / N
Indoor TXV installed correctly?	Y / N / NA	Outdoor TXV installed correctly?	Y / N / NA
Suction line insulated?	Y / N	Liquid line insulated?	Y / N
Mode Tested:		<input type="checkbox"/> Heating	<input type="checkbox"/> Cooling
% Full Capacity Tested			
Outdoor Dry-Bulb Temperature (°F)			
Hot Gas Discharge Temperature (°F)			NA
Suction Pressure (psig) / Saturated Temp. (°F)	/		/
Suction Temperature (°F)	NA		
Superheat (°F)	NA		
Head Pressure (psig) / Saturated Temp. (°F)	/		/
Liquid Line Temperature (°F)			
Subcooling (°F)			
Entering Dry-Bulb Temperature (°F):			
Entering Wet-Bulb (°F) (if cooling mode):			
Leaving Dry-Bulb Temperature (°F):			

* This form is not required but may serve as a guideline for the SRTM overseeing the installation of the data logging equipment and to verify that heat pump is properly charged. Documentation should be included with details on how the SRTM verified the unit was properly charged.

Form 6a: Ducted Systems – Blower Airflow Data

NOTE: See Air-Source Heat Pumps Cold-Climate Field Performance Project Testing Protocol for additional details. A minimum of three fan speeds should be tested and tests should be repeated at the conclusion of the testing period.

As-found filter condition: *	<input type="checkbox"/> New		<input type="checkbox"/> Somewhat dirty	
	<input type="checkbox"/> Filthy		<input type="checkbox"/> Missing	
Pressure Units:	<input type="checkbox"/> Pascal	<input type="checkbox"/> in. H ₂ O	<input type="checkbox"/> Other:	
	Test 1	Test 2	Test 3	Test 4
Mode tested (circle one)	Htg / Clg	Htg / Clg	Htg / Clg	Htg / Clg
Stage/Percentage/Nominal CFM Tested				
Return Static Pressure (downstream of filter)				
Normal Supply Operating Pressure (NSOP)				
TrueFlow Supply Operating Pressure (TFSOP)				
Correction Factor (NSOP/TFSOP)^{0.5}				
Plate (14 or 20)				
Plate Pressure				
Raw Flow				
Corrected Flow				
Blower True Power (RMS Watts)				

** Prior to all data collection a new filter must be installed. In addition, ask the homeowner to replace the filter on a quarterly basis.*

Form 7: Data Logger Channel List

Indoor Data Logger (CR1000)

Measurement	Sensor Model #	Wire Channel	Photo?	Notes
Supply Air Temp. #1	Thermocouple	1H – Blue 1L – Red ⊥ – Jumper to 1L ⊥ – Shield	<input type="checkbox"/>	
Supply Air Temp. #2	Thermocouple	2H – Blue 2L – Red ⊥ – Jumper to 2L ⊥ – Shield	<input type="checkbox"/>	
Supply Air Temp. #3	Thermocouple	3H – Blue 3L – Red ⊥ – Jumper to 3L ⊥ – Shield	<input type="checkbox"/>	
Return Air Temp.	Thermocouple	4H – Blue 4L – Red ⊥ – Jumper to 4L ⊥ – Shield	<input type="checkbox"/>	
ID Coil Ref. Mid. Temp.*	Thermocouple	5H – Blue 5L – Red ⊥ – Jumper to 5L ⊥ – Shield	<input type="checkbox"/>	
ID Coil Ref. Htg. Out Temp.	Thermocouple	6H – Blue 6L – Red ⊥ – Jumper to 6L ⊥ – Shield	<input type="checkbox"/>	
T&RH Air Return	Vaisala HMP110	7H – Green (T) 7L – White (RH) 12V – Red G – Black ⊥ – Shield (Clear)	<input type="checkbox"/>	
T&RH Air Supply	Vaisala HMP110	8H – Green (T) 8L – White (RH) 12V – Red G – Black ⊥ – Shield (Clear)	<input type="checkbox"/>	
Indoor Unit Total Energy	WNB-3D-240-P	C6 – WattNode P1 5V – 10 kΩ res. to C6 G – WattNode COM	<input type="checkbox"/>	ΦA CT ΦB CT CT size =
Indoor Unit Blower Energy	WNB-3D-240-P	C7 – WattNode P1 5V – 10 kΩ res. to C7 G – WattNode COM	<input type="checkbox"/>	ΦA CT ΦB CT CT size =

Outdoor Data Logger (CR1000)

Measurement	Sensor Model #	Wire Channel	Photo?	Notes
Outdoor Air Temp. (or OD coil entering temperature)	Thermocouple	1H – Blue 1L – Red ⏚ – Jumper to 1L ⏚ – Shield	<input type="checkbox"/>	
OD Coil Ref. Mid. Temp. (if accessible)*	Thermocouple	2H – Blue 2L – Red ⏚ – Jumper to 2L ⏚ – Shield	<input type="checkbox"/>	
OD Coil Ref. Clg. Out Temp.	Thermocouple	3H – Blue 3L – Red ⏚ – Jumper to 3L ⏚ – Shield	<input type="checkbox"/>	
Outdoor Unit Total Current	JC10F-50A-V	5H – Sensor Signal (+) ⏚ – Sensor Ground (-) ⏚ – Sensor Shield	<input type="checkbox"/>	
Compressor + Inverter Current	JC10F-50A-V	5L – Sensor Signal (+) ⏚ – Sensor Ground (-) ⏚ – Sensor Shield	<input type="checkbox"/>	
Crankcase Heater Current (if present)	JC10F-5A-V	6H – Sensor Signal (+) ⏚ – Sensor Ground (-) ⏚ – Sensor Shield	<input type="checkbox"/>	
Drain Pan Heater Current (if present)	JC10F-5A-V	6L – Sensor Signal (+) ⏚ – Sensor Ground (-) ⏚ – Sensor Shield	<input type="checkbox"/>	
T&RH Air Outdoor	Vaisala HMP110	8H – Green (T) 8L – White (RH) 12V – Red G – Black ⏚ – Shield (Clear)	<input type="checkbox"/>	
Outdoor Unit Total Energy	WNB-3D-240-P	C6 – WattNode P1 5V – 10 kΩ res. to C6 G – WattNode COM	<input type="checkbox"/>	ΦA CT ΦB CT CT size =
Inverter Voltage Frequency	ACCT-0750-005	P1 – CT wire 1 G – CT wire 2	<input type="checkbox"/>	

* Mid-coil refrigerant temperature measurements should be located on a return bend at the approximate midpoint of a selected heat exchanger circuit. NOTE: The mid outdoor coil temperature measurement should only be completed if a mid-coil return bend is accessible without having to remove the fan.

Form 8: Home Thermal Audit

Use accompanying grid paper for sketches; make sure all dimensions and associated R-values/window types are clearly shown/labeled. See last page of protocol for a U-factor reference table. Indicate clearly on the sketch where insulation values are estimated.

- Areas of all components but windows/doors can be reported to the nearest 10 ft². Windows/doors should be measured to the nearest 1 ft². Accuracy is more important in poorly insulated houses.
- Using out-to-out or in-to-in dimensions is fine. For vaulted ceilings, use best judgement on how to adjust attic area to account for vault slope.
- Slab on grade or slab below grade features are assigned F-factors (vs. U-factors) and we need to know the running feet of these features (vs. ft²)
- Record ceiling heights (by floor); add 1 foot for upper stories to account for framing. Calculate house volume. Account for half-stories, etc. as best you can.
- For windows, the big break is between single and double-glazed units; within double-glazed units with metal frames, older units have smaller air spaces and non-thermally improved frames. It is not necessary to draw elevations but make sure to double-check each elevation and to make sure all windows/doors are accounted for.
- Indicate approximate thermostat location.

Additional notes:

Heated Floor Area: _____ ft²

Heated House Volume: _____ ft³

Ducts

Measure feet of supply and return ducts in unheated buffer spaces (attics, crawlspaces, most garages). For duct R-values, use nominal R-value on duct or best guess (or thickness). Record R-values for all unique duct dimensions and enter below. Average R-value is okay; if there is a lot of missing/damaged insulation, use Notes field.

Supply Ducts

Duct Type (metal/flex/other)	Duct Location	Duct Perimeter (inches)	Estimated Duct Length (feet)	Duct Insulation (estimated R-value)*	Notes

Return Ducts

Duct Type (metal/flex/other)	Duct Location	Duct Perimeter (inches)	Estimated Duct Length (feet)	Duct Insulation (estimated R-value)*	Notes

<u>Round Duct Size (in)</u>	<u>Perimeter</u>	<u>Round Duct Size (in)</u>	<u>Perimeter</u>
5	15.7	10	31.4
6	18.8	12	37.7
7	22	14	44
8	25.1	16	50.2
9	28.3	20	62.8

Blower Door Test

Depressurize to near 50 and 25 Pa with respect to outside. Note the house pressure WRT outside doesn't have to be exactly 50 or 25 Pa; the actual values will be corrected to 50 Pa during analysis. The test will should be done in depressurization mode but can be done in pressurization mode if needed to reduce disruption and to save time for the duct test.

Was test done in pressurization mode? Y N

Blower Door (BD) Test Procedure:

1. Close all windows and doors to the outside. Open all interior doors and supply registers.
2. Turn off whole-house ventilation system. Leave intentional return leaks in their as-found condition. Make sure all exhaust fans and clothes dryer are off.
3. Make sure doors to interior furnace cabinets are closed. Also make sure crawlspace hatch is on, even if it is an outside access. Check attic hatch is closed position. Put garage door in normal position; note below if garage door is always open and run test with it open.
4. Set fan to depressurize house. If test done in pressurization mode, run outside pressure tap out through door shroud.
5. Depressurize house to 50 Pa or thereabouts. Record house pressure, BD flow pressure, and BD ring (below, "Test 1" line). If you cannot reach 50 Pa, get as close as possible and record information. If test done in pressurization mode, make sure that the BD fan pressure is measured WRT outside.
6. Now take the house down to 25 Pa WRT outside and record information on "Test 1" row.

Blower Door Tests	House P (~50 Pa) (P₅₀)	BD Fan Pressure (Pa)	BD Ring	BD Flow (~ 50 Pa) (Q₅₀)	House P (~25 Pa) (P₂₅)	BD Fan Pressure (Pa)	BD Ring	BD Flow (~25 Pa) (Q₂₅)
Test 1								
Test 2 (if needed)								

7. To check test, calculate the flow exponent, n . Use the following formula, $n = \ln(Q_{50}/Q_{25})/\ln(P_{50}/P_{25})$. Note Q_{50} and Q_{25} are the flows through the blower door at the testing pressures (which are denoted P_{50} and P_{25}). Depending on the test, you may not get the house to exactly 50 or 25 Pa WRT outside. Use the exact ΔP you measure when checking the flow exponent. For example, if the house gets to 48 Pa for the high ΔP , use this as the P_{50} in the equation. If the flow exponent is not between 0.50 and 0.75, repeat the test and record results on the "Test 2" line.

Note any unusual testing conditions (wind, etc.):

Exterior Duct Leakage Testing

1. Exterior house doors and garage doors should be closed for exterior duct leakage test.
2. Pressurize the house to about 50 Pa WRT outside.
3. Pressurize tested part of duct system to about 50 Pa with smallest flow ring possible.
4. Measure pressure of ducts WRT house. Make sure blower door flow does not impinge on pressure tap measuring house pressure.
5. Adjust duct tester speed controller so that duct pressure WRT house is zero or very close.
6. Re-check pressure of ducts WRT outside.
7. Measure duct tester fan pressure. Look up flow in table, use gauge (make sure gauge is paired with the right duct tester) or use flow equation. Record duct pressure WRT out, DB fan pressure, DB fan ring.
8. If you cannot reach 50 Pa, test to the highest pressure you can reach and enter this in the '50 Pa' column. Use a test pressure of half this pressure for the low-pressure test.
9. Repeat steps 2–7 with house and ducts at about 25 Pa WRT outside.
10. Check flow exponent (as above for blower door test).
11. Put in system split (taped-off TrueFlow often best) and do a one-sided test. Specify side tested (supply or return) on form.

Note any unusual testing conditions (wind, etc.):

Use the following formula: $n = \ln(Q_{50}/Q_{25})/\ln(P_{50}/P_{25})$. Note Q_{50} and Q_{25} are the flows through the Duct Blaster at the testing pressures (which are denoted P_{50} and P_{25} .) Depending on the test, you may not get the ducts to exactly 50 or 25 Pa WRT outside. Use the exact ΔP you measure when checking the flow exponent. For example, if the ducts get to 48 Pa for the high ΔP , use this as the P_{50} in the equation. If the flow exponent is not between 0.50 and 0.75, repeat the test and record results on the "Test 2" line.

	Test Type (enter below) <i>both sides supply return</i>	Duct P (near 50 Pa) (P_{50})	DB fan pressure	DB Ring	DB flow near 50 Pa (Q_{50})	Duct P (near 25 Pa) (P_{25})	DB fan pressure	Ring	DB flow near 25 Pa (Q_{25})
Test 1									
Test 2									
Test 3									
Test 4									